# Effect of the fractionation and immobilization on the sorption properties of humic acid

## Moustafa Khalaf

# Effect of the fractionation and immobilization on the sorption properties of humic acid

*Moustafa Khalaf*

# Acknowledgments

me to the world of NMR spectroscopy and for their hospitality during my unforgettable visit to Brookings, USA.

Sincere thanks are due to Dr. E. Tombácz, Department of Colloid Chemistry, University of Szeged, whose helpful comments and suggestions have had a considerable impact on this thesis and for her hospitality during my visit to Szeged, Hungary.

I would like to thank Dr. E. Koglin for performing the "ab initio" calculations and his useful discussion to interpret the FT-IR spectra. Thank you also for Dipl.-Ing. H. Schlimper for performing the FT-IR measurements.

For the nice working atmosphere and the warmhearted helps and valuable discussions, I am grateful to my colleagues in the physicochemical soil functions group at the institutes of "Chemistry and Dynamics of the Geosphere" and "Applied Physical Chemistry". Special thanks to:

A. Muren, who helped me get started in laboratory,

A. de Nijs and A. Csiszar for their sense of humor and for being not only colleagues but also good friends.

No words are sufficient to thank my wonderful and beautiful wife "Naglaa". The patience, love, sacrifice, encouragement, care and support freely given by her which I experienced during my study were invaluable and made all the difference. The youthful spirit of our son "Hazem" gave me the energy and perspective to finish this work.

Last but not least, I would like to thank my parents and my sisters for their love and their unconditioned and never-ending support of whatever will make me happy. As a whole, my family has taught me the things that are truly important in life: faith, love, and integrity. Thank you.

# Abstract

Humic substances modify the surface of inorganic soil constituents changing the nature and amount of adsorption sites for contaminants and also influencing the particle-particle interactions and thus the mobility and transport behavior of the soil particles. The aim of this PhD work was to investigate the effects of the interactions between two important soil components, aluminum oxide and humic acid, on the sorption behavior of 2,4-dichlorophenol under laboratory conditions selected to model the soil systems.

Humic acid is very heterogeneous in terms of physical and chemical properties. To reduce the chemical heterogeneity of the extracted humic acid (from the $A_p$ horizon of the Orthic Luvisol, Merzenhausen, Germany), a fractionation scheme using the ultrafiltration technique was used to obtain eight size fractions of the humic acid. The extracted humic acid and its fractions were characterized by potentiometric acid-base titration, elemental analysis and different spectroscopic methods (NMR, UV-VIS and FT-IR spectroscopy). Clear chemical differences between the humic acid size fractions were observed. Smaller size fractions of the soil humic acid contained more chargeable functional groups and larger percentage of aromatic carbon than the larger size fractions. Conversely, the percentage of aliphatic carbon increased with increasing apparent molecular weight. Moreover, the solid-state $^{19}$F-NMR was used to study the sorptive uptake of hexafluorobenzene by the humic acid and its fractions. It was found that humic acid molecules have different chemical environments into which organic pollutant such as hexafluorobenzene can sorb. Small humic acid molecules have at least three sorption sites ("rigid", "soft" and other new domains) that are more clearly defined and homogeneous than the sorption domains found in larger humic acid molecules.

The effect of the pH and the electrolyte concentration on the adsorption of the humic acid onto alumina surfaces as well as on the colloidal stability of these systems were studied. To better understand the binding mechanisms these

results were also compared to those of polyacrylic acid. The adsorption of humic acid or polyacrylic acid to alumina varied with pH and electrolyte concentration, suggesting that the conformation of the humic acid or polyacrylic acid in solution significantly determines their structures on the mineral surface. At low pH (< point of zero charge (PZC) of alumina), increasing amounts of humic acid or polyacrylic acid are adsorbed on the alumina surface with increasing concentrations of solutes, resulting in a charge reversal from positive to negative net total particle charge whilst at high pH (> PZC), the electrophoretic mobility was shifted to more negative values. The colloidal stability of the alumina dispersions containing increasing amounts of the added humic acid and polyacrylic acid, respectively, was monitored using the dynamic light scattering technique. The maximum aggregate size was observed around the zero electrophoretic mobility, indicating the importance of the charge neutralization mechanism.

By comparing the adsorption of the humic acid fractions on alumina surfaces, it was found that the adsorbed amount increases with increasing humic acid molecular size. Furthermore, an increase in the rise of the adsorption isotherm in the plateau regions by increasing the humic acid fraction size was also observed which indicates a higher contribution of the hydrophobic interactions due to the increase in the aliphatic carbon and the decrease in the chargeable groups.

The sorption results of 2,4-dichlorophenol on the immobilized humic acid at different pH and salt concentrations revealed that the value of the sorption coefficient decreases as the ionic strength decreases or the pH value increases which gives direct evidence for the importance of the conformation of the immobilized HA. These sorption isotherms can be described as a linear isotherm, which indicates that the sorption of 2,4-dichlorophenol is predominantly a partitioning process between the aqueous phase and the immobilized humic acid.

# Contents

# 1    Introduction

Humans have always built up their own order at the expense of some order in the environment; in recent history, however, they have multiplied destruction of environmental order to build up increasingly intricate structure of cultural and technical civilization (1). Increasing development of civilization has always been a primary driving force for humans, and has been particularly enhanced by men's unmatched ability to exploit natural resources. However, it has become evident in the past years that industrial and economic growth has not been without environmental cost (2). The development of cultural and technical civilization has been marked with increasing interference in hydrogeochemical cycles (3). As humans increasingly have disrupted the cycles connecting the soil, water and atmosphere, the ratio of pollutant fluxes to natural fluxes has multiplied.

What is pollution? People usually have a limited (typically egocentric) concept of what constitutes pollution. In a very broad sense, however, pollution is the alteration by humans of our surroundings in such a way that they become unfavorable to present ecosystems. Thus, pollution adversely affects not only people, but also causes other environmental catastrophes such as loss of species and diversity. This characterization implies that pollution not only results from addition of contaminants directly into the environment, but also from other direct or indirect consequences of human activity.

Over the last decades soil pollution has been recognized as a major topic of concern. Every now and then, pollution of the natural environment with for example heavy metal ions, fertilizers, and pesticides has been reported (4-8). The uptake of contaminants by living organisms mostly occurs by exposure to dissolved species. Plants are exposed to pollutants in the soil by their roots and animals mainly by drinking contaminated water (including contaminants bound to the dissolved soil components) or indirectly by eating contaminated plants or animals. Thus the concentration of the contaminants in the aqueous phase is of prime importance. These aqueous concentrations are affected by

soil factors such as pH, mineral oxide, clay, and organic matter content and the content of the toxic species. Further it is well known that the soil can immobilize toxic chemicals by precipitation, adsorption or (bio)transformation and that the soil acts as a buffer. The buffer capacity of the natural environment strongly influences the impact of toxic chemicals. Buffering in this sense is described as storage of the chemicals without a direct effect of these chemicals on the toxicity experienced at the contaminated site. Exceedance of this capacity may be harmful to the ecosystem because it implies an increased transport and an increased bio-availability of the toxic chemicals.

It has been generally recognized that not the overall concentration of a pollutant controls the toxicity of the contaminated site, but that the concentration of the different speciation forms of a pollutant and the bio-availability of each of the different species have to be considered. Besides the local interactions between contaminants and the soil components the transport of the dissolved species due to the soil water dynamics is an important factor when studying the risks associated with contaminated sites. Contaminants can be transported by the ground water. The species bound to the soil components that are soluble and transportable by the aqueous phase are considered as mobile. Species bound to the non-dissolvable or settled particles and the material bound to these particles belong to the immobile soil fraction. The transport of contaminants that bind strongly to the mobile soil components may be enhanced in the environment, this phenomenon is known as colloid facilitated transport. Binding of contaminants to the different soil components has often been recognized as a process which controls the bio-availability of the contaminants and affects the risks associated with the contamination (9). For example hydrophobic pesticides may be captured in the hydrophobic cavities of the humic substances (10) and thus the transport of these hydrophobic molecules is related to that of the organic matter. It was pointed out that, due to the partly hydrophobic structure of the humic material, adsorption of other hydrophobic organic compounds (HOCs) to the soil matrix was increased (9). Humic acids are generally more hydrophobic than the fulvic acids, thus the speciation of hydrophobic pollutants may be related to that of humic acid fraction. Adsorption of the humic acids will thus immobilize

the hydrophobic pollutants and the adsorbed humic matter also plays an important role in contaminant binding to mineral particles (9).

# 2    Outline of this thesis

The aim of the present study was to investigate the effects of the interactions between two important soil components, mineral oxides and humic substances, on the sorption of HOCs under laboratory conditions selected to model the soil systems. An understanding of sorption mechanisms, therefore, is an important key to describe the fate of HOC in the environment because sorption reactions directly affect the mobility, chemical reactivity, bioavailability, and toxicity of hydrophobic compounds. The model system used in this study consisted of aluminum oxide and an extracted soil humic acid. 2,4-Dichlorophenol (2,4-DCP) was taken as a hydrophobic organic compound contaminant model because of its wide distribution due to anthropogenic inputs from industrial wastes.

To achieve this aim throughout this work the following major topics were studied:

- The HA was fractionated by the ultrafiltration technique (UF) to reduce the HA's chemical heterogeneity. The size-fractioned humic acids obtained from the UF fractionation were characterized by different spectroscopic methods ($^{13}$C-NMR, UV-VIS and FT-IR spectroscopy) to give more identification of differences in chemical structures and the functional groups of these macromolecules. The sorption of the Hexafluorobenzene (HFB) probe molecule was observed via solid-state $^{19}$F-NMR to obtain data about the local chemical environments of HA sorption domains. The sorption data were correlated with the other characterization data for each fraction to determine what chemical moieties in HA are responsible for the observed sorption domains.
- The adsorption of humic acid and its fractions onto the alumina particles was studied (Fig. 2.1, reaction 2). The effects of solution conditions (pH and salt concentration) on the adsorption were discussed. To better understand the binding mechanisms these results were also compared to those of polyacrylic acid (PAA).

- The HA was immobilized by adsorbing it on alumina to form a HA/Al$_2$O$_3$ complex. The sorption of 2,4-DCP onto the HA/Al$_2$O$_3$ complexes at different pH and salt concentrations was investigated (Fig. 2.1, reaction 4).
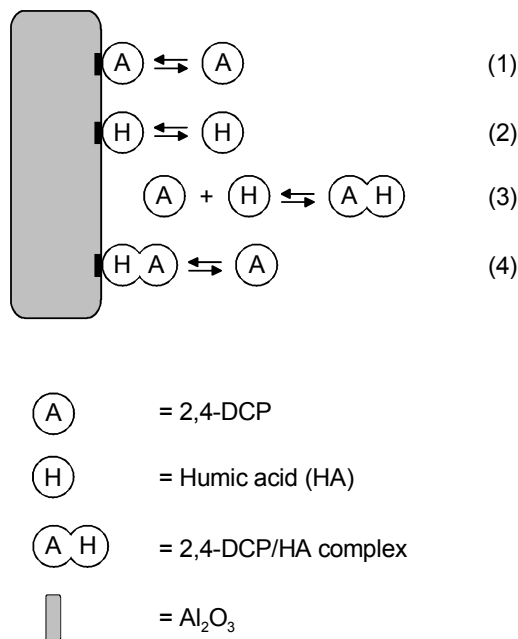


**Fig. 2.1.** *Mechanisms of interaction between Al$_2$O$_3$, humic acid and 2,4-DCP [after Ref. (11)].*

# 3    Theoretical background

## 3.1    Humic substances in the environment

The terminology of humic chemistry has a long history dating from the early work of Achard (1786) who extracted peat with alkali to yield a dark precipitate that we would now call "humic substances". Humic substances (HSs) are found in all soils and waters that contain organic matter (OM) (12). HSs are the result of biological and chemical processes, and the amounts generated in soil are several times greater than those in waters. Labile plant materials decompose rapidly on entering aerobic soil environments with adequate water supplies, but more resistant components transform slowly in the same environment. Because of the compositional diversities and the differences in the transformation modes of the components, it is impossible to define the gross mixtures that compose soil organic matter (SOM), or the dissolved organic matter (DOM), or the particulate organic matter (POM) of waters.
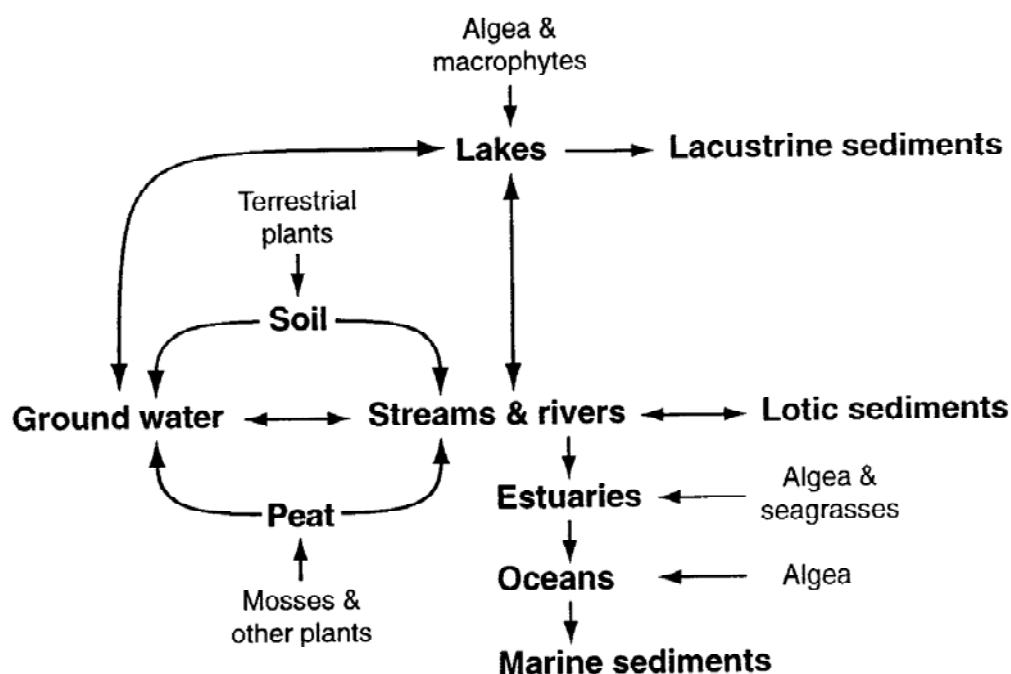


***Fig. 3.1.*** *Diagram of the many possible environmental flowpaths of humic substances (12).*

The diagram in Figure 3.1 shows the different flowpaths of the dissolved humic substances in the natural environment. Figure 3.1 further indicates that all humic substances are interconnected through the medium of water, and that it is primarily by means of water that these substances are transported in the environment. Soil and peat humic substances found in the different terrestrial systems may leach into the groundwater and can be transported until they settle in one of the sediments. The composition of the different ecosystems is controlled by a net balance of formation, degradation, and transfer of the humics (4, 13, 14). The contribution of the latter to this balance is relatively small although it can not be neglected (15, 16).

The classical definitions of HSs are operational and based on aqueous solubility. Aiken et al. (12) state that humic substances are "*a general category of naturally occurring heterogeneous organic substances that can generally be characterized as being yellow to black in color, of high molecular weight, and refractory*". Hays and Swift (17), considered humic substances to be the amorphous, macromolecular, brown-colored components of soil organic matter which bear no morphological resemblances to the plant or animal tissues from which they were derived, and which can be differentiated into broad general classes on the basis of solubility differences in aqueous acids and bases.

Soil humic substances play many different vital roles in the soil. Humic substances form stable bridges between cations and mineral grains resulting in the crumb structure found in fertile soils (4, 18). It is the crumb structure which allows water and air to permeate the top layer of soil enhancing the potential for the growth of significant vegetation. Humic substances also have a large capacity for the retention of water and can release stored water to plants during brief drought conditions (19). Ionized carboxylic groups in the soil humus electrostatically adsorb many micronutrients and function as buffers for those ions, storing and releasing them to plant systems through basic equilibrium processes. In addition to acting as ion buffers, carboxylic groups, and to a lesser extent, phenolic and amino acid groups, act as

hydronium ion buffers resulting in stable pH ranges conducive for plant and microbial growth.

Many authors list properties of HSs that are important for soil conservation and for crop growth (4, 17, 18). Even though the SOM composition of mineral soils is usually in the range of 1-5%, it would not be possible to achieve the agricultural productivity that is needed to sustain the world population in its absence. Humus can be more than 90% of the SOM. SOM is vital to the formation and stabilization of soil aggregates, and Swift (19) has outlined how polysaccharides and HSs have different roles in the formation and in the stabilization, respectively, of the aggregates.

HSs are important as cation exchangers, in the release of plant nutrients (especially N, P, and S) when mineralized, and in the binding of anthropogenic organic chemicals. The biological activity of most aromatic anthropogenic organic chemicals is decreased or lost on contact which HSs, and HSs in waters are not hazardous to health. Some research indicates that HSs have healing effect (20). However, dissolved HSs are chlorinated during water treatment, and the products can have deleterious health effects (21, 22).

## 3.2    Extraction and separation of soil humic substances

Humic materials are traditionally divided into three operationally defined fractions based on their solubility in aqueous solutions at different pH values (12, 13, 17, 23-24). Humic and fulvic acids are traditionally extracted from soils and sediment samples as the sodium salts by using sodium hydroxide solution. The material that remains contains the insoluble humin fraction (Figure 3.2). Fulvic acid is defined as the *"fraction of humic substances that is soluble under all pH conditions"*, humic acid is *"the fraction of HSs that is not soluble in water under acid conditions but becomes soluble at greater pH"*, and humin is defined as *"that fraction of HSs that is not soluble in water at any pH value"*.

HUMUS

*extract with alkali*

(soluble)

*treat with acid*

(insoluble)          (precipitated)          (not precipitated)
**Humin**            **Humic Acid**           **Fulvic Acid**

←————— increase in intensity of colour ————
←————— increase in degree of polymerization ———
←————— increase in molecular weight ————
←————— increase in carbon content ————
←————— decrease in acidity, oxygen
        content and degree of solubility ————
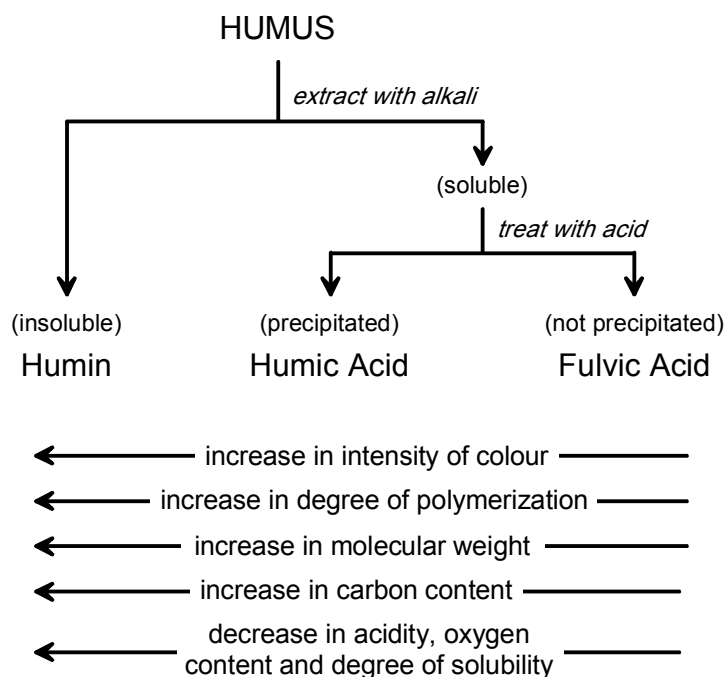
**Fig. 3.2.**      *Scheme for the fractionation of soil organic matter (humus) [after Ref. (4)] and the general properties of these fractions [after Ref. (25)] .*

Fulvic acid has the highest carboxylic content of the three humic fractions resulting in its high water solubility. It also has the lowest average molecular weight with typical weights ranging between 300 to 1200 daltons (14, 26). The relative ratio of fulvic acid to humic acid as found in soils ranges between 0.4 to 3.3 (4)

Humic acid has lower carboxylic content as well as much higher molecular weights than fulvic acid which makes it largely insoluble in acidic solutions. It is only under basic to neutral conditions fully water soluble, when a large number of the acidic groups are ionized. Reported molecular weights for humic acid vary widely based on the technique used for separation and have a reported range from 1,000 to 200,000 Daltons (14).

Humin typically represents more than 50% of the total organic carbon of soils (14, 27, 28). However, it is the least studied of the fractions (29, 30), primarily due to the difficulty in separating it from the inorganic matrix and its insolubility

in aqueous solutions. The elemental and functional group composition of humin has been shown to be similar to that found in humic acid (14).

## 3.3    The structural concepts of humic acid

An extremely wide variety of different diagenetic processes and biologically derived starting materials are responsible for the formation of humic materials (31-33). The varied combinations of starting materials and reaction mechanisms involved in the humification process produces a very large number of different molecular species. These molecules are different both in functional group distribution and molecular size. Humic acid (HA) is the alkaline soluble, acid insoluble fraction of humic materials and is itself a complex mixture. Observations show that the specific range of functional groups and properties displayed by HA is strongly influenced by it's genesis and degree of humification (34). Generally, the properties of HA are the result of the interactions of a great variety of aliphatic, aromatic, carbohydrate, and amino substructures irregularly connected together and substituted by a broad spectrum of functional groups. These molecules form three-dimensional networks having considerable aromatic and aliphatic functionality which have been shown to contain inter- and intramolecular hydrophobic domains of various size (35, 36). These hydrophobic domains are an important consideration for hydrophobic organic compound (HOC) transport because they have been shown to allow HOC inclusion (36).

Unfortunately an unified structure of humic acid (macro)molecules does not exist. Therefore the structure and the geometry of the molecules always has to be approximated. To study the adsorption of these natural polyelectrolytes and the conformation of the adsorbed molecules and that of the molecules in solution a model would be appropriate. Several models have been proposed to describe the humics (13). The most frequently cited structures are those described by Ghosh and Schnitzer (37) and Cameron et al. (38). Computational analytical chemistry has been used to calculate a three dimensional structure of humic substances (39). These calculations resulted

in a more or less spherical structure with a significant amount of space within the boundary of the humic acid entities.

Schulten and Schnitzer (36) developed a schematic structure for humic acid based on $^{13}$C-NMR, analytical pyrolysis, and oxidative degradation data. The structure (Fig. 3.3) consists of aromatic rings linked by long-chain alkyl structures so as to form a flexible network containing voids that trap and bind other organic components. Both COOH and OH groups are present in abundance, and they occupy positions on both the aromatic ring and aliphatic side chains.
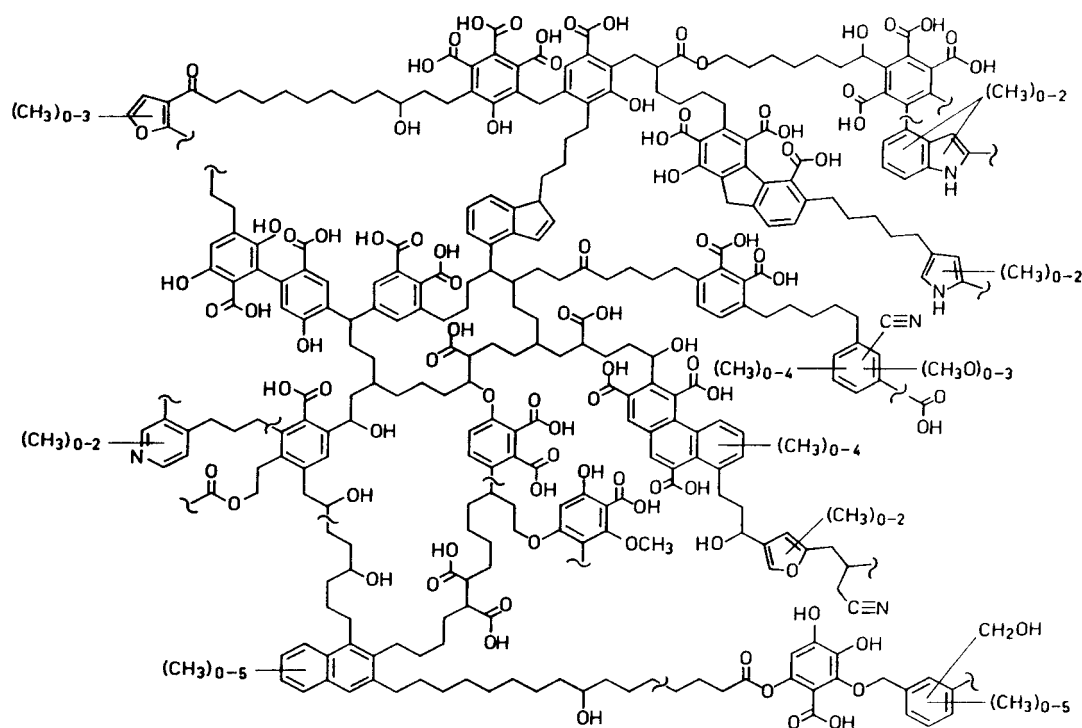


**Fig. 3.3.**     *Chemical network structure of humic acid. Adopted from Schulten and Schnitzer (36).*

## 3.4    Polyelectrolyte properties of humic acids

Based on the structural features of humic substances, humic acids molecules are often described as fairly flexible polyelectrolytes (37, 38, 40-42). Chen and Schnitzer (40) mentioned that humic and fulvic acids behave like flexible,

linear, synthetic polyelectrolytes, and concluded that the humics are not exclusively composed of condensed ring, but that there must be numerous linkages about which relatively free rotation occurs. Ghosh and Schnitzer (37) showed that humic acids can be described as flexible linear colloids under the conditions that normally prevail in natural soils. Cameron et al. (38) visualized the humic acid molecules in solution as a series of charged, occasionally branched strands. They concluded that the strands coil and wind randomly with respect to both space and time so that the mean distribution of molecular mass is spherical and Gaussian about the center. Branching results in an increased coil density within the molecule giving rise to more compact spheres compared with a linear molecule of equivalent weight. They described the humic acid molecules as a structure that is perfused with solvent molecules which are able to exchange with bulk solvent molecules.

## 3.5   Fractionation of humic acid

The molecular size of HAs are reported to range from several hundred to several hundred thousand Daltons (Da). In addition, the observed chemical structures show no clear repetitive pattern (43-45). Extremely wide ranges of characteristics are common among complicated mixtures, such as HAs. Few studies are available on the chemical heterogeneity of HAs in relation to molecular size distribution (46-52). The results of the studies published to date are somewhat contradictory. However, they do seem to suggest that chemical composition varies with molecular size and that differences in the chemical composition between size fractions may have significant consequences on the environmental chemistry and geochemistry of humic substances. In general, the low molecular weight humic fractions are expected to be more hydrophilic and mobile in soils and groundwater than the high molecular weight, hydrophobic fractions (53).

In the case of soil HA, the most valid argument for their fractionation is the fact that many interactions and processes of HA in the environment can be more or less dependent on their molecular size, for instance their binding capability towards pollutants (54) and their sorption behaviour onto mineral

surfaces (55). Among the fractionation methods available, ultrafiltration (UF) using different suitable membrane filters is a reasonably simple method to differentiate polydisperse mixtures of molecules (44, 45). Therefore, molecular size fractionation and classification of HA by UF (56), performed under reproducible and reliable conditions (57), enables such processes to be differentiated as a function of their molecular size.

Ultrafiltration is one of the few separation methods functioning without additional separation media and auxiliary reagents, thus avoiding blank substances as interferents. The simple and reliable scale-up of UF from the micro to the macro dimension in commercial UF units, which allows the rapid fractionation of relatively large quantities of humic acid, is another relevant advantage of this separation method (45).

## 3.6    Adsorption isotherms

The mineral and organic surfaces of soils (referred here as the adsorbent) may adsorb solute molecules (the adsorptive) weakly or strongly depending on the strength of the adsorbate-adsorbent interaction. Strong interaction is indicative of chemical adsorption, or chemisorption, in which a covalent or short-range electrostatic bond forms between the molecule and the surface. Weak adsorption, on the other hand, is characteristic of physical adsorption, in which the bonding interaction is not very energetic.

Adsorption data are most commonly represented by an adsorption isotherm, which is a plot of the quantity of adsorptive retained by a solid (the adsorbate) as a function of the concentration of that adsorbate in the bathing solution phase that is at equilibrium with the solid. The shape of this isotherm line suggests information about the adsorbate-adsorbent (organic-surface) interaction; to this end, isotherms have been classified into four types, diagrammed in Figure 3.4:

(1) The S-type isotherm suggests "cooperative adsorption", which operates if adsorbate-adsorbate interaction is stronger than the adsorbate-adsorbent interaction. This condition favors the "clustering" of adsorbate molecules at the surface because they bond more strongly with one another than with the surface.

(2) The L-type (Langmuir) isotherm reflects a relatively high affinity between the adsorbate and adsorbent, and is usually indicative of chemisorption.

(3) The H-type isotherm, indicative of very strong adsorbate-adsorbent interaction (i.e., chemisorption), is really an extreme case of the L-type. This isotherm is not often encountered with organic molecules because few of them form strong ionic or covalent bonds with soil colloids but it is typical for the polyacrylic acid (PAA) adsorption on the oxide minerals.

(4) The C-type (constant-partitioning) isotherm, which suggests a constant relative affinity of the adsorbate molecules for the adsorbent, is usually observed only at the low range of adsorption. Deviation from the linear isotherm is likely at high adsorption levels. Nevertheless, because many nonlinear organic compounds of interest in soils are adsorbed at quite low concentrations, the linear C-type isotherm is often a reasonable description of adsorption behavior.
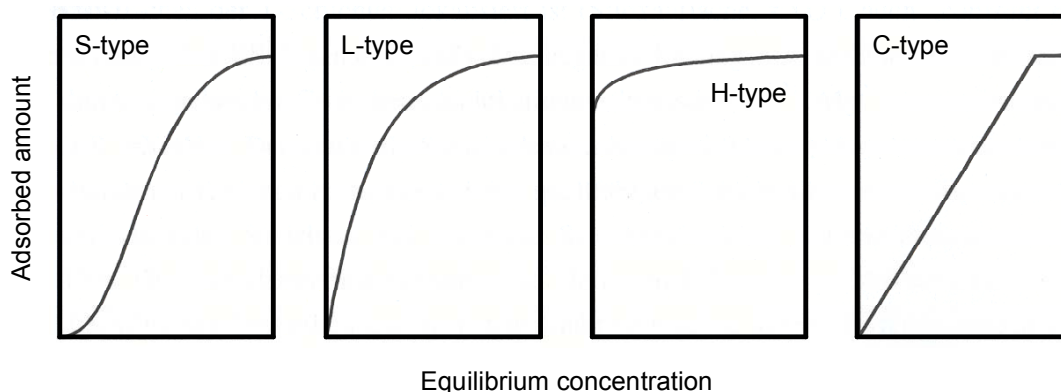


**Fig. 3.4.** *Classification of adsorption isotherms. [After Refs. (58, 59)].*

## 3.7    Binding mechanisms of the natural and synthetic amphiphilic macromolecules with the soil mineral particles

The geochemistry, and ultimately the fate, of particles and particle-reactive compounds is strongly dependent on chemical reactions that occur at the solid-liquid interface of particles. These reactions can greatly affect the mobility, bioavailability, reactivity and toxicity of pollutants. Organic surface coatings modify particle-pollutant interactions which occur at the solid-liquid interface or on particle surfaces.

Summers and Roberts (42) studied the effect of preferential adsorption of polydisperse humic acid samples on the measured adsorption isotherms and reported that previously developed concepts for well defined synthetic polymers (60-63) were also applicable to macromolecules of natural origin whose chemical composition was less well defined.

Throughout this study the properties of simple polyelectrolytes will be compared with the properties of humic substances. It has to emphasized that the humics are not described as simple polyelectrolytes, only the properties of both components are shown to be similar. Naturally the degree of branching affects these similarities, but this was shown to be a second order effect.

### 3.7.1  Adsorption of polyelectrolytes

Adsorption of polyelectrolytes must imply changes in their shapes. The usual description of conformations at an adsorbing interface, first proposed by Jenkel and Rumbach (64) and depicted schematically in Fig. 3.5, is in terms of three types of subchains: *trains*, which have all their segments in contact with the substrate, *loops*, which have no contacts with the surface and connect two trains, and *tails* which are non-adsorbed chain ends.
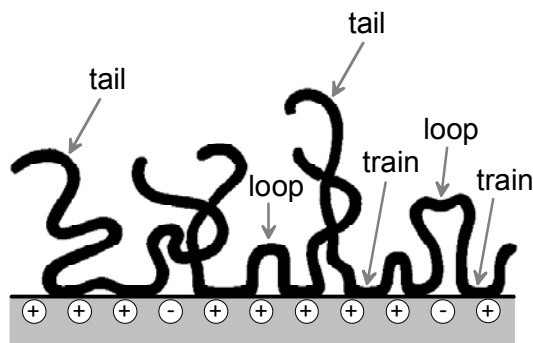
**Fig. 3.5.**     *Schematic representation of an adsorbed polyelectrolyte layer. Loops, tails and trains are indicated (after Ref. 65).*

In polyelectrolyte adsorption electrostatic interactions play a very important role. Since this interaction is of variable range and strength, depending on charge densities (for both the surface and the polyelectrolyte chain) and salt concentration, the adsorbed amount depends strongly on these two variables. At low salt concentrations, one usually finds that highly charged polyelectrolytes adsorb in small amounts, or hardly at all (66). When salt concentration is increased, the adsorption increases in the majority of cases. A schematic representation of the adsorbed layer for various situations is given in Fig. 3.6 (a – c).  The polyelectrolyte is assumed to be negatively charged, and the adsorbent surface charge density  is  constant.  The  two left-hand side cartoons [Fig. 3.6, (a) and (b)] refer to low ionic strength solutions where the adsorption is dominated by the electrostatics. At acidic pH region (low polymer dissociation degree), the increase in the PAA adsorption is quite common which is attributed to the coiled conformation at this pH (coiled because it is slightly ionized, and exhibits no intrapolymer-chain electrostatic repulsion) [Fig. 3.6 (a)]. At basic pH range, the polyelectrolyte adsorbed amount becomes low due to the ionization of PAA which generates negative charges in the polymer chain and reduces the extent of coiling, with the result that less of the polymer is needed for complete surface coverage [Fig. 3.6 (b)]. Diagrams (c) correspond to the high ionic strength, the adsorbed amounts and the conformations of the polymers are the same because the charges associated with the polyelectrolytes are screened by the salt ions and

consequently the polyelectrolyte molecules show a tightly coiled and compact conformation in solution.
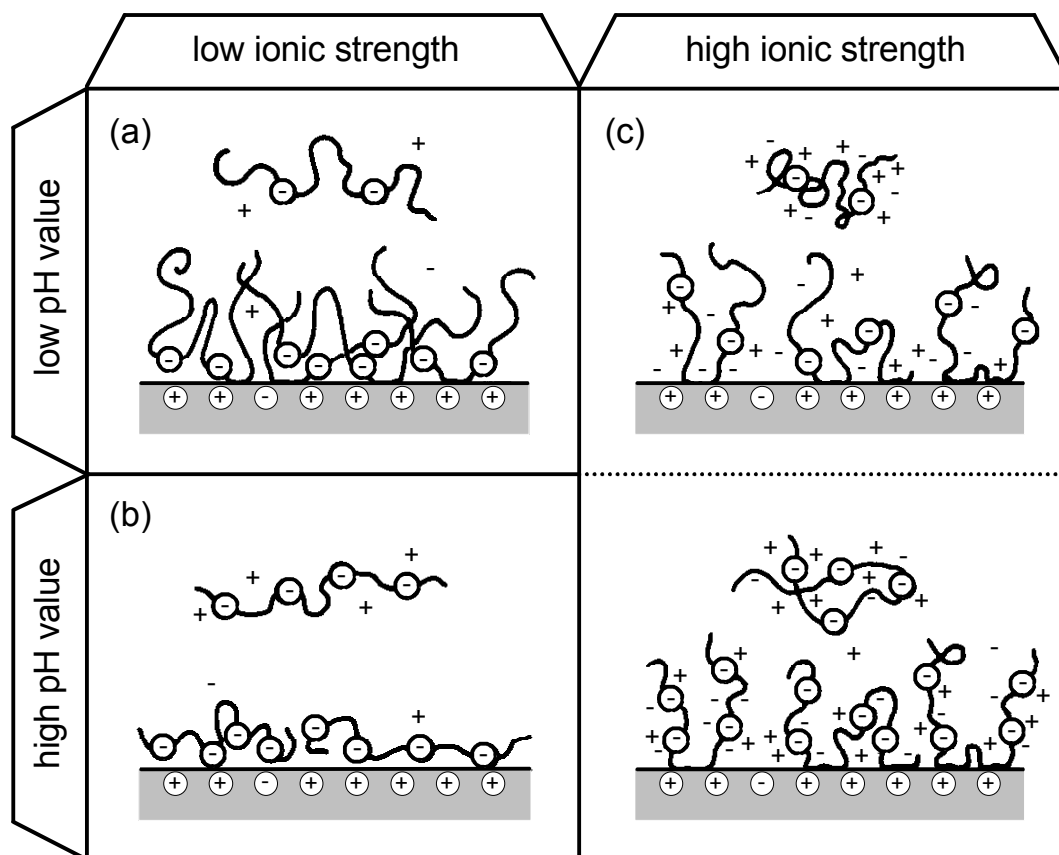


**Fig. 3.6.**     *Schematic representation of polyelectrolytes at surface under various conditions for the polymer charge density and the ionic strength (after Ref. 65).*

### 3.7.2  Adsorption of humic acid

Several authors studied the adsorption of humic substances onto mineral particles. Adsorption isotherms of humic acid on alumina (54, 67, 68), iron oxides (69-72) and manganese (73) were reported as well as the adsorption onto clays (10, 74-76). It is commonly observed that the adsorption increases with decreasing pH and in most studies the adsorption was found to increase with increasing salt concentration. The effect of these interactions on the speciation of the different components and complexes depends strongly on

the conditions and more specifically on the conformation of the adsorbed humic acid (77).

According to Sposito different interaction mechanisms for the adsorption of humic substances to mineral particles have to be considered (78), the major ones are: *ion exchange or physical adsorption* (purely coulombic interactions), *ligand exchange or surface complexation* (specific segment surface interactions), *divalent cation bridging* and *hydrophobic interactions*. It is generally accepted that all of these interactions may be important rather than only one of them. The importance of the different mechanisms for a given system depends on the mineral particles under investigation and the solution conditions during the experiments (67, 42, 79).

For the adsorption of humic acids on positively charged minerals, in general, an increase in adsorption is observed with decreasing pH and increasing salt concentration (67, 72, 79, 80). This behaviour is explained in various ways. According to Summers and Roberts (42), *physical adsorption* occurs next to specific binding and the differences in the adsorbed amount are mainly due to the charge difference between the mineral particles and the organic matter, and shielding of the lateral interactions by the indifferent electrolyte.

Of the principal adsorption mechanisms, the most important is considered to be ligand exchange. Ligand exchange refers specifically to direct bond formation between a carboxylate group and either Al(III) or Fe (III) in minerals possessing inorganic hydroxyl groups (42, 67, 71, 78-81). With increasing pH the adsorbed humic molecules may become more negatively charged which leads to a repulsion of the negative groups of the adsorbed humic that are not involved in ligand exchange, decreasing the overall affinity for the surface. The net energy for bond formation via ligand exchange will also decrease due to the change of the surface potential with increasing pH.

The chemical bonds formed in the inner-sphere complexes are stronger than the electrostatic bonds involved in anion exchange or in the two bridging mechanisms. Evidence for ligand exchange in carboxylate adsorption

reactions of humic substances with mineral surfaces is abundant though indirect (53, 72); adsorption is thought to be analogous to inorganic oxyanion ligand-exchange reactions.

Adsorption of humic substances by a ligand-exchange mechanism is thought to proceed by the following sequence (78, 81, 82):

$$>SOH + H^+ \quad \rightleftharpoons \quad >SOH_2^+ \qquad (3.1)$$

$$>SOH_2^+ + Hu\text{-}C(O)O^- \quad \rightleftharpoons \quad >SOH_2^{+\ -}O(O)C\text{-}Hu \qquad (3.2)$$

$$>SOH_2^{+\ -}O(O)C\text{-}Hu \quad \rightleftharpoons \quad >SO(O)C\text{-}Hu + H_2O \qquad (3.3)$$
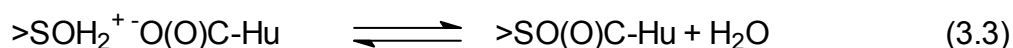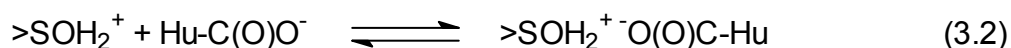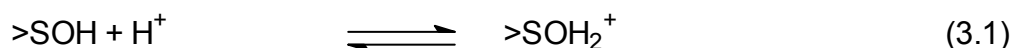
Where $>SOH$ represents a surface hydroxyl group on the mineral (S is the metal cation Al(III) or Fe(III)) and $Hu\text{-}COO^-$ represents the humic carboxyl group. The protonation step in equation (3.1) makes the surface hydroxyl group more exchangeable, but may not be necessary if the concentration of humic carboxyl groups is sufficiently high (78). Humic carboxyl groups may then form outer-sphere complexes with the protonated surface hydroxyl groups (equation (3.2)), and ligand exchange occurs in equation (3.3) in which $Hu\text{-}COO^-$ replaces $OH_2$ and forms an inner-sphere complex with the metal cation.

*Divalent cation binding* also affects the adsorption of humic acid onto mineral particles (69, 72, 83). In the presence of divalent ions, like $Ca^{2+}$ and $Mg^{2+}$, Tipping (72) reported slightly higher values for the adsorption. It was shown that the extra capacity was associated with coadsorption of $Ca^{2+}$ and/or $Mg^{2+}$ ions. Tipping postulated that the cations compete with the oxide for the anionic groups on the humic acid molecules, causing fewer contacts per humic acid molecule and consequently an increased adsorption. Due to the formation of metal ion-humic acid complexes also the lateral electrostatic repulsion is decreased and this also may contribute to the increased adsorption. Tipping mentioned that a non Langmuir behaviour was observed in the case where $Ca^{2+}$ and $Mg^{2+}$ were present, which was ascribed to the

screening by the divalent ions. Engebertson and Wandruszka (83) showed that humic acid undergoes a number of organizational rearrangements when subjected to metal ions in solution. According to these authors the formation of intermolecular humic acid/metal ion pseudomicelles precedes intermolecular interactions. Aggregates of humic acid molecules in the presence of metal ions should be regarded as more compact and more micelle-like in nature than analogous hydrophobic moieties that exist in dissolved humic acid when no metal ions are present. Due to such a compact structure the increased adsorption was explained.

A final aspect concerning the characteristics of the adsorption isotherms are *hydrophobic interactions*. Humic substances are of amphiphilic nature, they contain both hydrophobic and hydrophilic moieties. Due to these interactions the shape and the absolute adsorbed amount of the adsorption isotherms may be influenced. For instance Amal et al. (84), suggested for the adsorption of fulvic acid to hematite particles first coverage in a monolayer due to electrostatic interaction, followed by further adsorption or "hemimicelle" formation through hydrophobic effects between the first and successive layers. This type of adsorption was reflected by the fact that the adsorption isotherms described by Amal, first show a pseudo plateau, followed by a second step.

## 3.8    Sorption    mechanisms    of    hydrophobic    organic compounds

Humic materials appear to be the most important soil component for the binding of pollutants in soil (85). The interactions of HAs are particularly important because of their many interactions with both organic and inorganic contaminants. Associations between HA and the hydrophobic organic compounds (HOCs) are especially important since they impart, and often control HOC solubilization, transport, and retention in the environment (11, 86). A detailed understanding of the nature of HOC interactions with HA should significantly aid the prediction of their movement in the environment. This understanding is important for accurately modeling contaminant fate and

establishing realistic environmental management and remediation strategies. Numerous studies have been performed with humic materials and contaminants in an effort to develop such understanding (87-90). Almost all of these studies have utilized macroscopic experiments. One subset of these experiments has focused on the development of sorption models to form a conceptual picture of SOM-HOC interactions.

Currently discussed sorption models can be differentiated by the proposed sorption mechanism. Two mechanisms, "partition" and "sorption", have been frequently suggested to describe HA-HOC association (85-87). The "partition" model employs the gel polymer concept of HA in which the material is viewed as a loose three-dimensional tangle of macromolecules that offers an organo-lipophilic phase, analogous to organic liquids, for the movement of HOCs from the lipophobic environment of water (86, 87, 91, 92). In the "sorption" model, HA may be viewed as a mixture of macromolecules possessing specific three dimensional hydrophobic domains where HOCs, thermodynamically excluded from the aqueous phase due to their hydrophobicity, may preferentially "bind" (71, 93).

Schlautman and Morgan (94) noted that the binding of HOCs by dissolved humic materials depended on the hydrophobicity as well as the size of the solute molecules which are both important properties in determining their ability to fit into proposed hydrophobic cavities in humic materials. This reasoning alludes to a host/guest phenomena as being a likely mechanism for the association of polycyclic aromatic compounds with humic substances. Conceptually, sorption occurring by the "partition" mechanism can be compared to the sorption of HOCs to rubbery polymers (93) and sorption occurring by the "sorption" mechanism can be compared to sorption of HOCs to glassy polymers (95). Despite the large number of studies supporting "partition" model sorption through linear sorption of HOCs to HA (90, 96, 97), many recent studies give evidence for partition character by reporting nonlinear sorption isotherms (89, 98-104), solute-solute competition (88, 95, 98), and desorption hysteresis (105-109). These observations cannot be

adequately explained by a purely partitioning model and have been explained by attributing "dual-mode" sorption properties to SOM (110-115).

Polymers have been shown to possess both rubbery and glassy states and have been described as dual-mode sorbents (116, 117). The glassy state is characterized by a more condensed three-dimensional structure where the polymer segments have measurably higher cohesive forces than in the rubbery state (118-121). Sorption of gases and organic molecules to the rubbery state occurs by dissolution, while sorption to the glassy state occurs by concurrent dissolution and hole-filling mechanisms. The holes are postulated to be local regions of physical voids having molecular-sized dimensions where a limited number of sorbate molecules may undergo an adsorption-like interaction with an internal surface.

A number of investigators have drawn analogies between HA and synthetic organic polymers. Humic substances have been described as having expanded and condensed regions (111, 113, 114), which may be analogous to rubbery and glassy states found in polymers. This theoretical treatment of polymers states that sorption into rubbery ("soft") domains is fast and displays linear isotherms while that into glassy ("hard") domains is slow and displays nonlinear isotherms (102, 110, 112, 115). There has been significant discussion regarding, among other experimental data, linear and nonlinear sorption isotherms of contaminants to soil systems. These discussions have produced a number of studies that have resulted in the proposition of several different conceptual models for soil humic matter that can broadly be encompassed under the term "dual-mode" sorption.

"Dual-mode" sorption models make specific claims about the presence of microscopic HA domains (88, 89, 95, 98, 99, 101-105, 108, 109, 111-115, 122). The existence of these domains cannot be proven through macroscopic sorption experiments. Among these claims there is question over the actual existence of different organic matter phases (104, 123) or distinctly different local chemical moieties that are cited as being responsible for nonlinearity in sorption isotherms, competitive sorption, desorption hysteresis, and other

results that seems to contradict "partition" uptake. A recent review of the chemical interactions of hydrophobic organic contaminants with soil organic matter recognized the need for "direct observational data" of the location of sorption interaction (122). Such data is difficult to obtain due to the heterogeneity of SOM. In light of this heterogeneity, solid-state NMR may be the best technique for these observations because of its ability to describe the local chemical environment of NMR-active nuclei. Incorporating such a nuclei in a suitable molecular probe allows the observation of different chemical domains that may be present in a sorbent such as HA. Using this technique, dual-mode sorption domains in SOM have been observed by examination of the sorption of HFB to SOM (124).

# 4.    Materials and methods

This chapter provides information about the materials and methods used in the subsequent research discussion. All chemicals, unless otherwise stated, were reagent grade or better without further treatment. Water purified through Millipore filters was used in all experiments. All experiments were performed at room temperature (25°C).

## 4.1    Materials

### 4.1.1   Humic acid

One batch of soil extracted humic acid was used in all experiments, the amount of HA obtained was large enough to perform the characterization, fractionation and the adsorption studies.

#### 4.1.1.1 Extraction of humic acid

Soil material was taken from the $A_p$ horizon of the Orthic Luvisol, Merzenhausen, Germany (125). The field-moist soil was passed through a 5-mm sieve and stored at -17°C. As described in Fig. 4.1, the humic acid was isolated using standard extraction and purification procedures as recommended by the International Humic Substances Society (126). Briefly, 500 g of moist soil material was suspended in 5 L of Argon purged 0.1 M NaOH, shaken for 24 h at 25°C, and centrifuged for 15 minutes at 13 000 rpm. The supernatant solution containing fulvic and humic acids was filtered through glass wool and acidified to pH 1.0 with HCl to flocculate the humic acids. To achieve complete separation of fulvic acid, the precipitated humic acid was resuspended in 0.1 M NaOH and flocculated twice with HCl as described above. The humic acid fractions were collected and treated three times with a 0.1 M HCl-0.3 M HF solution to remove mineral impurities. The precipitated humic acid was dissolved again with the NaOH solution. The ash-free humic acid was then dialysed against slowly, flowing deionized water

using Spectra/Por 6 tubing (MWCO 1000) for one month. The humic acid obtained in this way is in its proton form, it is freeze-dried and stored in the dark at 3°C.
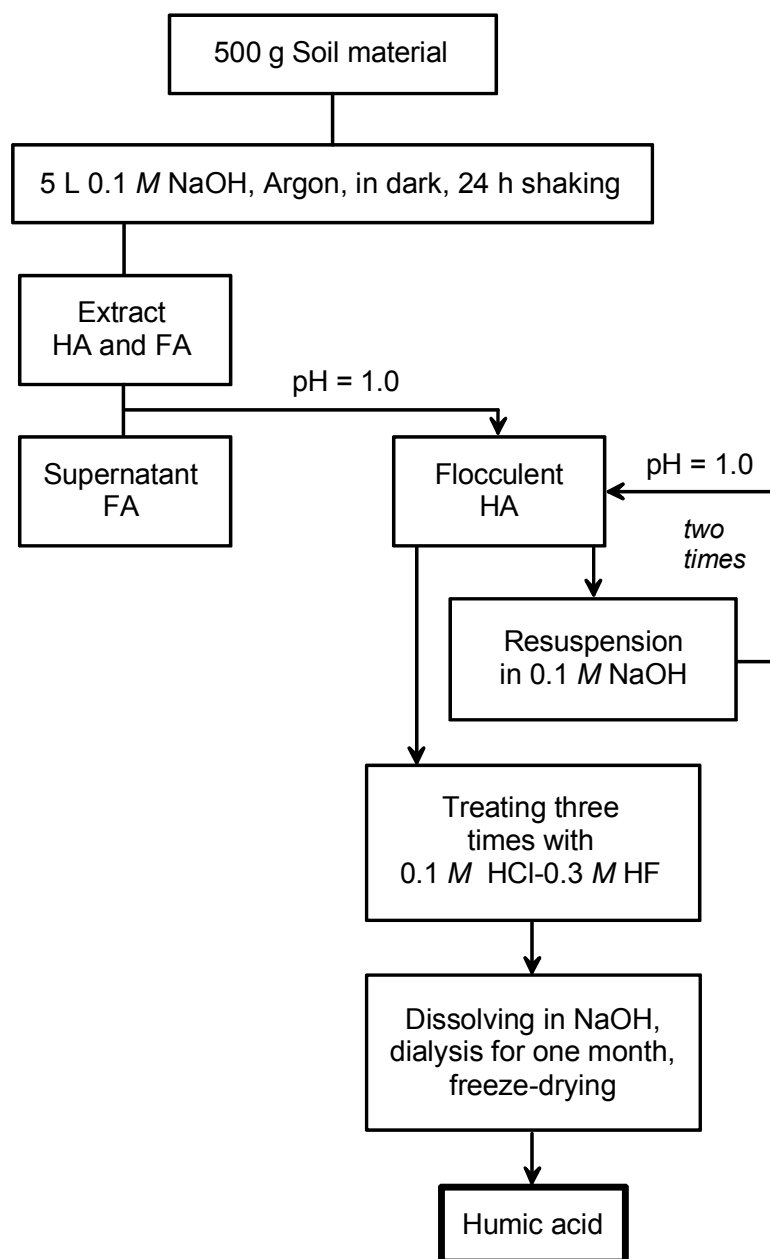


**Fig. 4.1.** *Scheme of humic acid extraction from the soil material.*

### 4.1.1.2 Fractionation of humic acid

The isolated and purified humic acid was separated (as described in Fig. 4.2) into eight molecular size fractions by using the ultrafiltration technique (UF) (127, 128). An alkaline solution of humic acid (1 g/50 ml) was microfiltrated by using a 0.2 $\mu$m Nylon filter and an Amicon ultrafiltration stirred cell (model 8050) under a pressure of 2.5 bar from an Argon tank. The stirring speed

Alkaline HA solution

Retentate
Fr0

*Filtration through 0.2 $\mu$m Nylon filter*

Filtrate

Retentate
Fr1

*Filtration through XM300 membrane*

Filtrate

Retentate
Fr2

*Filtration through YM100 membrane*

Filtrate

Retentate
Fr3

*Filtration through XM50 membrane*

Filtrate

Retentate
Fr4

*Filtration through YM30 membrane*

Filtrate

Retentate
Fr5

*Filtration through YM10 membrane*

Filtrate

Retentate
Fr6

*Filtration through YM3 membrane*

Filtrate

Retentate
Fr7

*Filtration through YC05 membrane*

Filtrate

**Fig. 4.2.**    *Graphical depiction of the HA fractionation by using the UF technique.*

was maintained at 450 rpm. The retentate was washed with small portions of Millipore water until colorless liquid passed through the microfilter. The washed retentate (Fr0) was sucked carefully out of the above membran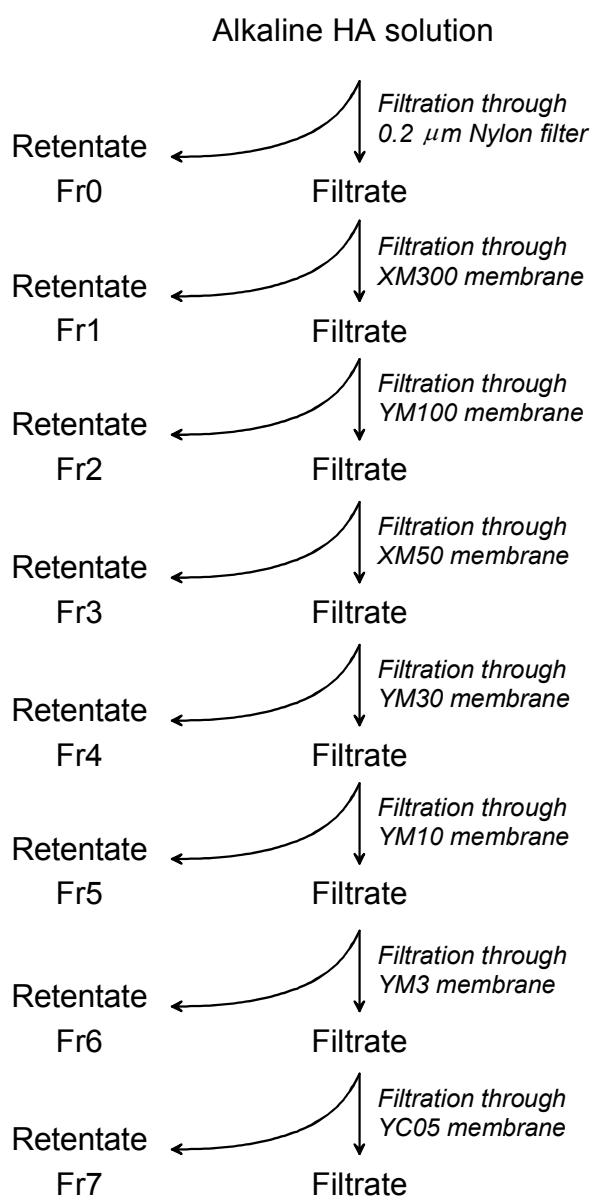e space of the ultrafiltration cell. The filtrate obtained was then fractionated by using an Amicon ultrafiltration cell (model 8400) and a series of Amicon membranes of successively smaller pore size to obtain HA fractions with different nominal molecular size which were classified as Fr1, larger than 300 000 Da; Fr2, 300 000-100 000 Da; Fr3, 100 000-50 000 Da; Fr4, 50 000-30 000 Da; Fr5, 30 000-10 000 Da; Fr6, 10 000-3 000 and Fr7, 3 000-1000 Da. All separations were performed under identical conditions. After each run, the membrane was removed, rinsed with distilled water, and stored overnight at 0-4°C. The complete separation process was repeated at least three times to assess the reproducibility of the fractionation results using the Amicon ultrafiltration technique. The separated fractions of the humic acid were freeze-dried, weighed and stored in the dark at 3°C.

### 4.1.2  Polyacrylic acid

Polyacrylic acid (PAA) was supplied as aqueous solution, and used as received. Table 4.1 summarizes some physicochemical properties of the PAA.

**Table 4.1.**    *The physicochemical properties of PAA.*
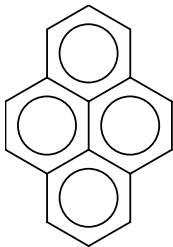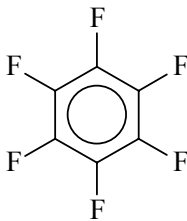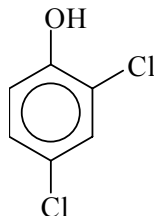
| | |
|---|---|
| Molecular weight (g/mol) | 50 000 |
| Structure | $\left[ CH_2-CH-\underset{\underset{O\quad OH}{\overset{\parallel}{C}}}{} \right]_n$ |
| Monomer molecular weight (g/mol) | 72 |
| Supplier | Polyscience |

### 4.1.3 Organic chemicals

The organic markers used in this study were pyrene and Hexafluorobenzene (HFB) and the pollutant was 2,4-dichlorophenol (2,4-DCP). Relevant physicochemical properties of these compounds are listed in Table 4.2.

***Table 4.2.*** *Physicochemical properties of the organic chemicals used.*

|  | Pyrene | HFB | 2,4-DCP |
|---|---|---|---|
| Molecular weight (g/mol) | 202.26 | 186.06 | 163.00 |
| Structure | | | |
| Solubility in water (mg/l) | 0.135[a] | 342[b] | 4400[c] |
| Log $K_{o/w}$ | 5.18[a] | 2.55[b] | 3.23[c] |
| pK value | — | — | 7.85[c] |
| Supplier | Aldrich | Aldrich | Merck |

[a] Ref (129)
[b] Ref (130)
[c] Ref (131)

### 4.1.4 Aluminum oxide

The hydrous oxide particles used in this study were $\gamma$-$Al_2O_3$ (Degussa, Aluminum oxide C). Aluminum oxide C is produced by flame hydrolysis of anhydrous aluminum chloride and Debye-Scherrer x-ray diffraction patterns reveal that it has primarily a gamma structure. The chemical purity is >99.6% and the density is 2.9 g/cm$^3$. The average primary particle size is 13 nm (132). To exclude chloride contamination, the aluminum oxide was pretreated by heating for 6 hours at 1000°C. Other additional data are listed in Table 4.3.

**Table 4.3.**     *The physicochemical properties of $Al_2O_3$.*

| | |
|---|---|
| Specific surface area (BET) ($m^2$/g) | $85\pm5$[a] |
| Average particle size in suspension (nm) | $215$[b] |
| pH value at the isoelectric point | $8.8$[a] |

[a] determined by this work,
[b] determined by dynamic light scattering at pH 5.5 and 0.01 M $KNO_3$

## 4.2   Methods

### 4.2.1   Analytical methods

#### 4.2.1.1 Polyelectrolyte titration technique

According to the polyelectrolyte titration technique, the basis of the determination of HA and PAA is the formation of a polysalt with the polycation. The polysalt reaction occurs quantitatively according to 1:1 charge saturation as shown schematically in Fig. 4.3. At the end point, the chromotropic cationic titrant reacts with an anionic dye. The corresponding color change is ascribed to a polymer-induced interaction of dye molecules with one another, which occurs when the distances between the molecules are small. A high structural charge density and thus a small distance (<1 nm) between the charge centers is a prerequisite for the chromotropic properties of a polyelectrolyte. The dye molecules may then interact to produce a metachromatic shift in the absorption bands and hence a detectable color change.

Both the polysalt formation and the indicator reaction are based on electrostatic and cooperative interaction. The equilibrium constants $K_1$ and $K_2$ differ owing to differences in the degree of cooperativity of the polymer/polymer versus the polymer/dye interaction. With a sufficiently large ratio of the two constants ($K_1/K_2 > 100$), the dye binds with excess polycations only after complete polyanion-polycation reaction. This is expressed by a sharp color change and an exact end point.
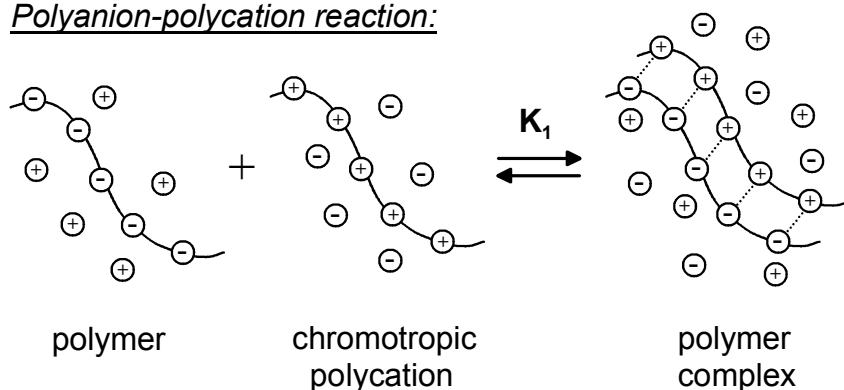
29

*Polyanion-polycation reaction:*



| polymer | chromotropic polycation | polymer complex |

*Indicator reaction:*



| chromotropic polycation | ECBT | ECBT-polymer complex |
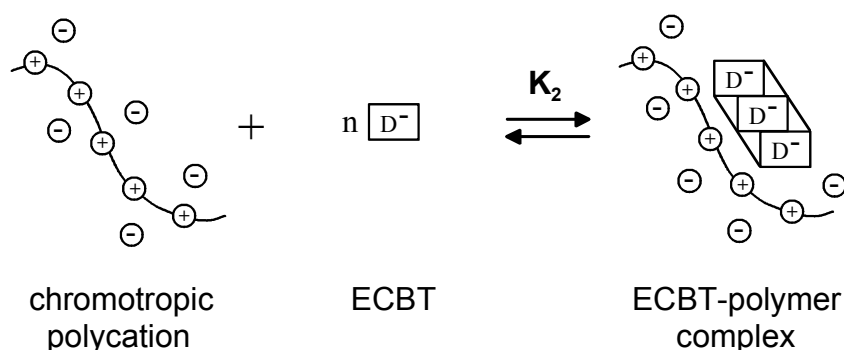
**Fig. 4.3.**      *Reaction scheme for the direct determination of anionic polyelectrolytes using chromotropic polycations and an anionic metachromatic dye for end-point detection. [after Ref. (133)]*

The HA and PAA were estimated quantitatively by direct polyelectrolyte titration using a phototitrator, Type 90, from BASF (two light-emitting diodes having emission maxima at 635 nm and 565 nm). The Dosimat, type 665 from Metrohm was used as a motorized burette.

The titrations were carried out in a Plexiglas cuvette (100 ml volume). The cuvette was filled with 50 ml argon saturated millipore water (pH = 10). Owing to the pH sensitivity of the daily fresh prepared Eriochrome black  T  (ECBT), 1 ml of $NH_3/NH_4^+$ buffer solution (0.01 mol/l, pH = 10-11) was added to the titration solution. 1 ml 0.1 mol/l EDTA was also added to complex polyvalent metal ions which may have been present, and which can interfere with the

colour reaction, even in traces. x ml of the HA or PAA and 1 ml of fresh daily prepared ECBT were added. Finally the titration solution was filled up to about 100 ml by using the argon saturated millipore water (pH = 10). After 5 min of stirring, the solution was titrated by using 30 mg/l 3,6-ionene bromide solution (Polybren, Aldrich Chemie) as a titrant. The accuracy of this method is ±5%.

### *4.2.1.2 Potentiometric acid-base titration*

The pH-dependent surface charge was determined by potentiometric acid-base titration under a $CO_2$-free atmosphere. $KNO_3$ was used as an indifferent background electrolyte to maintain a constant ionic strength ranging between 0.01 and 1.0 mol/l. The titrations are performed in a glass jacketed, 100 ml Duran vessel that is kept at a constant temperature (25°C) using a circulating water bath. The titration vessel is sealed with a polypropylene screw cap. A silicon rubber ring provides a gas-tight seal between the screw cap and the glass cell. The polypropylene screw cap is equipped with five sockets that provide access to electrodes, burettes and argon gas lines. The glass cell is cleaned very thoroughly, rinsed with high-purity water and dried before use. The burette cylinders and the tubing connecting the burettes with the cell are rinsed several times with the titrant in order to eliminate contaminants and/or trapped air bubbles. The suspension/solution was mixed by a magnetic stirrer with a clean dry Teflon-coated stirring bar. Clean freshly rinsed electrodes, dried with a lint-free tissue, are placed in the cap that is subsequently connected to the glass cell.

Before the experiment can be started the suspension/solution is outgassed extensively. Argon was used to continually purge for at least half an hour and keep the system free of $CO_2$. During this procedure the suspension/solution is stirred continuously. Measurement of a stable pH can be used as an indicator for the state of the cell. Once the cell is prepared for a titration it should remain closed, additions (titrant, reagent) have to be made through a septum in order to prevent carbon dioxide entrance.

Titrants were prepared from commercial volumetric standards (Tritrisol, Merk); 0.1 mol/l $HNO_3$ was used as acid titrant and 0.1 mol/l KOH as base. All of them prepared with millipore water, which had been boiled and allowed to cool in $CO_2$-free argon atmosphere. The exact base concentration was determined by titration with a standard benzoic acid solution.

A given amount of equilibrated suspension/solution containing 0.5 g of aluminum oxide, 0.02 g PAA or portions of electrolyte-free humic acid solution containing 0.02 g of humic acids was diluted with $KNO_3$ solution to give a volume of 50 ml. A titration cycle always started with a forward titration of an acidified solution of low ionic strength with base, followed by a backward titration with acid, and ended with the addition of solid $KNO_3$ to adjust the ionic strength to the next higher level. During each forward or backward titration and after the addition of titrant, the rate of drift was measured over a 2 minutes interval after an initial delay of 20 seconds to allow adequate mixing. The electrode readings were accepted when the drift was less than 0.2 mV/min. A maximum reading time of 20 minutes was set for two successive additions of titrant. The doses of $HNO_3$ and KOH were calculated by the interface to obtain a constant mV change of 5 mV for each addition, in order to obtain a good distribution of data points over the pH range studied. Such cycles were performed for different ionic strengths by using a developed titration system (GIMET-1, Szeged University) with 665 Dosimat (Metrohm) burettes, argon bubbling, magnetic stirrer and high performance potentiometer, yielding a whole series of forward and backward titration curves in a single experiment. The whole system (mV-measure, stirring, bubbling, amount and frequency of titrant) was fully controlled by a PC using AUTOTITR software (Szeged University). A Metrohm combination pH electrode was calibrated for three buffer solutions to check the Nernstian response. The hydrogen ion activity vs. concentration relationship was determined from reference solution titration so that the electrode output could be converted directly into hydrogen ion concentration instead of activity.

The net proton surface excess amount ($\Delta q$, mmol/g) is defined as the difference of $H^+$ ($\Gamma_{H^+}$) and $OH^-$ ($\Gamma_{OH^-}$) surface excess amounts related to unit mass of solid, $\Delta q = \Gamma_{H^+} - \Gamma_{OH^-}$. The surface excess amount defined for the adsorption (134) is determined from the initial and equilibrium concentration of the solute. The values $\Gamma_{H^+}$ and $\Gamma_{OH^-}$ were calculated at each point of titration from the electrode output using the actual activity coefficients from the slope of the straight lines of $H^+/OH^-$ activity vs. concentration functions from the corresponding background electrolyte titration. The surface excess concentration of $H^+$ or $OH^-$ was calculated as a function of pH. The amount of charged sites defined as the net proton surface excess ($\Delta q = \Gamma_{H^+} - \Gamma_{OH^-}$) was related to the unit mass of alumina, PAA or humic acid and plotted as a function of pH.

### 4.2.1.3 UV-VIS spectroscopy

### 4.2.1.3.1 Determination of $E_{465}/E_{665}$

The UV-VIS absorption spectra of the HA and its fractions were recorded over the wavelength region from 200 nm to 700 nm by means of Uvikon 920 spectrophotometer (Kontron Instruments) using 1 cm quartz cuvettes. The cuvettes are rinsed three times with the measured samples solutions before the measurement process. All samples were diluted to obtain 0.5 g/l humic acid and the humic acid fractions. The measurements were carried out in a 0.05 mol/l $NaHCO_3$ solution, which was also used as the blank. The $E_{465}/E_{665}$ ratios were calculated as the ratio of absorbance at 465 nm and 665 nm (135).

### 4.2.1.3.2 Determination of 2,4-DCP

The UV-VIS absorption spectra of the 2,4-dichlorophenol (2,4-DCP) were recorded over the wavelength region from 180 nm to 450 nm by means of a Uvikon 920 spectrophotometer (Kontron Instruments) using 0.1 cm quartz

cuvettes. The cuvettes are rinsed three times with the measured sample solutions as described in 4.2.1.3.1.  In order to eliminate light scattering effects of the remaining very small solid particles, the 2,4-DCP concentration was evaluated through the second derivative of the measured absorption spectra (derivative spectroscopy).

### 4.2.1.4 FT-IR spectroscopy

Humic substance (2 mg) was ground with 100 mg oven-dried potassium bromide (IR grade; Aldrich) and turned into a pellet. Infrared spectra were recorded on the pellet under nitrogen with a BRUKER EQUINOX-55 spectrometer equipped with a DLATGS detector. All spectra were recorded between 500 and 4000 $cm^{-1}$ over 22 scans at 4 $cm^{-1}$ resolution.

The "ab initio" calculations were performed with the DGauss suite of programs on a Cray supercomputer (SV1). The geometry was fully optimized without imposing external symmetry constraints using the BLYP/6-31G$^{*}$ basis set. Thereafter a force constant calculation was performed to obtain the vibrational frequencies and the corresponding FT-IR intensities. For comparison with the experimental results of FT-IR spectroscopy, the calculated wavenumbers were multiplied by a constant factor of 0.98.

### 4.2.1.5 NMR spectroscopy

### 4.2.1.5.1 $^{13}$C-NMR spectroscopy

Comparative solid-state $^{13}$C-NMR spectra of the dried humic materials were obtained on a Bruker DSX 200 operating at a frequency of 50.3 MHz using 7 mm OD zirconium rotors with KEL-F caps. A ramped cross polarization magic angle spinning technique (6.8 kHz spinning rate) $^{1}$H-pulse was used to circumvent spin modulation of Hartmann-Hahn conditions (136). A contact time of 1 ms and a 90° $^{1}$H-pulse width of 5.3 µs were used for all spectra (52). The $^{13}$C-chemical shifts were referenced to tetramethylsilane (= 0 ppm), using

glycine as an external standard (COOH: 176.04 ppm). Between $2 \times 10^4$ and $10 \times 10^4$ scans were accumulated using a pulse delay of 400 ms (137). Prior to Fourier transformation, a line broadening of 0 to 75 Hz was applied, depending on the sensitivity of the sample. The relative intensity of the peak areas was obtained by integration of the specific chemical shift ranges using an integration routine supplied with the instrument software. For data analysis, as shown in Fig. 4.4, the spectra were divided into chemical shift regions assigned to the chemical group classes alkyl C (0-45 ppm.), O-alkyl C (45-110 ppm.), aromatic C (110-160 ppm.), phenolic C (140-160 ppm.), carboxyl C (160-185 ppm.), and carbonyl C (185-220 ppm.), respectively.
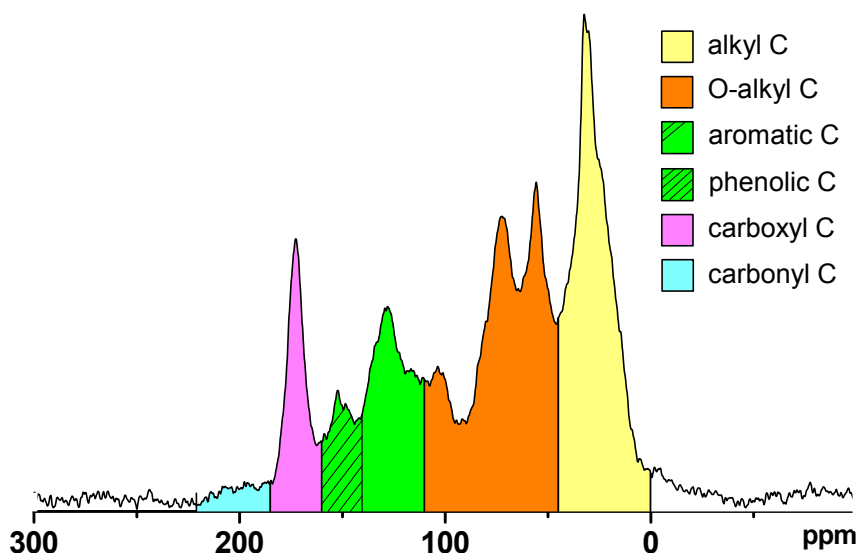


**Fig. 4.4.**     *Solid state $^{13}$C-NMR spectrum of humic acid and its different group classes.*

### 4.2.1.5.2 $^{19}$F-NMR spectroscopy

The $^{19}$F-NMR measurements were performed at the Chemistry and Biochemistry Department, South Dakota State University.

Initial ^{19}F NMR experiments were performed in the single-pulse mode to optimize the acquisition rate and 90 degree pulse angle while avoiding saturation of the nuclei due to inappropriately short recycle or delay times. Subsequent static and MAS ^{19}F NMR experiments were performed in the single-pulse mode (4.3 ms pulse, 49 kHz window, 0.334 s acquisition, 1.00 s delay between pulses) on a Bruker Avance 300 spectrometer equipped with a 4 mm solid state probe at a frequency of 282.414 MHz and externally referenced with respect to $CFCl_3$ (neat HFB taken as $-163.0$ ppm) (138). Rotor spin rates were held constant for each spectrum acquired but were varied between 4 and 15 kHz for identification of spinning sidebands. A line broadening of 50 Hz was applied to all spectra except the fine detail inserts, which have no line broadening applied.

### 4.2.1.6 Electrophoretic measurements

Measurements of the electrophoretic mobility of the bare alumina and of the PAA/alumina and HA/alumina complexes were carried out with the Laser Zee Meter, model 501 (PENKEM, USA) at pH = 5.5, 7.5 and 9.5 and 0.01 M $KNO_3$. Using the Smoluchowski approximation the zeta potential can be calculated (software Z-Trac, COLLOTEC, Germany). The electrophoretic mobility (EM) is recalculated from the mean value.

Alumina and PAA or HA were mixed and equilibrated for a given time. Dilute suspensions (100 mg/l) were prepared by diluting a small fraction of the sediment in the 0.01 M $KNO_3$ background electrolyte. The sample was ultrasonicated for 60 s in a sonicator bath before performing the measurements. In order to obtain reliable values of electrophoretic mobility, the electrophoretic cell was filled three times with the dilute suspension and six measurements were repeated. The electrokinetic results are thus mean values of 18 measurements.

### 4.2.1.7 Dynamic light scattering

Dynamic light scattering (DLS) was shown to be a valuable tool for studying the colloidal stability of alumina as a function of different PAA or HA adsorbed amounts. The measurements were performed using a ZetaSizer 4 (MALVERN) apparatus operating at $\lambda = 633$ nm produced by an He-Ne laser at a scattering angle of 90°. Particles from the alumina suspension, PAA-$Al_2O_3$ or HA-$Al_2O_3$ complexes were dispersed in 0.01 M $KNO_3$ solution at a certain pH values, the suspension was placed in the cell and measured directly.

The correlation functions were evaluated by cumulant analysis (139). The first-order autocorrelation function, $g^1(t)$, can be given as

$$\left| g^1(t) \right| = \exp(-\Gamma t + (\mu_2/2!)\, t^2 + (\mu_3/3!)\, t^3 + ...)$$

where $\Gamma$ is an average decay rate, $\Gamma$ characterizes the mean, $\mu_2$ the width and $\mu_3$ the skewness of the distribution. If $qR \ll 1$, the translational diffusion is the dominant dynamics, the diffusion coefficient can be calculated

$$\Gamma = D_t\, q^2$$

where the scattering vector, $q$, is

$$q = (4\pi n/\lambda)\, \sin(\theta/2)$$

and according to the Stokes-Einstein equation

$$D_t = kT/6\pi\eta\, R_H$$

the average diffusion coefficient, $D_t$, is related to the hydrodynamic radius, $R_H$, where k is the Boltzmann constant, T is the temperature, $\eta$ is the viscosity of the medium, n is the refraction index of the solution, $\lambda$ is the laser wavelength and $\theta$ is the scattering angle.

### 4.2.1.8 Elemental analysis

The elemental content (C, H, N, S) of the HA and its fractions were determined using a Leco CHNS-930 elemental analyzer in the Central Department of Chemical Analysis, Research Center Jülich. Elemental measurements were performed immediately after freeze-drying so that moisture interference would be minimal. The ash content was determined from mass lost after heating the humic acid at 750°C, until a constant mass was obtained.

### 4.2.2 Adsorption measurements

Stock humic acid solutions were prepared by dissolving humic acid in 0.005 M KOH aqueous solution, sonicating for 3 min, and finally shaking for 1 hour. $HNO_3$ (or KOH) was then added to adjust its pH. Weighted amounts of $KNO_3$ were added to HA solutions to adjust to the desired ionic strength (0.01, 0.1 and 1.0 M).

The alumina suspensions (15 g/l) were prepared for use as working stocks in order to obtain consistent solid concentrations in the equilibrium adsorption experiments. These suspensions were made in 0.01, 0.1 and 1.0 $M$ $KNO_3$ for the PAA or HA adsorption isotherms (or KCl for the 2,4-DCP adsorption experiments) at the desired pH value over a period of 14 days.

### 4.2.2.1 Adsorption of organic macromolecules on aluminum oxide

### 4.2.2.1.1 Adsorption of humic acid

A fraction of the well-mixed alumina suspension (at the desired pH and ionic strength value) was then pipetted into series of humic acid solution at varying concentration (2-420 mg/l) to give the final volume of 30 ml in 50-ml polyethylene centrifugation tubes. The suspensions were shaken for 24 h on a horizontal shaker (Janke & Kunkel) to reach equilibrium. The final alumina

concentration for all adsorption experiments was 7.5 g/l. Preliminary experiments verified that after 18 h no measurable change occurred in the adsorbed amount. 5 ml aliquot was removed for the subsequent electrophoretic and DLS measurements. The remaining portion of each sample was centrifuged for 30 minutes at 20 000 rpm (Sorvall company). The supernatant was transferred to separate bottles. The amount of HA adsorbed was calculated from the difference between the total added HA concentration and the HA concentration in the supernatant by direct polyelectrolyte titration (4.2.1.1). Calibration curves were made for each required pH and salt level.

### 4.2.2.1.2 Adsorption of polyacrylic acid

The adsorption experiments were performed exactly as in the case of HA adsorption experiments (as described in 4.2.2.1.1). The total added concentration of PAA generally varied from 2 to 250 mg/l. Preliminary experiments verified that during the course of an adsorption experiment at pH = 5.5 and 7.5, little variation in pH was observed. This problem was solved by performing the experiments in the presence of 4 $\mu$M acetic acid/sodium acetate buffer (to adjust the system pH at 5.5) or 2 $\mu$M Tris buffer (to adjust the system pH at 7.5).

### 4.2.2.2 Adsorption of 2,4-DCP on HA/Al$_2$O$_3$ complex

The alumina particles were coated with humic acid by adding 75 ml of a well-mixed alumina suspension (30 g/l) (at the desired pH and ionic strength value) to a 75 ml of varying amounts of dissolved HA solution (120, 240, 400 or 560 mg/l) at the same pH and ionic strength value in 250-ml polyethylene centrifuge bottles. After shaking for 24 h, the HA/Al$_2$O$_3$ complexes were centrifuged for 45 minutes at 13 000 rpm (Sorvall company). 100 ml of the supernatant solution in each bottle was aspirated into a plastic container. 100 ml of KCl solution (at the same pH and ionic strength value) was added to the complex.

The $HA/Al_2O_3$ complexes were resuspended for 24 h in the (Janke & Kunkel) horizontal shaker. This washing step was repeated seven more times to exclude the free HA from the solution. The aspirated supernatant of each washing step was stored for HA measurement (see Fig. 4.5). The stock $HA/Al_2O_3$ suspensions were stored in the dark at 3°C.
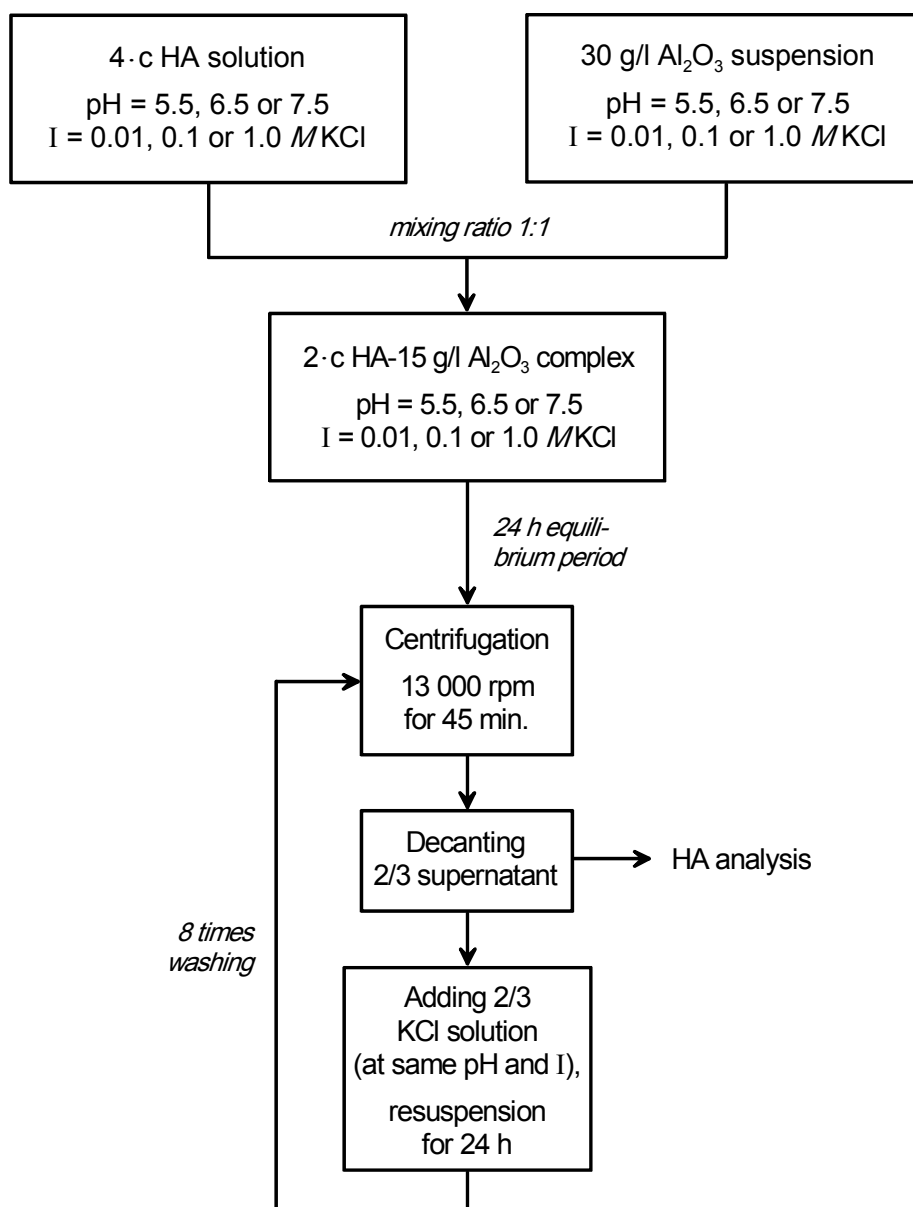


**Fig. 4.5.**     *The preparation scheme of HA/Al$_2$O$_3$ complexes.*

5 ml of the well-mixed HA-alumina complex suspension (15 g/l) (at the desired pH and ionic strength value) was then pipetted into series of 2,4-DCP portions at differently varying concentrations to give the final volume of 10 ml in 16-ml polyethylene centrifugation tubes. The 2,4-DCP stock solution used was pre-adjusted at the same pH and ionic strength concentration. The suspensions were shaken for 24 h in an overhead shaker (Heidolph company). The samples were centrifuged for 45 minutes at 20 000 rpm (Sorvall company). The 2,4-DCP adsorbed amount was calculated from the difference between the initial concentration of the 2,4-DCP and the 2,4-DCP equilibrium concentration in the supernatant by using the UV-VIS spectroscopy technique (as described in 4.2.1.3.2).

# 5      Results and discussion

## 5.1    Materials characterization

The interaction between HA and charged solid particles such as amphoteric aluminum oxide in aqueous media is essentially influenced by the pH and ionic strength and depends on the charge of both the solute molecules and the solid particles. To understand the influences of these solution parameters on the surface charges a quantitative characterization using potentiometric acid-base titration was necessary. Moreover, HA and its fractions were characterized using different spectroscopic methods (NMR, UV-VIS and FT-IR spectroscopy) to obtain more information on the chemical structures and the functional groups of these macromolecules. For comparison, investigations with polyacrylic acid (PAA) were also carried out.

### 5.1.1  Characterization of the organic macromolecules

### 5.1.1.1 Acid-base properties of polyacrylic acid

A unified structure of humic acid does not exist. Therefore, the structure and the geometry of these (macro)molecules always have to be approximated. To study the adsorption of these natural polyelectrolytes and the conformation of the adsorbed molecules a model system would be helpful.

Based on the structural features, humic acid molecules are often described as fairly flexible polyelectrolytes (37, 38, 40-42). Compared to humic substances, which contain various functional groups, polyacrylic acid (PAA) are much simpler molecules, containing only carboxylic groups and linear $-CH_2-CH_2-$ chain, but they facilitate the understanding of the adsorption of HA on alumina or the influence of HA on the colloidal stability of alumina particles. Therefore, throughout this study the influence of humic acid will be compared with those of PAA. It has to be emphasized that the humics are not described as simple

polyelectrolytes, only certain properties of both substances are shown to be similar.

The charge density of the PAA's ionizable carboxyl groups is controlled by varying the pH. The polyelectrolyte features of PAA are characterized by a locally strong electrical field that exerts a long-range influence on charged species, such as colloid surfaces. In Fig. 5.1 the pH-dependence of the specific amount of negatively charged sites on polyacrylic acid is shown for different salt concentrations (0.01, 0.1 and 1.0 mol/l $KNO_3$). It can be shown that an increase of the ionic strength from 0.01 to 1.0 mol/l facilitates the deprotonation of carboxylic groups through a salt-screening effect of the polyelectrolyte charge, which can induce conformational changes in the PAA in solutions. The role of these phenomena will be discussed in 5.3.1.The PAA molecules become more negatively charged with both increasing pH and ionic strength, and the maximum value was attained at a pH of about 9.7. Above this pH, the net proton consumption becomes constant in all $KNO_3$ solutions.
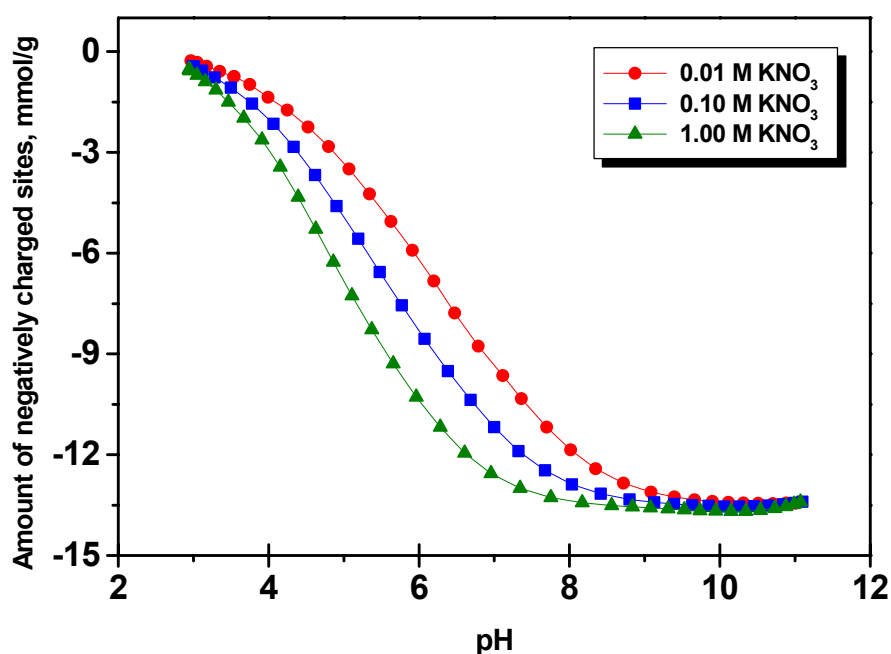


**Fig. 5.1.**     *pH and ionic strength dependence of negatively charged sites amount of PAA in the presence of $KNO_3$.*

### 5.1.1.2 Acid-base properties of humic acid

Humic acids behave like weak-acid polyelectrolytes, in addition to COOH groups, their negative charges may arise from the presence of phenolic OH and enolic OH, etc. (4). Humic acids develop negative charges and form electric double layers (EDLs) spontaneously due to the dissociation of the acidic groups. The electrostatic field inside and around the humic macroions shows considerable pH and ionic strength dependence. On the basis of potentiometric acid-base titration the net proton surface excess of the original orthic luvisol humic acid was determined over the range of pH 3.0 to 11.0 at different $KNO_3$ concentrations (0.01, 0.1 and 1.0 mol/l). The pH-dependence of the specific amount of negatively charged sites on humic acid can be seen in Fig. 5.2.
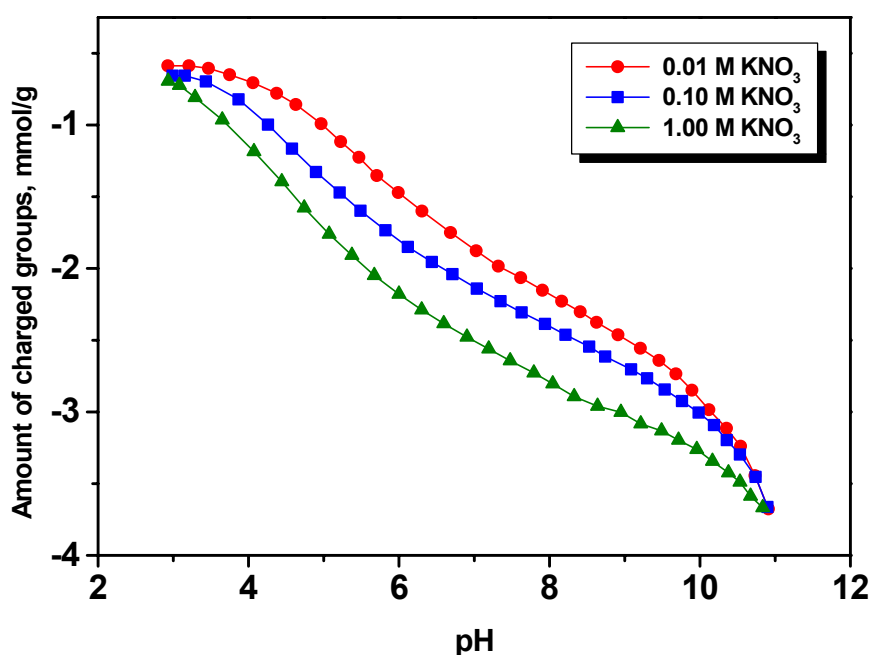


**Fig. 5.2.**    *pH and ionic strength dependence of the HA charged groups amount in the presence of $KNO_3$.*

The humic acid particles became more negatively charged with both increasing pH and ionic strength, and the maximum value was attained at a

pH of about 10.5. Above this pH, the net proton consumption started to become independent of ionic strength and increased infinitely, approaching pH ~ 11, due to the alkaline hydrolysis (140).

The existence of two dissociation steps related to the stronger and weaker acidic groups (carboxylic and phenolic) of humic acid was assumed. Among the numerous models available to describe the electrostatic effect, the diffuse double layer (DDL) approach has been chosen in this work. The net proton surface excess curves at different ionic strengths were fitted using the FITEQL(v.3.2) (141) software choosing the option of two p$K$s and the DDL electrostatic model. The sum of the stronger and weaker acidic groups calculated from the fitted curves agrees relatively well with the measured values at pH ~ 10.5. The calculated p$K$ values are p$K_1$ = 3.5 ± 0.1 for carboxylic groups and p$K_2$ = 5.7 ± 0.1 for phenolic groups.

### 5.1.1.3 Fractionation of humic acid and elemental composition of the fractions

From both chemical and structural points of view, humic acid is an inherently composite material. It can be considered as a cross-linked network having aromatic functionality and a variety of aliphatic functional groups and side chains. The most serious hindrance in the characterization of HA, however, is the fact that analytical signals observed from HA and their processes generally are sums of numerous slightly different sub-signals, leading to their broadening and, thus, lowering their resolution and specificity.

Due to the extreme complexity of HA mixtures, a fractionation method like ultrafiltration (UF) using different suitable membrane filters was used in this work (as described in 4.1.1.2) to differentiate such polydisperse mixtures of macromolecules as a function of their molecular size.

The humic acid was fractionated into eight different fractions corresponding to nominal molecular size ranges. The mass balance of the eight fractions

showed an average recovery of ~87.8%. Table 5.1 lists the percent by weight of the humic acid fractions obtained from the fractionation process. The micro- and ultrafiltered fractions in decreasing size are labeled Fr0 to Fr7.

***Table 5.1.*** *The percent by weight of the humic acid fractions.*

| Size fraction | Wt% |
|---|---|
| Fr0 (> 0.2 $\mu$m) | 16.5 ± 4.9 |
| Fr1 (300 kDa-0.2 $\mu$m) | 7.8 ± 0.5 |
| Fr2 (100-300 kDA) | 8.5 ± 2.6 |
| Fr3 (50-100 kDa) | 12.3 ± 1.2 |
| Fr4 (30-50 kDa) | 6.1 ± 0.4 |
| Fr5 (10-30 kDa) | 6.0 ± 0.6 |
| Fr6 (3-10 kDa) | 10.7 ± 0.9 |
| Fr7 (1-3 kDa) | 19.9 ± 1.5 |

Elemental analysis is one of most simple and important means of characterizing humic acids (HAs). Along with some ratios such as O/C, H/C, N/C and S/C, analytical analysis can provide valuable information of the composition and possible structure of HA and its fractions (142). Table 5.2 lists the elemental analysis results for the original HA and its fractions.

Results for humic acid size fractions show a clear trend: C, H, N, and S contents decrease and O content increases with decreasing molecular weight. The composition of the total humic acid sample is consistent with the composition of its molecular size fractions (Table 5.2). The elemental O/C molar ratio data obviously show that the abundance of oxygen containing functional groups is larger in the smaller size fractions, which may gives an indication about the carboxylic and phenolic groups. They seem to increase regularly from Fr0 to Fr7, whilst the H/C atomic ratio, which as a measure of –HC=CH– bonds can be used as an indication of the degree of aromaticity, is substantially lower (greater aromaticity) for the smaller molecular size

fractions. These findings are in a good harmony with the results obtained from the acid-base titration, the FT-IR spectra and $^{13}$C-NMR measurements of the HA fractions (as described below). A similar increase in aromatic carbon content (143) or a decrease in the ratio of aliphatic to aromatic carbon (144, 145), and also an increase in the proportion of aromatic hydrogen (146) with decreasing size of ultrafiltered humic acid samples has been recently published.

**Table 5.2.** *Elemental composition and molar ratios of soil extracted HA and its fractions.*

| Sample | Elemental composition (wt%) [a] | | | | | Ash (wt%) | Molar ratio | | | |
|---|---|---|---|---|---|---|---|---|---|---|
| | C | H | N | S | O [b] | | O/C | H/C | N/C | S/C |
| HA | 43.4 ± 0.4 | 5.08 ± 0.1 | 3.94 ± 0.1 | 0.74 ± 0.0 | 46.84 | < 0.1 | 0.81 | 1.39 | 0.078 | 0.0064 |
| Fr0 | 48.3 ± 0.2 | 5.92 ± 0.2 | 4.96 ± 0.2 | 0.53 ± 0.0 | 40.29 | ND | 0.63 | 1.46 | 0.088 | 0.0041 |
| Fr1 | 46.7 ± 0.3 | 5.62 ± 0.2 | 4.51 ± 0.0 | 0.44 ± 0.0 | 42.73 | ND | 0.69 | 1.43 | 0.083 | 0.0035 |
| Fr2 | 45.5 ± 0.2 | 5.37 ± 0.1 | 4.38 ± 0.1 | 0.38 ± 0.1 | 44.37 | ND | 0.73 | 1.41 | 0.083 | 0.0031 |
| Fr3 | 42.9 ± 0.1 | 5.05 ± 0.1 | 4.01 ± 0.1 | 0.37 ± 0.0 | 47.67 | ND | 0.83 | 1.40 | 0.080 | 0.0032 |
| Fr4 | 41.8 ± 0.4 | 4.86 ± 0.1 | 3.82 ± 0.0 | 0.46 ± 0.0 | 49.06 | ND | 0.88 | 1.39 | 0.078 | 0.0041 |
| Fr5 | 40.7 ± 0.2 | 4.51 ± 0.0 | 3.52 ± 0.0 | 0.35 ± 0.0 | 50.92 | ND | 0.94 | 1.32 | 0.074 | 0.0032 |
| Fr6 | 40.2 ± 0.1 | 4.36 ± 0.2 | 3.12 ± 0.1 | 0.40 ± 0.0 | 51.92 | ND | 0.97 | 1.29 | 0.067 | 0.0037 |
| Fr7 | 37.5 ± 0.3 | 4.02 ± 0.1 | 2.49 ± 0.0 | 0.28 ± 0.0 | 55.71 | ND | 1.12 | 1.28 | 0.057 | 0.0028 |

[a]Standard deviation calculated from five measurements.
[b]Calculated as difference to 100%.
ND, not determined.

### 5.1.1.4 Acid-base properties of humic acid fractions

The net proton surface excess of the original HA, and of its fractions, was determined over the pH range from 3.0 to 11.0 at an ionic strength of 0.01 mol/l as can be seen in Fig. 5.3.

By comparing the data for the fractions, it can be seen that although the shapes of the curves are similar, the amount of negatively charged groups increases as the size of fractions decreased; i.e., the smaller the fractions, the larger their acidity over the entire range of pH. Assuming that beside phenolic groups (–OH) the most carboxylic groups (–COOH) are linked to aromatic rings of HA, the increase in acidity with decreasing size of fractions is in good harmony with the increasing aromaticity of samples, which was established by $^{13}$C-NMR (Fig. 5.9 and Table 5.5) and UV measurements (Fig. 5.4 and Table 5.4), as shown below, as well as with the increasing O/C molar ratio of fractions (Table 5.2). The $^{13}$C-NMR spectra show, however that Fr0 is almost entirely aliphatic, and aromaticity is very low for Fr1, yet there are carboxyl functionalities certainly linked to the aliphatic carbons such as, e.g., fatty acids supposed to be constituents of the high molecular weight fractions. The net proton consumption started to increase infinitely, approaching pH ~ 11.0 due to the alkaline hydrolysis (140).
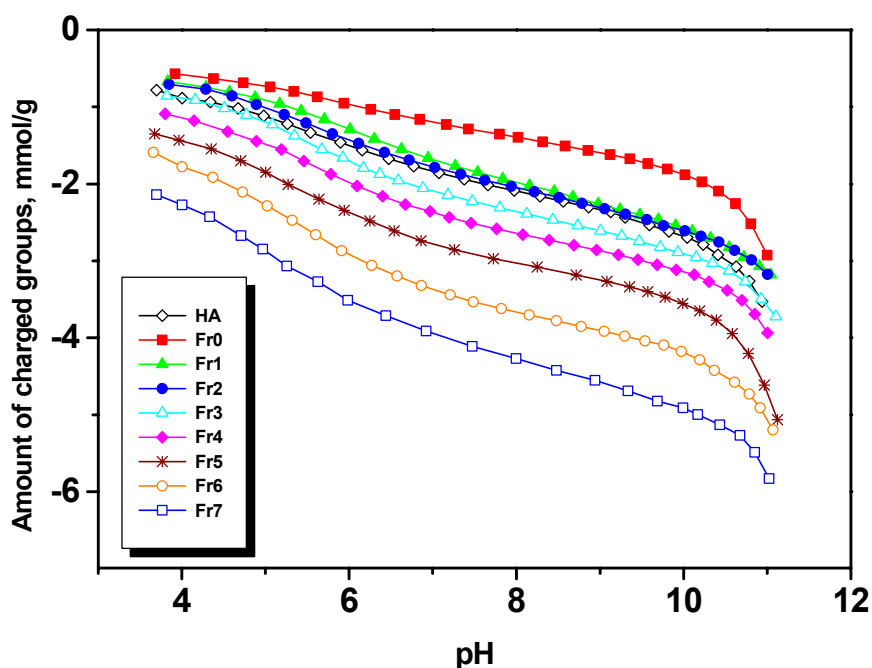


**Fig. 5.3.**     *pH-dependent ionization of the whole humic acid and of its ultrafiltered fractions.*

The curves were fitted using the FITEQL(v.3.2) choosing two pKs and the diffuse double layer (DDL) electrostatic model. The calculated pKs are summarized in Table 5.3. The calculated dissociation constants decreased with decreasing size of fractions ($pK_1$ 4.52 to 3.01, $pK_2$ 6.84 to 5.09). Perhaps the calculated two pKs values for each HA fraction are not true values but they only show us clearly the differences in the chargeable functional groups amounts between these HA size fractions where the carboxylic and phenolic groups amounts increase by decreasing the size of the HA fraction (from Fr1 to Fr7).

**Table 5.3.**    *The calculated ionization constants of the humic acid fractions.*

| Sample | $pK_1$ (strong) | $pK_2$ (weak) |
|--------|-----------------|---------------|
| Fr0    | 4.52            | 6.84          |
| Fr1    | 4.10            | 6.43          |
| Fr2    | 4.07            | 6.31          |
| Fr3    | 3.83            | 6.24          |
| Fr4    | 3.72            | 6.19          |
| Fr5    | 3.66            | 5.92          |
| Fr6    | 3.33            | 5.21          |
| Fr7    | 3.01            | 5.09          |

### 5.1.1.5 Spectroscopic characterization of humic acid and its fractions

### 5.1.1.5.1 UV-VIS spectroscopy

The spectroscopic characterization of humic acid fractions clearly shows their chemical diversity. The UV-visible spectra of dilute alkaline solutions of the original humic acid and its fractions are shown in Fig 5.4. The fractions exhibit almost the same, featureless spectra as the solution of unfractionated material did, only the absorbance values showed systematic change especially in the near UV region. The absorbance of sample Fr0 is the lowest

over the entire wavelength range. The spectrum of the original unfractionated humic acid is situated among those for its fractions. The ratio of absorbance at 465 and 665 nm ($E_{465}/E_{665}$ ratio) being inversely related to either the degree of condensation of aromatic group or the molecular weight (145) was also determined for the fractions (shown in Table 5.4). In general, fulvic acids should have higher $E_{465}/E_{665}$ values (7.0 to 8.0) than humic acids ($E_{465}/E_{665}$ ~3.0 to 5.0). It was found that the higher the $E_{465}/E_{665}$ ratio is, the higher the relative amount of the compounds of lower molecular weight.
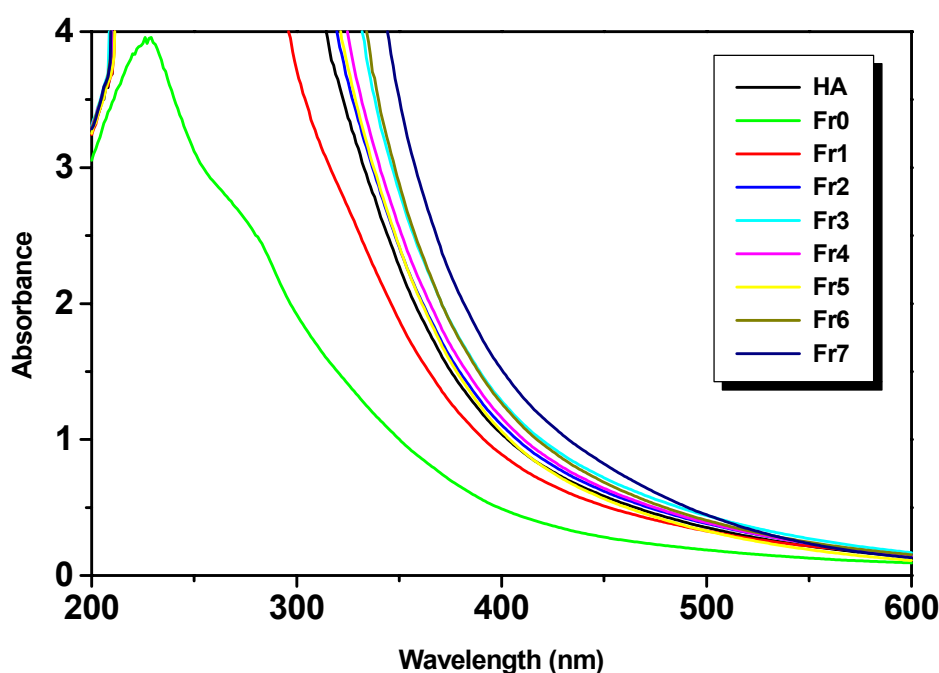


**Fig. 5.4.**     *UV-visible spectra for the humic acid and its ultrafiltered fractions.*

The $E_{465}/E_{665}$ ratio increases steadily from 5.30 to 11.57 with decreasing nominal size of fractions, and it is relatively high and rather match to the range of fulvic acids. The smaller size humic acids may be more compact than the larger ones. This is due to their larger content of aromatic carbon and a higher degree of condensation, as was indicated by the $E_{465}/E_{665}$ ratio, which increased with decreasing molecular weight. Similar findings for a fractionated humic acid have recently been reported (46, 52).

***Table 5.4.*** *The $E_{465}/E_{665}$ values of the humic acid and its fractions.*

| Sample | $E_{465}/E_{665}$ |
|--------|-------------------|
| HA | 7.60 |
| Fr0 | 5.30 |
| Fr1 | 6.17 |
| Fr2 | 7.36 |
| Fr3 | 7.66 |
| Fr4 | 8.08 |
| Fr5 | 8.28 |
| Fr6 | 9.60 |
| Fr7 | 11.57 |

### 5.1.1.5.2 FT-IR spectroscopy

FT-IR spectroscopy has provided considerable insight into the reactivity, structural arrangement of the functional groups and aromatic/aliphatic domains in humic acids (147, 148).

Fig. 5.5 shows the FT-IR spectra of the eight humic acid fractions of different nominal molecular size and of the unfractionated humic acid. In a more detail, the FT-IR spectra of two characteristic humic acid fractions (Fr1 and Fr7) are represented in Fig. 5.6. Absorption bands characteristic of humic acid (149) are observed in the FT-IR spectra as follows:

a) a broad band around 3400 cm$^{-1}$, generally attributed to O-H groups and, secondarily, N-H stretching of various functional groups,

b) a weak (shoulder) at about 3080-3060 cm$^{-1}$, attributed to aromatic C-H vibrations,

c) two peaks at about 2920 and 2850 cm$^{-1}$, preferentially ascribed to aliphatic CH$_3$ stretching (Fig. 5.8 a) and aliphatic CH$_2$ stretching modes (Fig. 5.8 b),

d) pronounced peaks between 1750 and 1650 cm$^{-1}$, due to aromatic -C=C-stretching, carbonyl vibrations (Fig. 5.8 c), phenolic R-C-OH and -C=O of H-bonded conjugated ketones,

e) the strong band centered between 1650 and 1580 cm$^{-1}$, assigned to the characteristic asymmetric stretching (Fig. 5.7 b) of the carboxylate group R-COO$^-$ K$^+$ (K$^+$-humate),

f) a band at 1547 cm$^{-1}$ is assigned to the amide II vibration,

g) the weak peak located at 1457 cm$^{-1}$ is attributed to CH$_3$ and CH$_2$ asymmetric bending modes (Fig. 5.8 d),

h) the strong band between 1400-1380 cm$^{-1}$ indicates the prominent symmetric R-COO- K$^+$ carboxylate vibration (Fig. 5.7 c),

i) broad peaks in the 1240 cm$^{-1}$ region are ascribed to C-OH bending modes of phenols (Fig. 5.7 d) and of tertiary alcohols,

j) a strong peak at 1050-1040 cm$^{-1}$, generally attributed to C-O stretching of polysaccharides or polysaccharide-like compounds and/or Si-O stretching of silica impurities.

The most interesting and important group of frequencies, from the point of view of interpreting the FT-IR spectra, is the group due to the R-COOH (R-COO$^-$ X$^+$) part of the humic acid molecule. When a carboxylic acid changes into carboxylate, the C=O and C-O bond groups are replaced by two equivalent carbon-oxygen bonds. The $\nu$(C=O) vibration, occurring in the carboxylic acid at about 1720 cm$^{-1}$, shifts to a lower wavenumber and two new bands appear near 1600 and 1400 cm$^{-1}$ corresponding to the R-COO$^-$ X$^+$ antisymmetric and symmetric vibrations. This carboxylate ion may coordinate to a metal ion (X$^+$ = Na$^+$, K$^+$, Ca$^{++}$ …) in one of the following modes: unidentate complex, chelating (bidentate) structure or a bridging complex.

The problem of FT-IR signal assignment however; as well as understanding the relationship between the observed spectral features and the molecular structure, can be difficult. Even the identification of fundamental vibrational frequencies often generates controversy. Several theoretical methods are useful in analyzing vibrational spectra. These theoretical methods can be
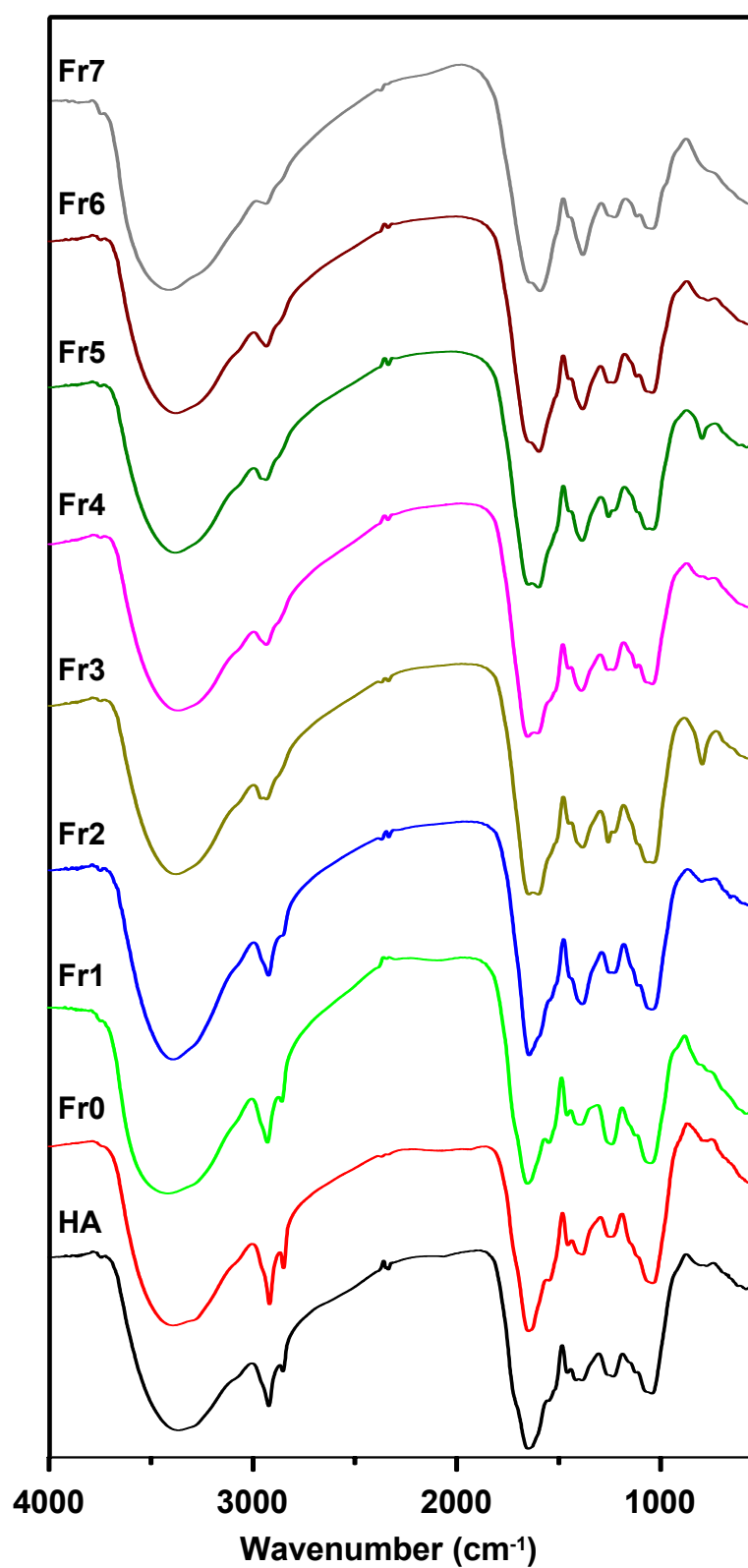
**Fig. 5.5.**     *FT-IR spectra of the humic acid and its ultrafiltered fractions.*
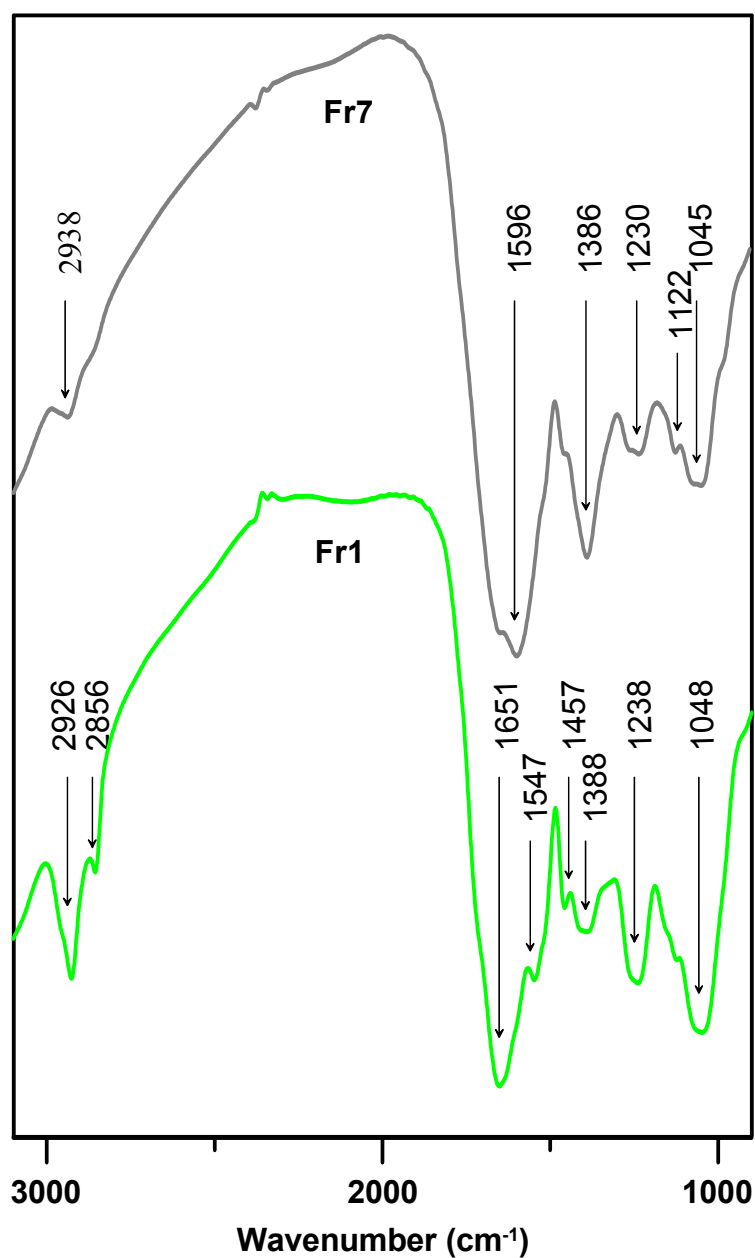
**Fig. 5.6.**    *FT-IR spectra of two characteristic humic acid fractions (F1 and F7).*

roughly divided into the following groups: classical methods, semi-empirical quantum mechanical methods and ab initio (first principal) quantum mechanical calculations. Straight forward ab initio molecular orbital calculation of the structure and vibrational frequencies has the advantage that the results are completely unbiased since there is no arbitrary assumption involved.

Therefore, quantum mechanical <u>D</u>ensity <u>F</u>unctional <u>T</u>heory (DFT) ab initio calculations on relatively short oligomers (humic acid model structures) may provide valuable information regarding the interpretation of the characteristic carboxylic acid group vibrations.

The calculated normal mode displacements (eigenvectors) of the most important vibrations are presented in Fig. 5.7 (in an aromatic model system) and in Fig. 5.8 (in an aliphatic model system).



$\nu_{sym}$ : -C= C- (1650 cm$^{-1}$)    $\nu_{as}$ : C-OO-K (1596 cm$^{-1}$)

$\nu_{sym}$ : C-OO-K (1387 cm$^{-1}$ )    $\nu_{sym}$ : C-O$_{ph}$ (1252 cm$^{-1}$)
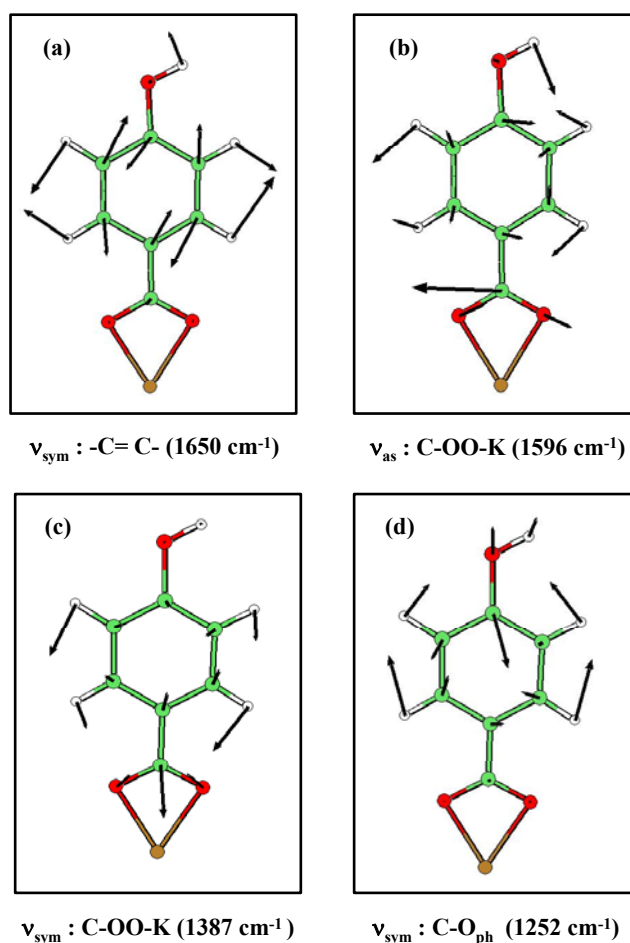
***Fig. 5.7.*** *Calculated normal mode displacements (eigenvectors) of the atoms in an aromatic model system.*

There is general agreement among FT-IR experts that one of the main chemical reactions in the neutralization and metal complexation of humic substances is the conversion of R-COOH into R-COO⁻ groups, which is indicated by the disappearance of the 1720-1710 cm$^{-1}$ band and the gain in intensity of the 1560-1600 cm$^{-1}$ and 1400 cm$^{-1}$ bands.

The complete absence of the FT-IR band in the 1720 cm$^{-1}$ region (Figures 5.5 and 5.6) indicates the total conversion of carboxylic groups into carboxylate anions (R-COO⁻ K⁺) in all fractions and in the original humic acid spectrum. Thus, untreated humic acid and the eight size fractionated humic acids show chemical alteration with the complete absence of all carbonyl group vibrations.

(a)

$\nu_{sym}$ : CH$_3$ str
(2920 cm$^{-1}$)

(b)

$\nu_{sym}$ : CH$_2$ str
(2850 cm$^{-1}$)

(c)

$\nu_{asym}$ : R-COOH str
(1720 cm$^{-1}$)

(d)

$\nu_{bend}$ : CH$_3$ ; CH$_2$
(1447 cm$^{-1}$)
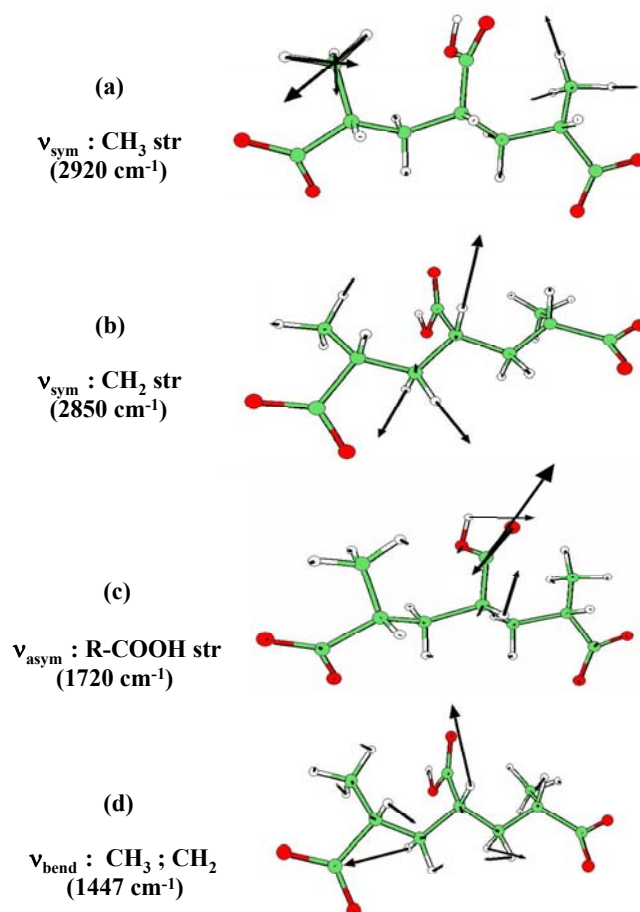
**Fig. 5.8.** *Calculated normal mode displacements (eigenvectors) of the atoms in an aliphatic model system.*

The FT-IR spectra of the eight fractionated humic acids presented in Fig. 5.5 show a strong decrease in IR intensity of the aliphatic vibrations (2920-2850 cm$^{-1}$) from Fr0 to Fr7. These results indicate that fractions with molecules of larger size contain humic molecules which are predominantly aliphatic.

The increase of the characteristic antisymmetric carboxylate band intensity ($v_{asym}$ R-COO$^-$ K$^+$) and the corresponding symmetric vibration ($v_{sym}$ R-COO$^-$ K$^+$) from fraction Fr0 to Fr7 point out that molecules of smaller size have a higher content of carboxylate carbon.

Using the Si-0 vibrational intensity as an internal standard one is able to determine the increase of the pronounced aromatic peak between 1660-650 cm$^{-1}$. Therefore, fractions with molecules of smaller size have higher contents of aromatic carbon.

These trends accord with the $^{13}$C-NMR results (Fig. 5.9, Table 5.5). However, the clear parallels between molecular weight and phenolic groups as well as the aromatic character can hardly be derived from the FT-IR spectra alone.

### 5.1.1.5.3 $^{13}$C-NMR spectroscopy measurements

Solid-state $^{13}$C-NMR is one of the most promising techniques for studying the chemical structure of humic substances. In this work, solid-state CP-MAS $^{13}$C-NMR spectroscopy was used to gain more detailed information about the structure of the humic acid fractions. The spectra of the humic acid, and the humic acid size fractions are presented in Fig. 5.9, and the relative intensities of the chemical shift regions as well as the values of the ratio of aromatic to aliphatic carbon are summarized in Table 5.5. $^{13}$C-NMR analysis of the humic acid fractions reveals that the chemical forms of carbon vary between the different size fractions of humic acid. These spectra of the humic acids contain strong peaks at 0-45 and 45-110 ppm (aliphatic carbons), broad peak at 110-160 ppm (aromatic carbon), strong peak at 160-185 ppm (carboxyl carbon) and broad peak at 185-220 ppm (carbonyl carbon) (52, 150, 151). This suggests that the bulk properties of the carbon functionalities of each
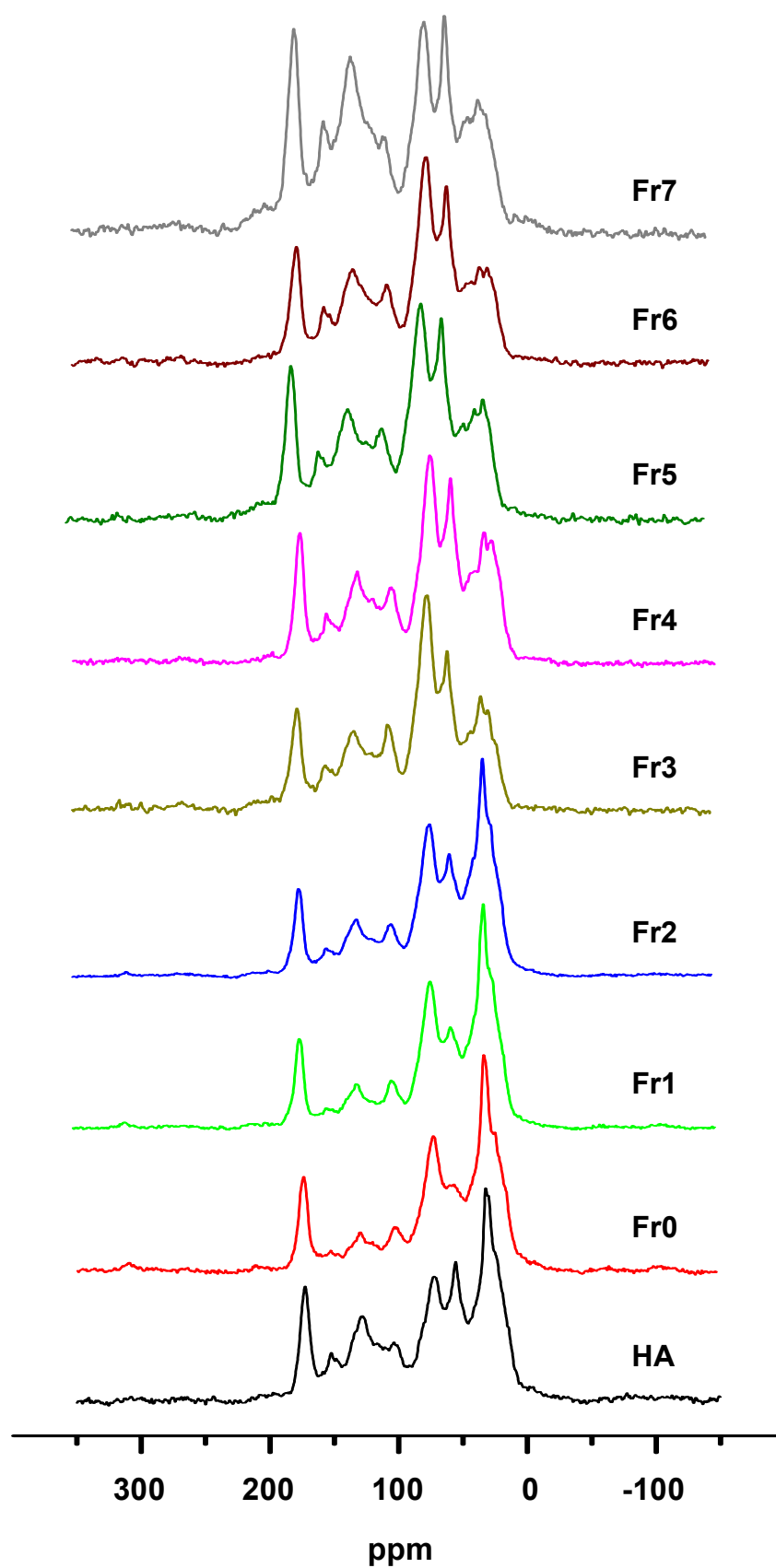
**Fig. 5.9.**    *Solid state $^{13}$C-NMR spectra of the original humic acid and its ultrafiltered fractions.*

humic acid fraction are similar to one another. However, the relative intensities of the different carbon shifts in the spectra differ significantly in the humic fractions.

These measured values indicate that the Fr0, Fr1 and Fr2 fractions contain humic molecules which are predominantly aliphatic (0-110 ppm) with lower contents of aromatic and carboxyl carbons. By contrast, the Fr5, Fr6 and Fr7 fractions with molecules of much smaller size have much higher contents of aromatic (110-160 ppm) and chargeable groups (phenolic and carboxyl carbons) (140-160 ppm and 160-185 ppm, respectively) and lower levels of aliphatic carbons. These findings agree with the results obtained from the FT-IR spectra (see 5.1.1.5.2). A detailed evaluation of these results can be seen in the discussion of the $^{19}$F-NMR measurements (see 5.2).

**Table 5.5.**     *The relative intensities of different type carbons in humic acid and humic acid fractions determined by solid state $^{13}$C-NMR spectroscopy.*

| | **Percentage distribution of carbon within indicated p.p.m. regions** | | | | | | |
|---|---|---|---|---|---|---|---|
| **Sample** | **0-45 alkyl C** | **45-110 O-alkyl C** | **110-160 aromatic C** | **140-160 phenolic C** | **160-185 carboxyl C** | **185-220 carbonyl C** | **$C_{arom.}/C_{aliph.}$** |
| HA | 32.8 | 37.1 | 19.6 | 5.40 | 9.2 | 1.3 | 0.280 |
| Fr0 | 39.7 | 39.6 | 10.7 | 3.02 | 8.9 | 1.1 | 0.135 |
| Fr1 | 38.8 | 40.6 | 11.3 | 2.97 | 8.1 | 1.2 | 0.142 |
| Fr2 | 36.3 | 40.9 | 14.0 | 3.62 | 7.5 | 1.3 | 0.181 |
| Fr3 | 20.3 | 48.9 | 19.3 | 5.28 | 9.0 | 2.5 | 0.279 |
| Fr4 | 23.4 | 44.4 | 19.9 | 4.97 | 9.6 | 2.7 | 0.294 |
| Fr5 | 19.8 | 44.9 | 21.6 | 6.16 | 10.6 | 3.1 | 0.334 |
| Fr6 | 19.7 | 44.5 | 22.6 | 6.84 | 9.8 | 3.4 | 0.352 |
| Fr7 | 18.8 | 36.9 | 27.9 | 8.28 | 12.8 | 3.6 | 0.501 |

### 5.1.2 Surface charge characterization of aluminum oxide

The pH-dependence of the surface charge ($\sigma_0$) of aluminum oxide in aqueous medium at different concentrations of indifferent electrolyte ($KNO_3$) can be seen in Fig. 5.10. It is observed that at low pH ($<$ point of zero charge, PZC), $\sigma_0$ becomes more positive with increasing background electrolyte concentration, whereas at high pH ($>$ PZC) it becomes more negative. The PZC can be identified as the intersection point of $\sigma_0$ vs. pH curves belonging to the different ionic strength. The experimental PZC value is at pH = 8.8.

At low pH, although protons have a very high affinity for the surface, their adsorption cannot proceed, because the positive charges that are already adsorbed repel newly arriving protons. Equilibrium is attained when the chemical attraction is just cancelled by the electrostatic repulsion. This repulsion depends on the way in which the countercharge from the electrolyte ($NO_3^-$) is distributed. If there are many $NO_3^-$ ions near the adsorbed protons
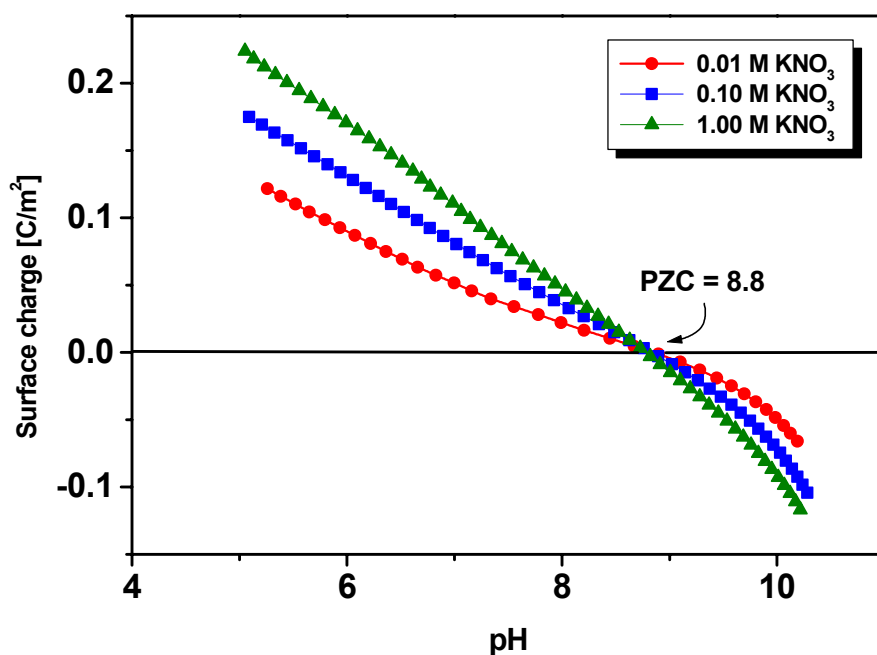


**Fig. 5.10.**      *The surface charge of aluminum oxide as a function of pH in the presence of different $KNO_3$ concentrations.*

(at high electrolyte concentration) then the surface charge is more effectively screened, so that at given pH more protons can be adsorbed. By the same token, at high pH, the $K^+$ ions are the counterions and the screening is improved if the $KNO_3$ concentration is raised. Generally, this behavior corresponds to double-layer theories that with increasing electrolyte concentration the distribution of the countercharge also changes in such a way that promotes the accumulation of charge in the region close to the surface.

## 5.2 Evaluation of the sorption properties of HA and its fractions based on $^{19}$F-NMR spectroscopy

Associations between HA and hydrophobic organic compounds (HOCs) are especially noted since they have important consequences with regard to HOC solubilization, transport, and retention (11, 86). To better understand these processes, a detailed knowledge of the nature of HOC interactions with HA is required.

The interaction mechanisms are poorly understood because of the HA heterogeneity. HA molecules have many different sorption chemical environments into which the HOC can sorb, and relative strength and mobility of those domains is highly dependent upon the carbon moieties available in the humic acid or individual fraction. One way to get better insight into these sorption mechanisms is to fractionate HA to decrease the chemical heterogeneity and to characterize a contaminant "$^{19}$F-labeled probe" molecule (like hexafluorobenzene, HFB) sorbed into these fractions. It would be an ideal way to "see" the environment that the contaminant experiences and to give direct spectroscopic evidence for the binding mechanisms between the HOC and HA.

The use of $^{19}$F-labeled probes has three distinct advantages in this respect. First, fluorinated analogues of many HOC are commercially available. Second, it is an element normally present at very low levels in most soils.

Third, the natural abundance of ^{19}F is 100%, and it has an NMR sensitivity almost equal to that of [1]H (138).

In the following, the solid-state ^{19}F-NMR study of the sorptive uptake of HFB by the humic acid and its fractions is discussed. The sorption data is correlated with the ^{13}C spectrum and molecular size range for each fraction to assess the impact of size fractionation on the interaction between HFB and HA.

**Humic Acid.** Integration of the unfractionated HA ^{13}C-NMR spectrum (Fig. 5.9, Table 5.5) shows that 69.9% of the carbon is aliphatic, 19.6% is aromatic, and 9.2% is carboxylic moieties.

The ^{19}F spectrum obtained for the interaction of HFB with the whole humic acid shows two distinct resonances that have been attributed to different HFB sorption domains (138) (Fig. 5.11, HA).

The most prominent domain is centered at -159.7 ppm. The resonance also has a broad, low intensity shoulder on the upfield side (~-170 to ~–175 ppm). The intensity in the sidebands from this peak is unevenly distributed with the downfield sidebands having more signal than the upfield sidebands, this is particularly evident when comparing the two sidebands nearest the central peak. This contains the majority of the ^{19}F signal, and thus the majority of the HFB sorbed to the system. The broadness of this resonance and the distance of observed sidebands give evidence of a significant amount of chemical anisotropy. Due to the apparent anisotropy this resonance is attributed to immobile or motionally restricted HFB.

The –168.1 ppm peak has no discernable sidebands and an 18 Hz line width at half height (LWHH), significantly more narrow than that of the –159.7 ppm
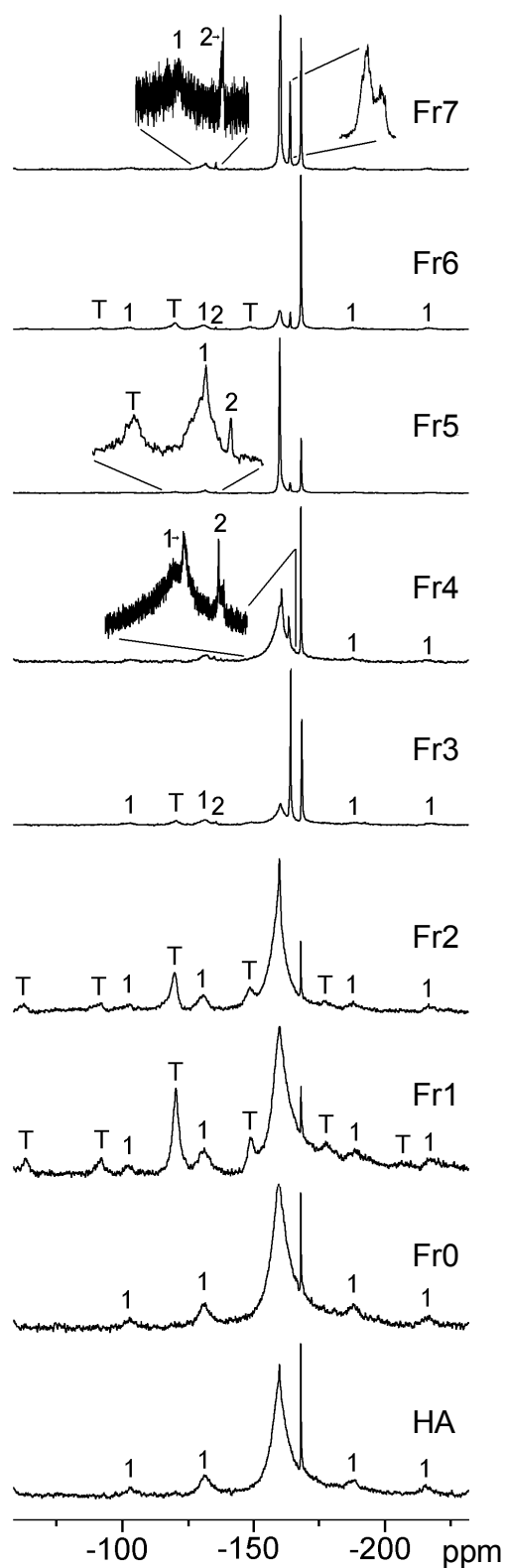
**Fig. 5.11.** $^{19}F$ *solid-state MAS NMR spectra of HFB sorbed to HA and its fractions.* Within the spectra T denotes signal due to PTFE contamination, 1 denotes spinning sideband for immobile domain, and 2 denotes spinning sideband for −163 ppm resonance.

resonance which has a 1500 Hz LWHH. Due to the narrowness of this peak it is attributed to loosely bound, mobile HFB.

The general progression of the chemical character of the fractionated humic acid with decreasing molecular size is a decrease in aliphatic character, increase in aromatic character, and increase in carboxylic character. Of these fractions the carboxylic character has the highest variability but clearly increases in relative amount with decreasing apparent molecular weight. The humic acid fractions can generally be divided into three different groups based on their molecular weight, ^{13}C-NMR (as shown in Fig. 5.9 and Table 5.5), and ^{19}F-NMR spectra as described below.

**Fr0, Fr1, and Fr2.** This fractions group has, on average, approximately 13 % more aliphatic, 39% less aromatic, and 10% less carboxylic carbon contents relative to the whole HA. These fractions account for 33% of the mass of the whole HA (Table 5.1).

All display a strong, broad signal in the ~–160 ppm HFB sorption domain, have high aliphatic, low aromatic, and low carboxylic contents. This dominant sorption domain is termed "rigid" due to its very broad nature (116, 138, 152). The broad nature of the resonance indicates a wide variety of different chemical moieties likely present with which HFB can interact (Fig. 5.11, Fr0, Fr1 and Fr2). This observation appears logical as the largest molecules would likely have the most heterogeneous composition and structural variability. The rigid sorption domains all have asymmetrical peaks with higher intensities being observed on the downfield side. This suggests that this sorption domain is skewed to moieties that yield lower electron density around the F nuclei. This would likely result from sites with high electron withdrawing strengths. Structures such as carbonyl or other oxygen bearing moieties could produce such results.

The −168 ppm resonance is very narrow in all of the spectra acquired. It is very sharp in both the 8 kHz MAS experiments and the static experiments. The fact that this peak does not appreciably broaden in the static experiments (Fig. 5.12) gives strong evidence that the resonance is the result of highly mobile HFB molecules. This mobility is not due to the HFB existing as a nonaqueous phase liquid (NAPL) phase because neat HFB resonates at −163.0 ppm. Nor can it be attributed to dissolved HFB in the aqueous medium present in the humic acid (the resonance of HFB in the aqueous medium was measured at −163.2 ppm). The most probable source of this resonance is highly mobile HFB which is weakly physisorbed to surface groups in which the molecule is free to rapidly "hop" from site to site. The rapid movement between different sites with rather weak interactions would result in a very sharp and well defined resonance.
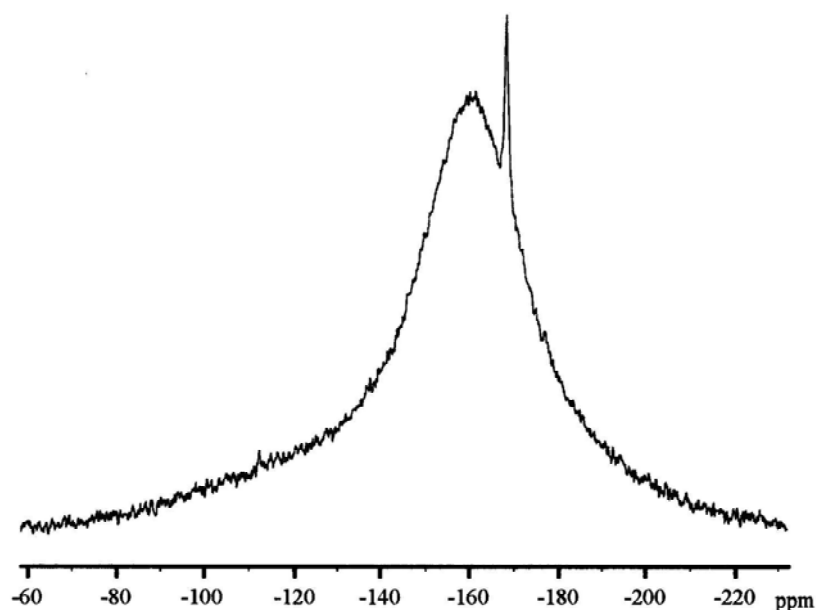


**Fig. 5.12.** $^{19}F$ *solid-state static NMR spectrum (32400 scans) of HFB sorbed to Fr0.*

The spectra of Fr1 and Fr2 display a signal due to PTFE contamination resulting from abrasion of the PTFE coating on the magnetic stir bar used

during ultrafiltration. The main PTFE resonance occurs at −120.4 ppm with two spinning sidebands located on either side of the main peak.

**Fr3 and Fr4.** Integration of the $^{13}$C spectrum for Fr3 and Fr4 (Fig. 5.9, Table 5.5) show that these fractions have intermediate aliphatic, aromatic, and carboxylic contents as well as intermediate apparent molecular weights. These fractions account for 18.4% of the mass of the whole HA. These fractions display HFB sorption spectra which can be perceived as transitioning from the sorption domains found in the heavy fractions to those observed in the light fractions.

The $^{19}$F spectrum obtained for the interaction of HFB with Fr3 or Fr4 show three distinct resonance regions at ~−160, ~−164, and ~−168 ppm (Fig. 5.11, Fr3 and Fr4). The ~−160 ppm sorption domain changes significantly from a very broad, somewhat featureless domain, to a smaller, narrower domain with multiple peaks and slightly different chemical shifts. Fr4 displays this transition the most clearly, where, the ~−160 ppm resonance is actually composed of two peaks, one broad resonance and a second, sharper resonance (see insert in Fr4 spectrum). These two resonances represent the averages of two different chemical environments, the broader domain centered at −159.9 ppm corresponds to the broad domain in the heavier fractions and the narrower resonance centered at −160.6 ppm corresponds to the broad domain in the lighter fractions. All peaks observed in all the other fractions are present to some degree in this fraction. The highly mobile peak at −168 ppm is clearly evident. The ~−164 ppm peak is also complicated and appears to be due to two resonances closely overlapping (again, see insert in Fr4 spectrum). The static spectrum from this experiment (Fig. 5.13) gives no indication that this resonance is caused by a separate HFB nonaqueous phase liquid (NAPL). This observable transition phase gives evidence that there are different sorption domains in humic acid which are dependent upon the molecular weight ranges and carbon moieties found in the humic matrix. This dependence gives indication that the different size fractions have different chemical and/or structural differences which have significant impact on the

type of sorption environment available to nonionic, nonpolar compounds. There is a very weak PTFE contaminant signal at –120 ppm in Fr3 spectrum but there is no discernable PTFE contaminant signal in Fr4 spectrum.
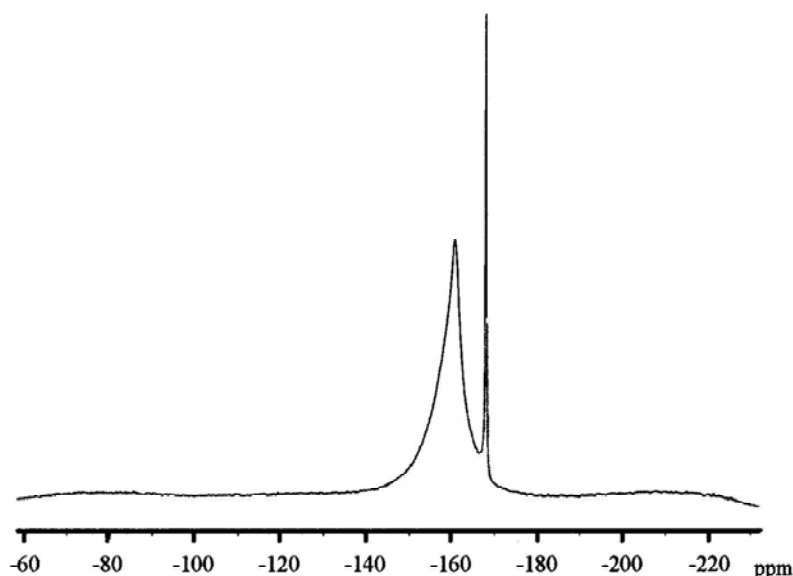


**Fig. 5.13.** $^{19}F$ *solid-state static NMR spectrum (32400 scans) of HFB sorbed to Fr4.*

**Fr5, Fr6 and Fr7.** Integration of the $^{13}C$ spectrum for these fractions (Fig. 5.9, Table 5.5) show that they have, on average, carbon contents that are approximately 12% less aliphatic, 22% more aromatic, and 20% more carboxylic relative to the whole HA. Thirty-seven percent of the mass of all the fractions is isolated in these three lightest fractions. These fractions have lower aliphatic, higher aromatic, and higher carboxylic contents than the whole HA. These fractions display three unique sorption domains. The –164 ppm sorption domain is very sharp, however it still results in an observable spinning sideband (~-136 ppm). This spinning sideband is evidence that this sorption domain is not due to liquid-like environment but a more rigid environment with a broad chemical shift range. This conclusion is also supported by the static spectrum which shows no evidence of a highly mobile resonance at –164 ppm. This resonance is actually a composite of two peaks at –164.1 and –163.9 ppm (see insert in Fr7 spectrum). In comparison, the

–168 ppm domain is much more narrow with a clear signal present in the static spectrum. The –160 ppm resonance is composed of two peaks, a sharper peak with the same average chemical shift as the broader peak. This is seen in the odd shape of the spinning sideband located at –130 ppm (see insert in Fr5 and Fr7 spectra) which suggests a sharper, narrow peak on top of a broader peak. These peaks suggest two different sorption domains in which HFB finds a similar local chemical environment which differs only in its relative mobility. There is a very weak PTFE contaminant signal at –120 ppm in Fr5 and Fr6 spectra but there is no discernable PTFE contaminant signal in Fr7 spectrum.

The previous $^{19}$F-NMR measurements indicate that the humic acid molecules have many different sorption chemical environments which nonionic molecules such as HFB can sorb into. The relative strength and mobility of those domains is highly dependent upon the carbon moieties available in the humic acid or individual fraction. Smaller humic acid molecules have at least three sorption sites that are more defined and homogeneous than the sorption domains found in larger humic acid molecules. The presence of these different sorption domains gives evidence that humic acid cannot be looked at strictly as a simple partitioning medium but a more complicated sorbent such as the soil organic matter sorbents depicted in recent articles by Weber et al. (153) and Pignatello et al. (154, 155).

## 5.3   Interaction between organic macromolecules and alumina

Interactions between hydrous oxides and naturally occurring organic materials such as humic and fulvic acids are of great importance in environmental processes. Natural soil and water systems, and relatively simple models of them (e.g. dispersions of metal oxides in organic acid solutions), have been described in comprehensive reviews (78, 156, 157). Most of these investigations are related to the pH dependence of the interactions since the

soil and water equilibria are largely pH-dependent, but less attention has been paid to the effect of the ionic strength.

Considering the charging behavior of the alumina in aqueous electrolyte solutions (Fig. 5.10), three particular pH values were chosen for the adsorption study. Table 5.6 shows the surface charges of alumina at the different pH values and salt concentrations used.

**Table 5.6.**    *The surface charge of the aluminum oxide at different pHs and ionic strengths.*

| pH | $\sigma_0$ (C/m$^2$) | | |
|---|---|---|---|
|  | 0.01 M KNO$_3$ | 0.1 M KNO$_3$ | 1.0 M KNO$_3$ |
| 5.5 | 0.112 | 0.155 | 0.198 |
| 7.5 | 0.036 | 0.058 | 0.077 |
| 9.5 | -0.021 | -0.035 | -0.047 |

### 5.3.1  Adsorption of polyacrylic acid on alumina

Based on the structural features of humic substances, the HA could be modeled by assuming that its molecules are strongly hydrated, fairly flexible, carboxylic groups containing, polyelectrolyte molecules (37, 38, 40-42). In view of these results, e.g. the characteristics of the HA adsorption isotherms observed in this work can be understood by applying PAA to compare its properties with those of natural polyelectrolytes. It has to be emphasized that the humics are not described as simple polyelectrolytes, only certain properties of both compounds are assumed to be similar.

The adsorption isotherms of the PAA on alumina at different pH values are given in Fig. 5.14. It is seen that the adsorption increased sharply at low PAA concentration (strong adsorption part) and reaches a plateau with increasing

PAA concentration for all pHs. In addition, the adsorption of PAA becomes smaller with increasing pH. The strong adsorption of PAA is derived from the electrostatic attraction force between ionized PAA and the positively charged sites on the alumina surface (ligand-exchange mechanism) as well as the interaction of hydrogen bonding between undissociated PAA and hydroxyl groups on the alumina surface. Since the PZC of alumina is 8.8 and the *pKa* of PAA is about 4.5 (158), the electrostatic attraction force between PAA and the alumina surface is decreased with increasing pH, resulting in the decrease of PAA adsorption with pH. At high pH, the decrease in the adsorption of PAA is also caused by the increased intersegmental repulsion between the already adsorbed dangled PAA and the newly arriving stretched ones.
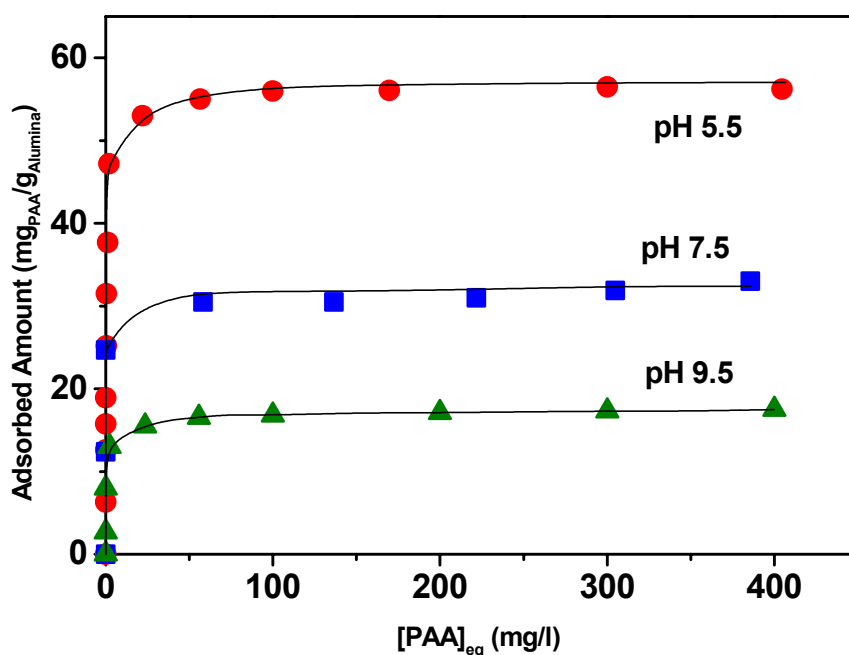


**Fig. 5.14.**     *Effect of pH on the adsorption isotherms of PAA on alumina at 0.01 M KNO₃.*

The increase in PAA adsorption with decreasing pH is quite common (159-161). The supposed polymer conformations on the alumina surface are shown schematically in Fig. 5.15. It is clear that the higher adsorption amount at the

low pH is attributed to the coiled conformation (coiled because the carboxylic groups are slightly ionized, where 34.5% are dissociated, and exhibit low intrapolymer-chain electrostatic repulsion) that causes more of the polymer molecules to be needed for a complete surface coverage. The PAA adsorbs and remains approximately in the same coiled conformation on the positively charged alumina surface [Fig. 5.15 (a)]. When the pH is raised, ionization of PAA generates more negative charges in the polymer chain (80.0% of the carboxyl groups are dissociated) which reduces the extent of coiling. The polymer still strongly adsorbs on the surface because of the positive charges on the solid  [Fig. 5.15 (b)] but the maximum adsorption amount that can be achieved is lower. By raising the pH above the PZC of alumina (PZC = 8.8) the solid particles became mainly negatively charged like the polymer and under these conditions the adsorption amount is much smaller than that  at pH = 7.5 (Fig. 5.14). The lowest adsorption amount at pH 9.5 is attributed to the PAA highly stretched conformation (98.9% of the PAA's carboxyl groups are dissociated), with the result that less of the polymer is needed for complete surface coverage. On the other hand, the strong electrostatic repulsion between the negatively charged PAA and the negative sites  on  the alumina particles surfaces at this pH would cause the polymer to 'dangle' from the particle into the aqueous phase, being held to the particle by the hydrogen bonding [Fig. 5.15 (c)].



(a)                              (b)                              (c)
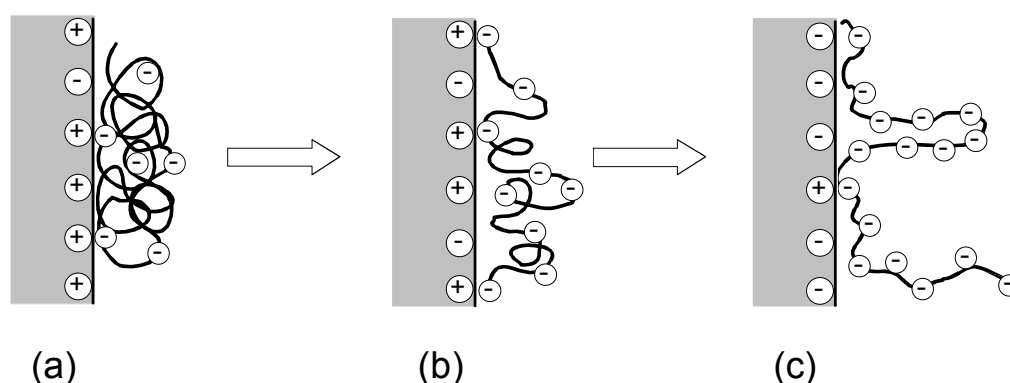
**Fig. 5.15.**     *Schematic representaion of the variations of PAA conformation at the alumina/water interface under changing pH conditions. (a) pH ~ 5.5; (b) pH ~ 7.5; (c) > 9.5.*

The importance of the ionic strength for PAA on alumina is shown in Fig. 5.16, the adsorption amounts increase significantly with increasing $KNO_3$ concentration at pH = 7.5. The effect of increasing ionic strength is to screen out the electrostatic repulsion between the carboxylic groups, and hence lead to an increase in the adsorption density of PAA on alumina.
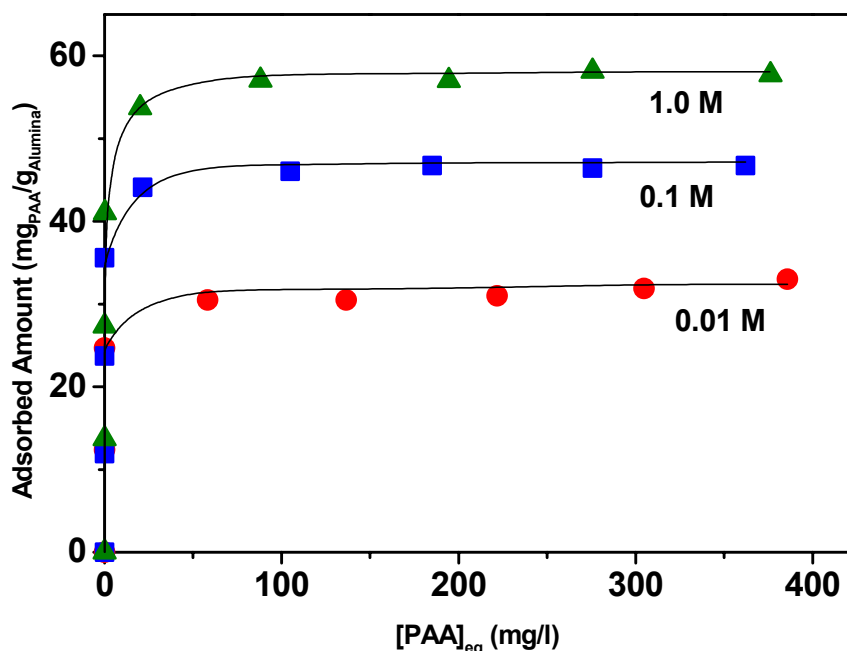


**Fig. 5.16.** *Adsorption isotherms of PAA on alumina at pH = 7.5, effect of ionic strength on the adsorption isotherm.*

From the experimental adsorption isotherms (Figures 5.14 and 5.16) one can determine the surface area occupied by one PAA molecule, $\sigma_m$, in the adsorbed state corresponding to the plateau by using the following dependence, $\sigma_m$ $(nm^2)$ $= MW_{PAA}/(\Gamma_{max} \ N_A)$ (162), where $MW_{PAA}$ is the polyelectrolyte molecular weight, $\Gamma_{max}$, is the amount of the adsorbed polyelectrolyte on a planar surface corresponding to the isotherm plateau (in $mg/m^2$), and $N_A$ is Avogadro's number. The value of $\sigma_m$ for the PAA calculated from the adsorption PAA isotherms in Figures 5.14 and 5.16 using the above equation is shown in Table 5.7.

**Table 5.7.**    *Area occupied by one PAA molecule on the alumina surface at different pH and ionic strength values.*

| Conditions | $\sigma_m$ (nm$^2$) | | |
|---|---|---|---|
| $C_{KNO_3}$ mol/l | pH = 5.5 | pH = 7.5 | pH = 9.5 |
| 0.01 | 127.77 | 202.58 | 377.53 |
| 0.10 | — | 151.01 | — |
| 1.00 | — | 123.97 | — |

From the data in Table 5.7, an important conclusion can be drawn. At high pH and low salt concentration (at pH = 9.5 and 0.01 M KNO$_3$) the polyelectrolyte molecules are adsorbed relatively flatly on the surface, which can be described by a large fraction of train segments. The few segments of the molecule that are not in direct contact with the surface protrude relatively far into the solution due to lateral repulsion effects. Consequently the adsorbed layer formed is very thin. At lower pH and higher salt concentration (at pH = 7.5 and 1.0 M KNO$_3$) the adsorbed polyelectrolyte layer can be described by a large fraction of adsorbed segments in loops and tails. Due to the high fraction of segments adsorbed in loops the adsorbed amount per surface area is relatively high.

### 5.3.2 Adsorption of humic acid on alumina

Figures 5.17 and 5.18 show the adsorption isotherms of humic acid, for varying aqueous chemistry conditions. It is observed that the humic acid adsorbed amount increases with decreasing pH and increasing ionic strength. The adsorption isotherms show an initial steep slope indicating a high affinity character, followed by a "pseudo" plateau at elevated equilibrium concentrations. These features of the adsorption isotherms are commonly observed for the adsorption of humic substances onto mineral particles (35, 67, 69, 72, 80, 84, 163). As shown in Fig. 5.2 the degree of HA dissociation increases with increasing pH value, thereby increasing the apparent solubility

of HA. Consequently, the adsorbing tendency between HA on $Al_2O_3$ is decreased due to a lowered hydrophobic interaction (67, 164). In addition, the surface of aluminum oxide, with the point of zero charge at around 8.8, becomes more negatively charged with an increase of the pH. This event further decreases the adsorption tendency owing to the increased repulsive force between HA, ionized and negatively charged molecules, and the sorbent (69).
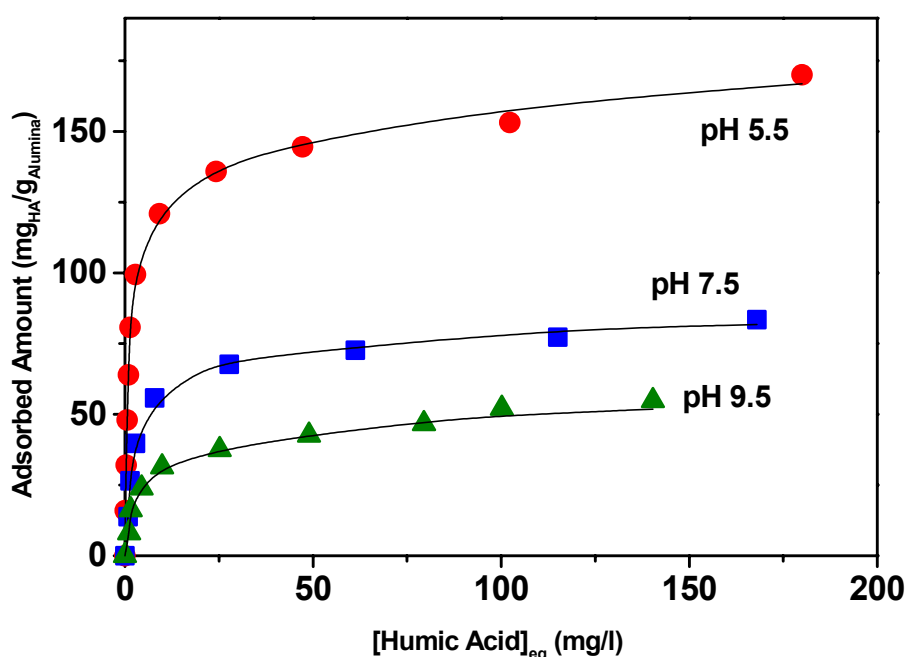


**Fig. 5 .17.**    *Adsorption isotherms of humic acid onto alumina, 0.01 M KNO₃.*
                   *Effect of pH on the adsorption.*

Sorption of humic acid increased with decreasing pH in response to positive charge development on the alumina particles. This pattern was consistent with the ligand-exchange mechanism, as previously suggested for humic substances by other authors (80, 165). Sorption of humic substances by ligand exchange is believed to occur in the following sequence (78):

$$\equiv AlOH + H^+ \rightleftharpoons \equiv AlOH_2^+ \qquad (5.1)$$

$$\equiv AlOH_2^+ + Hu\text{-}C(O)O^- \rightleftharpoons \equiv AlOH_2^+ {}^-O(O)C\text{-}Hu \qquad (5.2)$$

$$\equiv AlOH_2^+ {}^-O(O)C\text{-}Hu \rightleftharpoons \equiv AlO(O)C\text{-}Hu + H_2O \qquad (5.3)$$
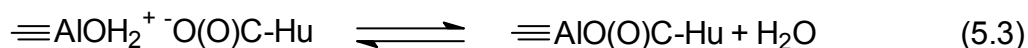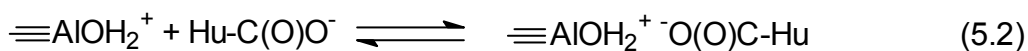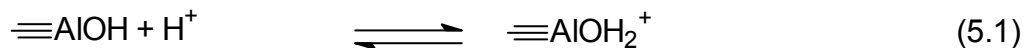
The first step of this process is protonation (eq. 5.1), which is believed to render the surface hydroxyl group more exchangeable. The protonation step is responsible, in part, for the pH dependence of the fractional sorption, but may not be necessary if the concentration of humic carboxyl groups is sufficiently high (78). The humic carboxyl groups may then form an outer-sphere surface complex with the protonated hydroxyl group (eq. 5.2). Ligand exchange occurs in (eq. 5.3) in which Hu-COO$^-$ replaces OH$_2$, yielding an inner-sphere complex.
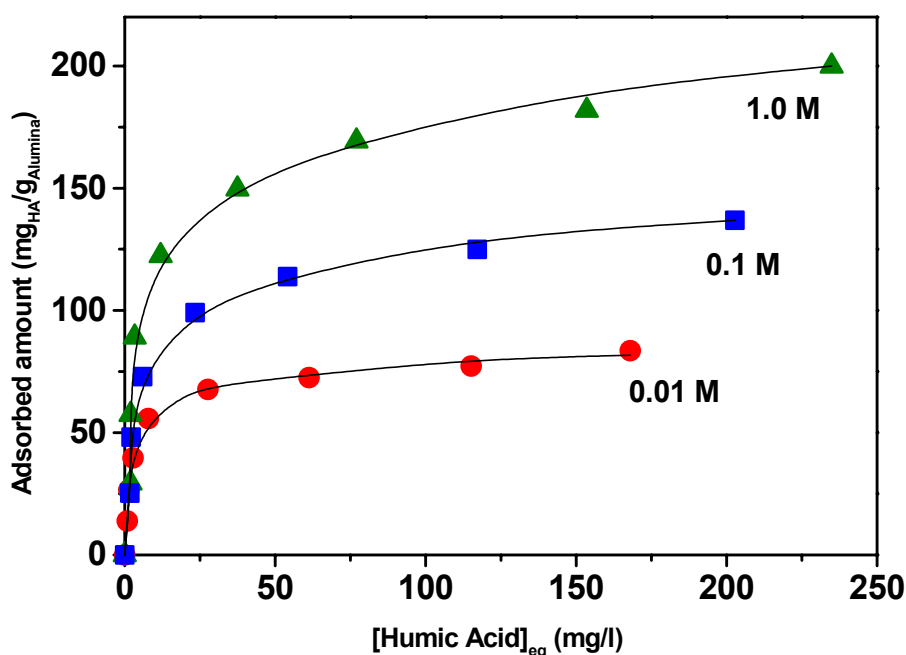


**Fig. 5.18.**     *Adsorption isotherms of humic acid onto alumina, pH = 7.5. Effect of ionic strength on the adsorption.*

The isotherms seem to be of the Langmuir type according to the classification of Giles et al. (58). The adsorption isotherms were modeled with the Langmuir isotherm equation. Monolayer adsorption capacities (apparent amounts adsorbed) calculated from the linearized form of the Langmuir equation are summarized in Table 5.8 and plotted in Fig. 5.19 as a function of pH and ionic strength. The most significant trend is the increase in the apparent amounts adsorbed with increasing ionic strength independent on the pH value. This is however most pronounced in the acidic region. This trend is expected since humate macroions are negatively charged at each pH (Fig 5.2), while the surface charge of aluminum oxide changes from positive to negative with increasing pH (Fig. 5.10).
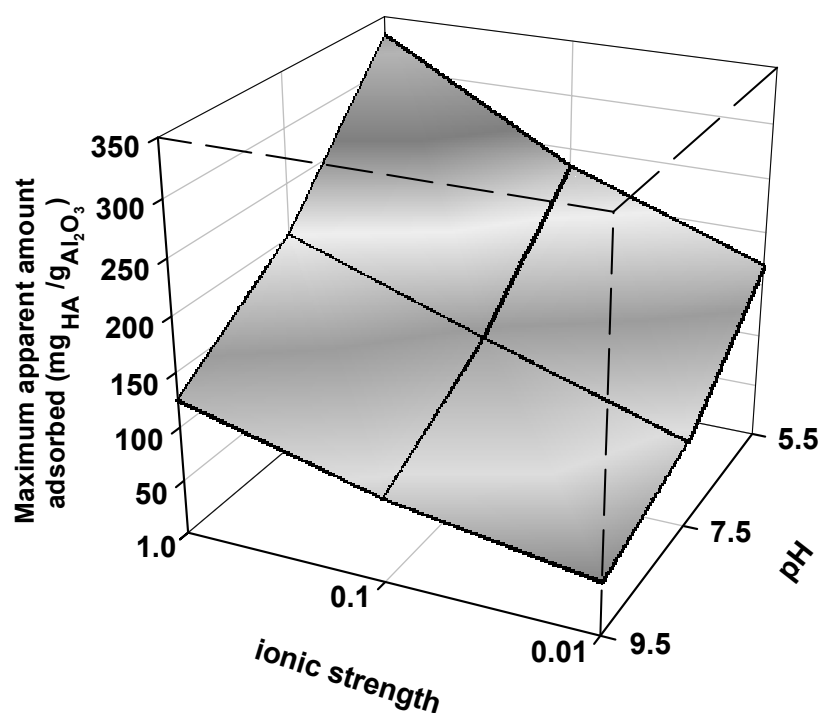


**Fig. 5.19.**    *Apparent amount of humate adsorbed on aluminium oxide at different pH and ionic strength.*

***Table 5.8.***   *Adsorption capacities of HA on alumina at different pH and ionic strength values evaluated by Langmuir equation.*

| Conditions | Adsorption capacity, mg/g | | | | | |
|---|---|---|---|---|---|---|
| | pH = 5.5 | | pH = 7.5 | | pH = 9.5 | |
| $c_{KNO_3}$ mol/l | Langmuir (regression) | Measured | Langmuir (regression) | Measured | Langmuir (regression) | Measured |
| 0.01 | 169.5 (0.97) | 170.2 | 81.9 (0.98) | 83.5 | 50.7 (0.98) | 54.8 |
| 0.10 | 234.5 (0.98) | 232.9 | 140.2 (0.97) | 136.8 | 78.6 (0.95) | 82.5 |
| 1.00 | 333.6 (0.99) | 336.6 | 203.7 (0.96) | 197.3 | 126.8 (0.95) | 132.1 |

Regarding the analogy between humic substances and polyelectrolytes like PAA, it seems probable that the conformation of the humic acid molecules in solution also influences the conformation of the adsorbed layer, as shown schematically in Fig. 5.20. As an example two cases with "extreme" conditions are discussed. The condition of the first situation is a low electrolyte concentration combined with a high pH value [Fig. 5.20 (a)]. At high pH values most HA functional groups (carboxylic and phenolic) are dissociated causing a high charge density. Due to electrostatic repulsion between these functional groups, HA molecules have a rather extended conformation in the bulk solution. Such an extended conformation is emphasized due to the absence of indifferent electrolyte; no screening by the salt ions occurs. After adsorption the majority of the charged groups of the HA molecules are in the vicinity of the surface, leading to a relatively flat conformation and a relatively low adsorbed amount. The other extreme is a high concentration of electrolyte combined with a low pH value [Fig. 5.20 (b)]. The few charges associated with HA, due to the low degree of dissociation, are screened by the salt ions and consequently the humic acid molecules show a tightly compressed and compact conformation in solution. The humic acid molecules adsorb as

compressed entities and retain their structure resulting in an enhanced adsorption.



(a)                                           (b)
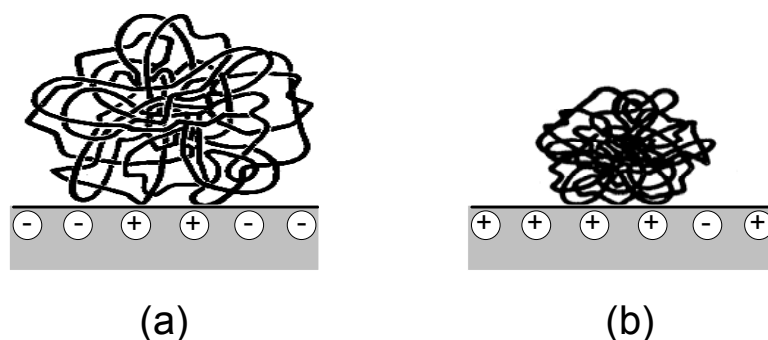
**Fig. 5.20.**     *Schematic representation of the variations of HA network-like conformation at the alumina/water interface under changing pH and ionic strength conditions.(a) low ionic strength and high pH; (b) low pH and high ionic strength.*

By comparing the adsorption isotherms of PAA (Figures 5.14 and 5.16) and HA (Figures 5.17 and 5.18) on alumina, the isotherms showed high affinity sorption at low surface coverage that rapidly reached sorption maxima for PAA, at which the alumina surface is completely covered by PAA. Further adsorption does not occur. This kind of isotherm followed a H-type curve. It could be proved by using the electrophoretic mobility measurements, where as shown in Fig. 5.25, in the plateau region the net negative electrophoretic mobility of alumina particles does not increase by increasing the PAA adsorbed amount. The isotherms of the sorption of HA on alumina followed a L-type curve, in which the isotherm showed high affinity sorption (at up to 60% HA surface coverage) exactly as in the case of PAA adsorption but in the plateau region, by increasing the HA concentration the adsorbed amount increases gradually presumably due to hydrophobic humic-humic interactions resulting in multiple layering of humic acids on alumina which could also be proved by measuring the electrophoretic mobility where the net negative electrophoretic mobility of alumina particles increases gradually by increasing the HA adsorbed amount in the plateau region of the HA adsorption isotherm as shown in Fig. 5.23. Consequently, PAA as a model for the HA adsorption on the mineral surfaces could not be applied in the plateau region.

### 5.3.3  Adsorption of humic acid fractions on alumina

Due to its extreme complexity, the HA was fractionated into three HA fractions to study their adsorption on alumina and to prove the chemical and structural differences between these HA size fractions. These HA fractions are classified as Fr(1,2) larger than 100 000, Fr(3,4) 100 000-30 000 and Fr(5,6) 30 000-3 000 daltons. The adsorption isotherms of Fr(1,2), Fr(3,4) and Fr(5,6) as well as the unfractionated HA on aluminium oxide at pH = 5.5 and 0.01 mol/l $KNO_3$, are shown in Fig. 5.21. All adsorption isotherms showed high affinity sorption at low surface coverage followed by a slight increase in the adsorbed amount in the plateau region, indicating an L-type adsorption isotherm. It is also evident here that the adsorbed amount increases with increasing the HA molecular size [Fr(1,2) > Fr(3,4) > Fr(5,6)] where the maximum adsorbed amounts of Fr(1,2) and Fr(3,4) are about 2.3 and 1.9 times respectively greater than that of Fr(5,6). As shown from the $^{13}$C-NMR results in Fig. 5.22, this observation suggests that the larger HA molecular size fractions which have more aliphatic carbons (more hydrophobic fractions)
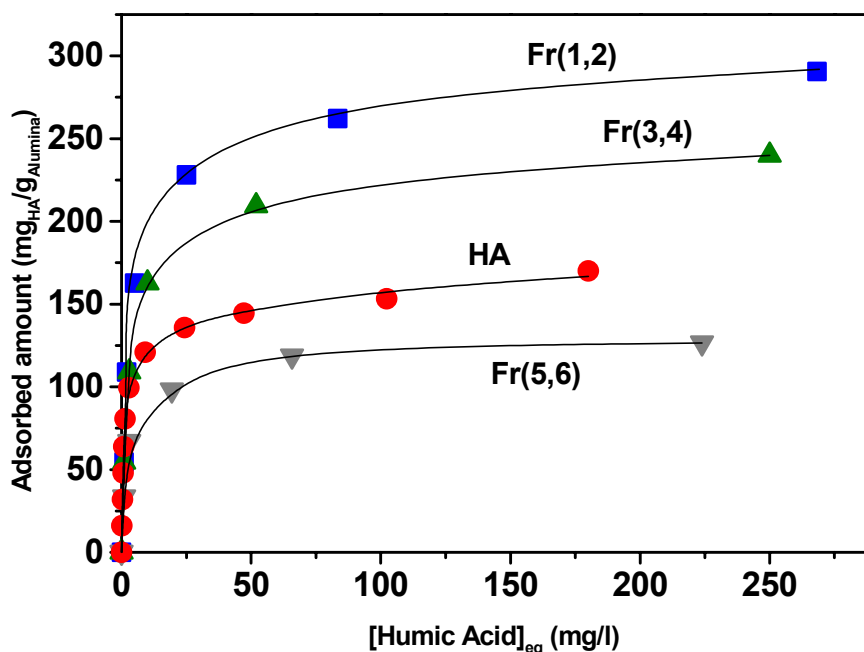


**Fig. 5.21.**    *Adsorption isotherms of humic acid and its fractions onto alumina at pH = 5.5 and 0.01 M KNO₃.*

are stronger adsorbed in comparison to the smaller molecular size fractions (more hydrophilic) which have higher contents of aromatic carbons. Moreover, because the adsorption is site specific through the hydroxyl functional groups on alumina surfaces, only limited numbers of chargeable groups of the three HA fractions may react with the alumina surfaces and by suggesting limited surface sites on alumina surfaces, so lower amount of Fr(5,6) was required to cover up the alumina surfaces compared with the Fr(3,4) and by the same token a lower amount of Fr(3,4) was required compared to Fr(1,2). It is also observed that, the decrease in the rise of the adsorption isotherm in the plateau regions by decreasing the HA fraction size  [from Fr(1,2)  to Fr(5,6)] which indicates a lower contribution of the hydrophobic interactions is due to the decrease in the aliphatic carbons as shown in Fig. 5.22. Similarly, previous workers (53, 70, 166) have directly or indirectly indicated that dissolved humic substances with higher molecular size exhibited higher adsorbed amounts on mineral surfaces compared to the smaller (more hydrophilic) ones.
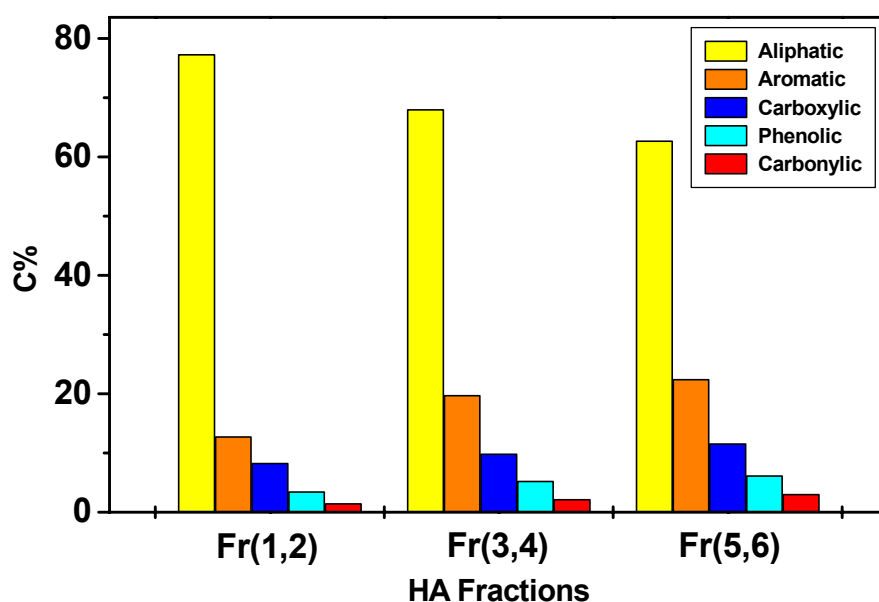


**Fig. 5.22.**    *Aliphatic, aromatic, carboxylic, phenolic and carbonylic carbon contents percentage of the HA fractions as measured by ^{13}C-NMR.*

The adsorption isotherms were modeled with the Langmuir isotherm equation. Monolayer adsorption capacities calculated from the linearized form of the Langmuir equation are summarized in Table 5.9. The most significant trend is the increase in the apparent amounts adsorbed with increasing HA fraction molecular size.

***Table 5.9.***   *Adsorption capacities of HA fractions on alumina evaluated by Langmuir equation.*

| HA fractions | Adsorption capacity, mg/g | |
| --- | --- | --- |
| | **Langmuir (regression)** | **Measured** |
| Fr(1,2) | 263.15 (0.98) | 268.3 |
| Fr(3,4) | 243.9 (0.99) | 240.1 |
| Fr(5,6) | 131.5 (0.99) | 126.6 |

### 5.3.4  Colloidal stability and electrophoretic mobility

Colloids play a decisive role in the distribution and transport of organic and inorganic pollutants in the environment. On the one hand, they are the most reactive constituents of aquatic and soil systems. A large proportion of contaminants are sorbed on their surfaces. On the other hand, colloids as carrier substances, are responsible for the long distance movement (migration or transport) of chemicals, e.g. for the landing of pollutants in the groundwater. Indeed, these transport processes strongly depend on the stability of the colloids (82, 167, 168). The interactions of humic substances with natural minerals constitute a puzzling domain of investigation and because of the heterogeneity of natural systems it is difficult to estimate the

importance of several factors controlling colloidal stability without using model systems. Based on the polyelectrolyte features of humic substances, polyacrylic acid (PAA) is a well defined polymeric substance that can be used as a model compound for the study of HA to facilitate the understanding of the influence of HA on the colloidal stability of alumina particles.

The influence of humic acid on the electrophoretic mobility and particle size of alumina particles in 0.01 M $KNO_3$ as a function of HA adsorbed amount at different pH values (5.5, 7.5 and 9.5) are shown in Figures 5.23 and 5.24. At pH = 5.5 and 7.5 [below the PZC of alumina (pH = 8.8)], pure alumina exhibited positive electrophoretic mobility (Fig. 5.23). As the HA adsorbed amount increased, the electrophoretic mobility decreased significantly causing reversal of surface charge from positive to negative whilst, above the PZC (at pH = 9.5), the addition of humic acid resulted in a strong shift in electrophoretic mobility toward more negative values. The hydrodynamic radius of alumina particles as a function of HA adsorbed amount can be seen in Fig. 5.24. According to the representation here, the colloidal suspension is stabilized when the z-average particle size is equal or close to 215 nm when alumina particles were determined in the absence of humic acid. On the contrary, the system is fully destabilized when its value reaches its maximum. Comparing the measured curves at different pH values containing only 0.01 M $KNO_3$, it is obvious, that pure alumina suspensions remained stable at pH values 5.5 and 7.5 (< PZC of alumina) due to the charge repulsion between the positively charged alumina particles [Fig. 5.27 (a)], but at pH 9.5 (near to the PZC) the negative surface charge on the pure alumina particles is not enough to stabilize the system. The addition of small amounts of humic acid ($\leq$ 63.1 and $\leq$ 24.3 mg HA/g $Al_2O_3$ at pH 5.5 and 7.5, respectively) resulted in aggregation and settling of the particles. Addition of larger amounts of humic acid again increased the colloidal stability due to increased negative surface charge [Fig. 5.27 (c)].
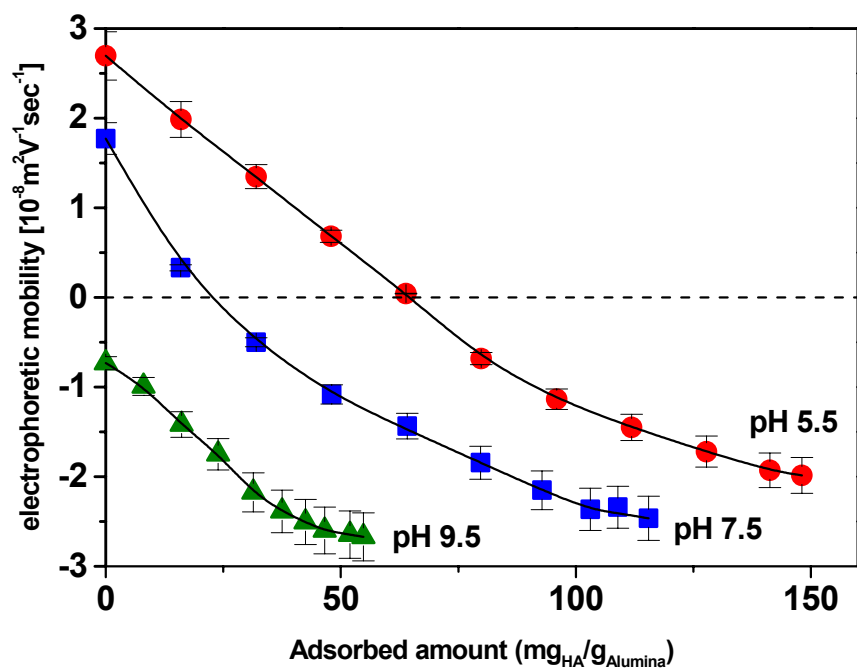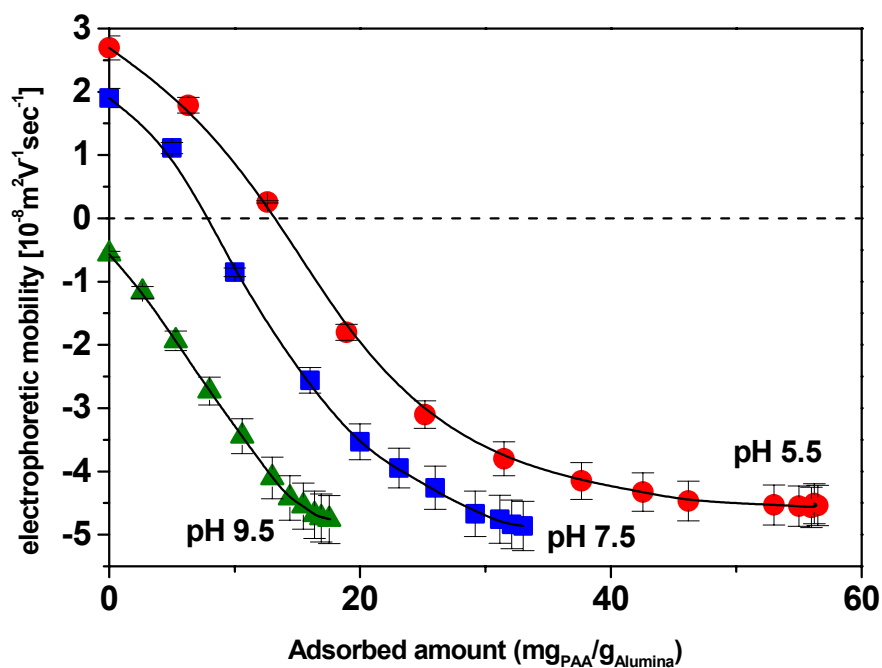
**Fig. 5.23.**    Influence of humic acid on the electrophoretic mobility of alumina at 0.01 M $KNO_3$.
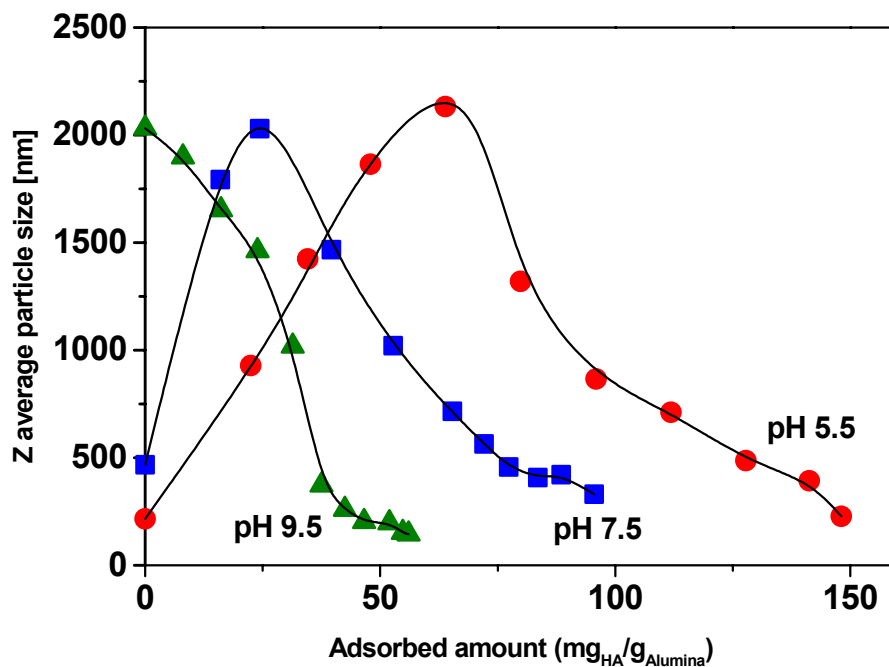


**Fig. 5.24.**    Hydrodynamic diameter of coated alumina particles as a function of HA adsorbed amount at 0.01 M $KNO_3$.

Likewise, Figures 5.25 and 5.26 show the electrophoretic mobility and the hydrodynamic radius of the alumina particles as a function of PAA adsorbed amount at different pH values (5.5, 7.5 and 9.5). Fig. 5.25 shows a rapid decrease in the electrophoretic mobility at PAA concentrations lower than in the case of HA (Fig 5.23). This is because the PAA's charge density is more negative under the given conditions of pH and $KNO_3$ concentration (Figures 5.1 and 5.2). This also results the occurrence of the full destabilization of the system at lower PAA adsorbed amount, as shown in Fig. 5.26, where small amounts of adsorbed PAA result in charge neutralization and destabilization of alumina suspensions compared to that in the case of the $Al_2O_3$/HA system (Fig. 5.24). The influence of humic and polyacrylic acids on the surface charge and colloidal stability of alumina particles is obviously in a quite analogous manner. Nevertheless, a marked difference is observed (Figures 5.23 and 5.25), where adsorption of the HA induces a decrease of the electrophoretic mobility when the HA adsorbed amount increases, whereas the adsorption of PAA induces a plateau value. The phenomenon responsible for the no existence of the electrophoretic mobility plateau in case of HA is presumably due to the hydrophobic humic-humic interactions.

To elucidate the colloidal stability mechanism of alumina particles, the values of electrophoretic mobilities and average particle size of alumina as a function of the HA adsorbed amount are compared in Fig. 5.27. To facilitate the comparison, the optimal HA and PAA flocculation dosages and the isoelectric points (IEPs) are presented in Table 5.10. The optimal flocculation dosages of HA and PAA are shifted to a lower concentration by increasing the pH values. This displacement corresponds exactly to a shift in the IEP of the particles. As shown in Fig. 5.27 and presented in Table 5.10, the results obtained in this study are consistent with the charge neutralization mechanism, where the optimum dosage for flocculation corresponds well to the IEP. This indicates that no electric repulsive forces exist between the alumina particles at this HA dosage (critical dosage of HA) [Fig. 5.27 (b)]. HA or PAA does not cause bridging flocculation because if bridging were important, a smaller dosage of HA or PAA (< IEPs) would be expected to flocculate the alumina particles at

**Fig. 5.25.** *Influence of PAA on the electrophoretic mobility of alumina at 0.01 M KNO₃.*
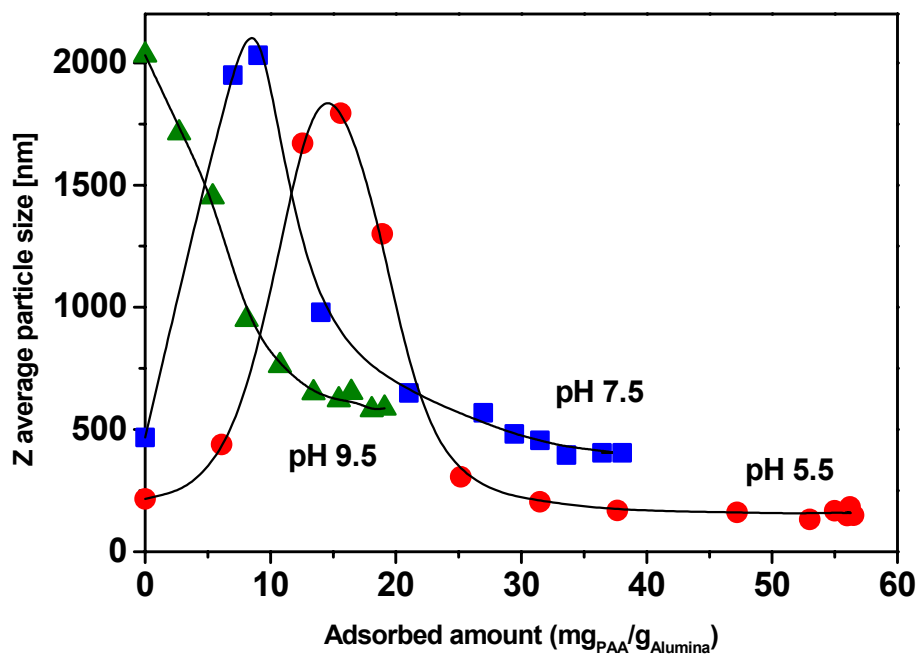


**Fig. 5.26.** *Hydrodynamic diameter of coated alumina particles as a function of PAA adsorbed amount at 0.01 M KNO₃.*

pH 7.5, where the conformation of HA or PAA is relatively expanded. The expanded HA or PAA could bridge the particles together. This is clearly contrary to the experimental observation made here. The flocculation is then mainly due to electrostatic interactions and the classic bridging mechanism plays an insignificant role in the present system.
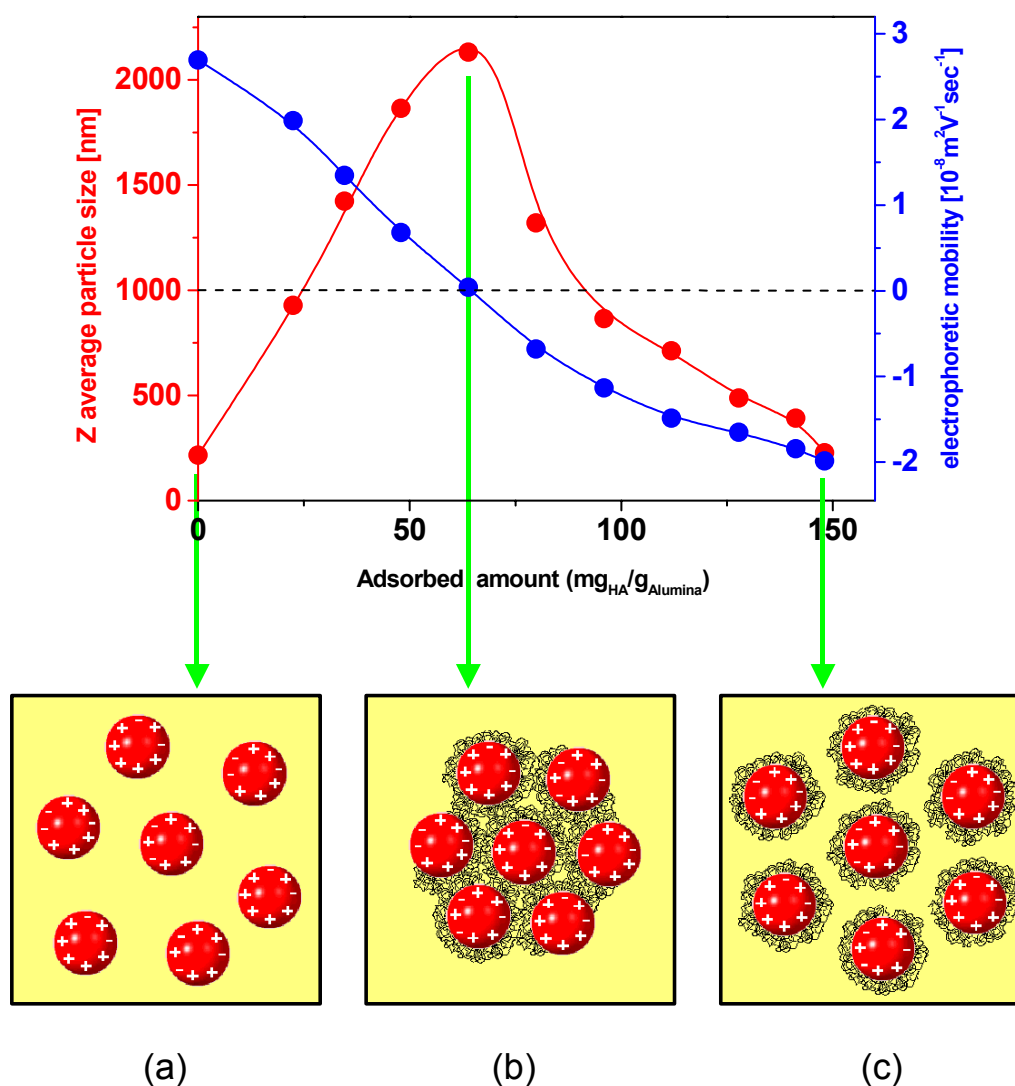


**Fig. 5.27.** *Schematic representation of the alumina particles stability at different HA coverage. (a) stabilization by electrostatic repulsion, (b) flocculation by charge neutralization, (c) restabilization by electrostatic repulsion.*

***Table. 5.10.*** *Optimal aggregation dosage and IEP in terms of relative HA and PAA concentrations (mg/g $Al_2O_3$).*

| pH values | HA | | PAA | |
|---|---|---|---|---|
| | 5.5 | 7.5 | 5.5 | 7.5 |
| Optimal aggregation dosage | 63.1 | 24.3 | 14.5 | 8.5 |
| IEP | 64.0 | 23.5 | 13.6 | 8.1 |

## 5.4. Interactions between 2,4-Dichlorophenol and HA/$Al_2O_3$ complexes

Naturally occurring soil colloids are multicomponent associations of minerals and organic matter (67, 71, 169). Organic matter modifies the hydrophilic/hydrophobic character of the mineral surfaces making them more hydrophobic and, therefore, more reactive to hydrophobic organic compounds (HOCs). Although some studies have addressed the interaction between HOCs and HA, much of them still remains unclear. This is partially due to the fact that systematic investigations in a wide range of environmental conditions are often thwarted by the experimental difficulty that humic acid, partially dissolves at natural pH and that there are only a few approaches by which the concentrations of the HOC can be readily measured in the presence of dissolved HA. One way to avoid this complication is to use immobilized humic acid by adsorbing it on alumina to form a HA/$Al_2O_3$ complex. Since this kind of complex can be easily separated from the supernatant, the measurement of the adsorption of 2,4-dichlorophenol (2,4-DCP) in this study becomes easy and is not influenced by the dissolved HA. Moreover, immobilized HA on $Al_2O_3$ can be studied in a wide range of environmental conditions such as pH and ionic strength as shown below.

Because the conformation and polarity of HA play an important role in its adsorption onto alumina (as described before in 5.3.2) and its ability to bind 2,4-DCP at the solid/liquid interface, a systematic study of the effects of pH and ionic strength was undertaken.

The sorption isotherms of 2,4-DCP on alumina that had been coated with different amounts of HA at pH 5.5 and ionic strength 0.01 M KCl are shown in Fig. 5.28. In these experiments, $f_{oc}$ values were varied over the range 0.0128-0.0599 (30-140 mg HA/g $Al_2O_3$) to encompass the low organic carbon concentrations found in soil. The adsorption of 2,4-DCP on the bare alumina is very low (the maximum measured adsorbed amount was 0.034 μmol DCP/g $Al_2O_3$ at 0.52 mmol/l equilibrium concentration of 2,4-DCP), while on HA/$Al_2O_3$ complexes the sorption is governed by the amount of adsorbed humic acid and expressed as μmol DCP/g HA/$Al_2O_3$ complex. The bound 2,4-DCP amounts increased by increasing the surface coverage with HA, but the general course of the isotherms were similar. These sorption isotherms can be described as a linear isotherm, which indicates a partitioning process between the 2,4-DCP and HA/$Al_2O_3$ complex or is due to physical trapping in the microvoids of the network of the adsorbed HA (170, 171). The sorption process can be discussed in terms of sorption coefficients that are
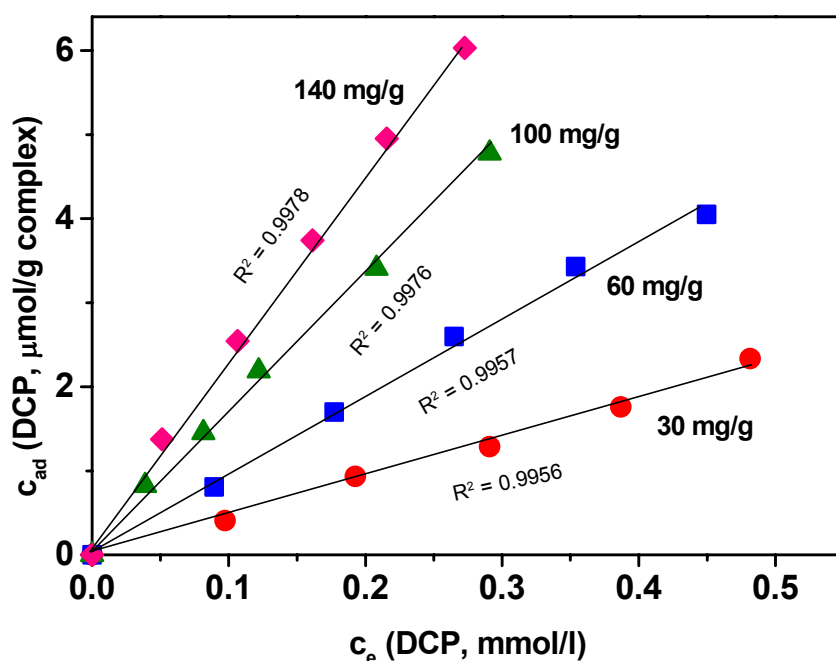


**Fig. 5.28.**    *Sorption isotherms of 2,4-dichlorophenol onto HA/$Al_2O_3$ complexes (30-140 mg HA/g $Al_2O_3$) at pH = 5.5 and 0.01 M KCl. Symbols represent experimental data and lines represent regression fits of respective isotherm equation.*

characteristic of the individual systems. The $R^2$ values (goodness of fit criterion) computed by linear regression for the adsorption isotherms are also presented in Fig. 5.28 for each complex.

The sorption coefficients are summarized in Table 5.11. When these values were plotted against the organic carbon fraction of the complexes, $f_{oc}$ (Fig. 5.29), the results indicate a linear relationship ($R^2$ = 0.9974). The slope of line is the organic carbon normalized partition coefficient with a value $K_{oc}$ = 373 ml/g or *log* $K_{oc}$ = 2.572. This is in good agreement with the $K_{oc}$ values reported in the extensive literature data for sorption of 2,4-dichlorophenol by soils and sediments (172) whilst it is a little bit lower than the value of 2.75 which was estimated mathematically (173) and those of 2.84 and 2.89 which were estimated experimentally in refs (174 and 175), respectively.

The above critical comparison verifies that the $K_{oc}$ values of the present study are reasonable. The reason for the smaller sorption constants (*log* $K_{oc}$ values shown in Table 5.11) obtained in the present study compared to the literature values is probably due to the slightly different soil conditions in which the HA was found.

**Table 5.11.** *Sorption coefficients of 2,4-DCP on the HA/Al$_2$O$_3$ complexes with different surface coverage.*

| HA/Al$_2$O$_3$ complexes | Sorption coefficients | | |
|---|---|---|---|
| | $K_d$ | $K_{oc}$ | log $K_{oc}$ |
| 30 mg/g | 4.56 | 354.8 | 2.550 |
| 60 mg/g | 9.26 | 357.5 | 2.553 |
| 100 mg/g | 16.04 | 382.0 | 2.582 |
| 140 mg/g | 21.99 | 367.1 | 2.564 |
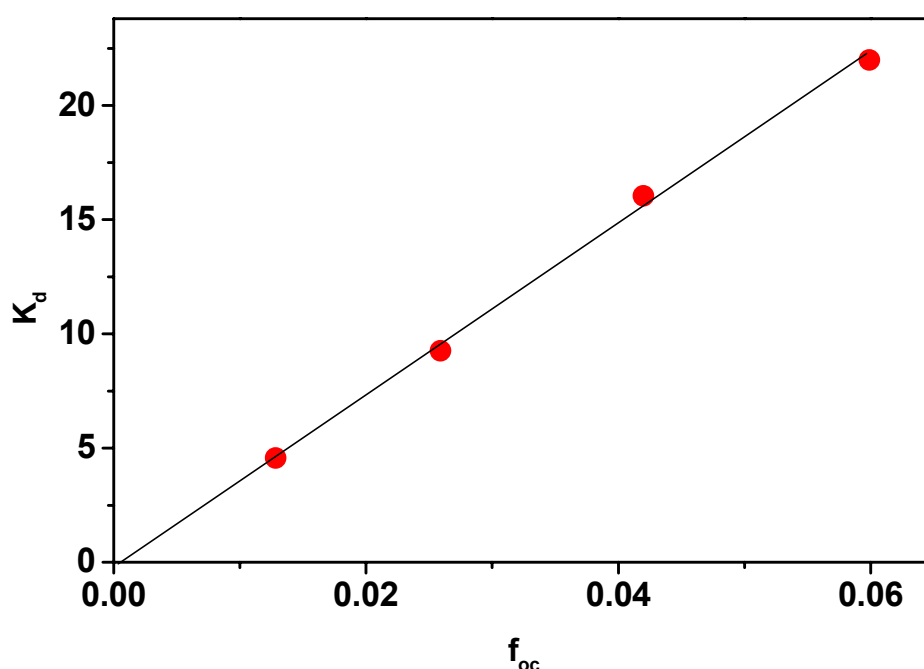
**Fig. 5.29.** *Dependence of 2,4-DCP sorption coefficient on the organic carbon fraction, $f_{oc}$.*

The effects of varying aqueous chemistry conditions on the sorption of 2,4-DCP on the HA/Al$_2$O$_3$ complexes which contains the smallest HA coverage (30 mg HA/gAl$_2$O$_3$, $f_{oc}$ = 0.0128) are shown in Figures 5.30 and 5.31 and the calculated partition coefficients at different pH and ionic strength values are listed in Table 5.12. They demonstrate that the magnitudes of the sorption coefficients of 2,4-DCP are strongly pH and ionic strength dependent (176, 177, 178-181). Figure 5.30 presents the adsorption isotherms for 2,4-DCP at three different pH values and at 0.01 M KCl. The sorption of 2,4-DCP decreases with increasing pH value. The decrease in the binding capacity with increasing pH is due to the dissociation of 2,4-DCP. The greatest adsorption occurs at pH 5.5, where most of the 2,4-DCP is present as the neutral phenol [pK= 7.85 (182)]. Considerably less adsorption occurs at pH 6.5 and 7.5 where the phenolate form is also present in solution ($\alpha$ = 4.27% and 30.87% at pH 6.5 and pH 7.5, respectively, that were estimated according to $\alpha = 1/(1+10^{(pK_a - pH)})$ (183). The increase of the pH
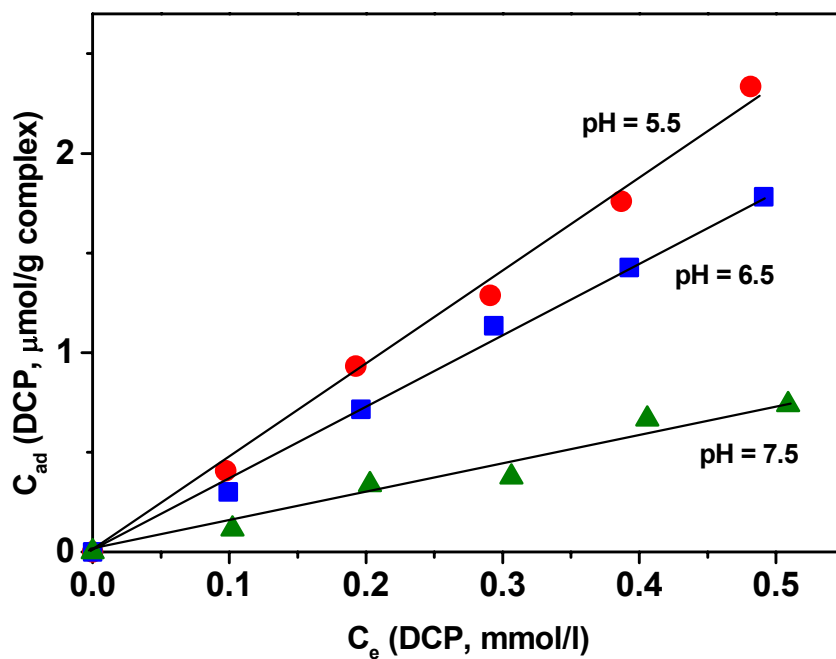
**Fig. 5.30.**     *Adsorption isotherms of 2,4-DCP on 30 mg HA/g Al$_2$O$_3$ complex at 0.01 M KCl and different pH values.*
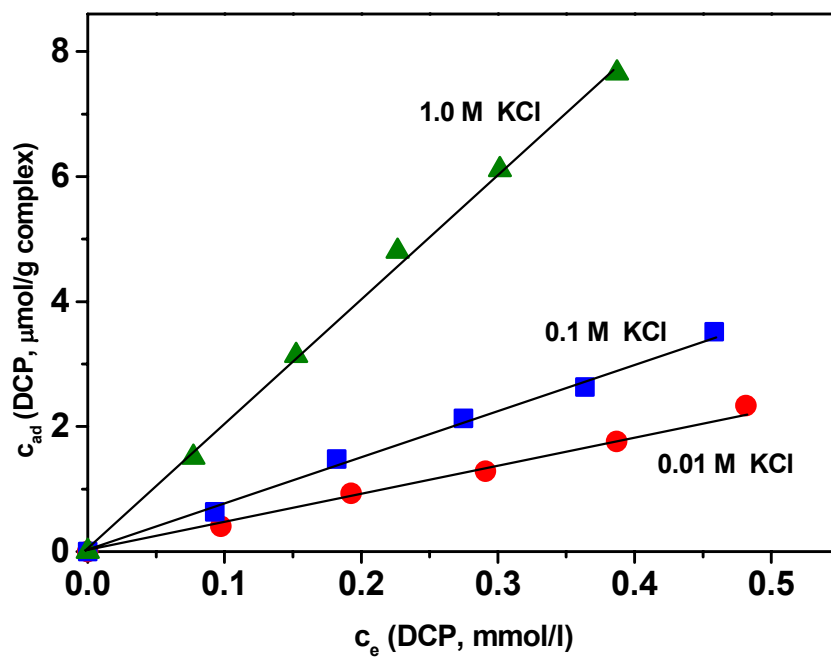


**Fig. 5.31.**     *Adsorption isotherms of 2,4, DCP on 30 mg HA/g Al$_2$O$_3$ complex at different ionic strengths and pH = 5.5.*

caused also a deprotonation of functional groups in the HA. Hence, both effects have to be considered responsible for the decreased sorption. On the one hand, the electrostatic repulsion increases between 2,4-DCP and HA/$Al_2O_3$. On the other hand, the hydrophobicity of the 2,4-DCP was decreased. Furthermore, it is also attractive to consider the change of the conformation of the HA to a more expanded form (see Fig. 5.20) leading to an overall loss of hydrophobic cavities for the sorption.

Similarly, at fixed pH value (pH 5.5) the adsorption of 2,4-DCP increases with an increase of the ionic strength according to Fig. 5.31. Such an increase is attributed to the screening effect (184). The higher the ionic strength, the better the screening of the electrostatic repulsion between the functional groups in the HA and the higher the bound amount of 2,4-DCP. Besides this, the adsorption ability of 2,4-DCP may also increase with ionic strength owing to the salting-out effect (82).

***Table.5.12.*** *2,4-DCP sorption isotherm parameters on the 30 mg HA/g $Al_2O_3$ complexes at different pH and ionic strength values.*

| Conditions | Sorption coefficients | | | | | | | | |
|---|---|---|---|---|---|---|---|---|---|
| $C_{KCl}$ mol/l | pH = 5.5 | | | pH = 6.5 | | | pH = 7.5 | | |
| | $K_d$ | $K_{oc}$ | log $K_{oc}$ | $K_d$ | $K_{oc}$ | log $K_{oc}$ | $K_d$ | $K_{oc}$ | log $K_{oc}$ |
| 0.01 | 4.56 | 354.8 | 2.550 | 3.50 | 272.0 | 2.435 | 1.471 | 114.4 | 2.058 |
| 0.10 | 7.58 | 589.7 | 2.771 | — | — | — | — | — | — |
| 1.00 | 20.02 | 1558.4 | 3.192 | — | — | — | — | — | — |

To demonstrate the role of the bound HA conformation and due to the available sorption domains in the binding of organic pollutants, the polarity parameter ($I_1/I_3$ ratio) of a non-polar hydrophobic organic compound (pyrene) on the bound HA was investigated. It is expected that the conformation changes depending on the solution parameters affect the sorption ability of

HA for HOC. The $I_1/I_3$ ratio of pyrene in the aqueous suspension of the 30 mg HA/Al$_2$O$_3$ complex at different pH and ionic strength values is shown in Fig. 5.32. It was found that, the hydrophobicity of the bound HA decreases (high $I_1/I_3$ ratio) by increasing the pH value or decreasing the ionic strength. As the pH increases or the ionic strength decreases, the enhanced ionization of HA may induce mutual repulsion among the negatively charged functional groups on it and the conformation of the HA is in a more stretched form as well. The "hydrophobic domains" of the HA are reduced by this change in conformation and the $I_1/I_3$ ratio is then increased. Similarly, by decreasing the pH value or increasing the ionic strength the negative charges on HA are screened and consequently the humic molecules show a tightly compressed and compact conformation, possibly altering the size of the "hydrophobic domains" which makes the pyrene environment more hydrophobic leading to a decrease of the $I_1/I_3$ ratio.
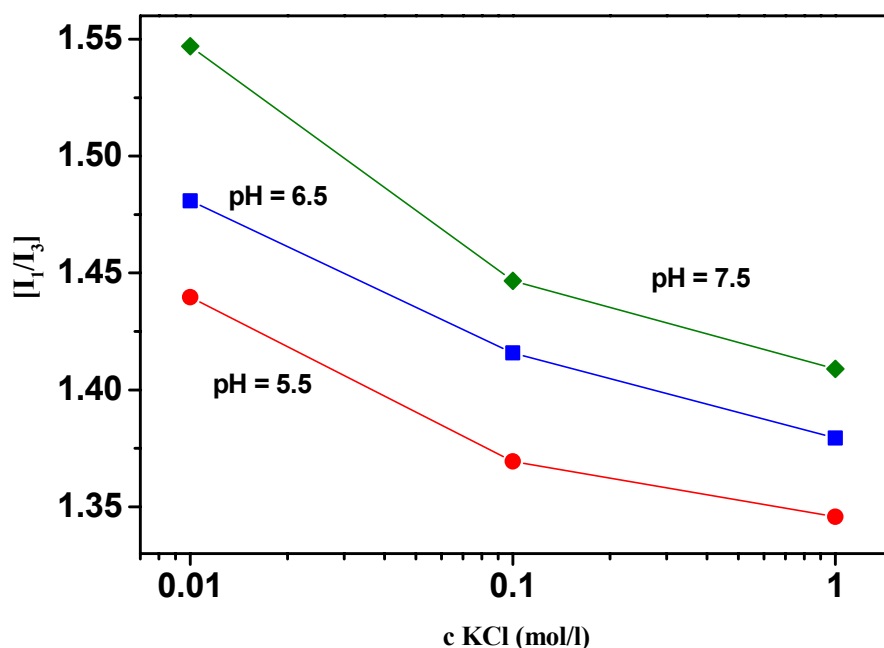


**Fig. 5.32.**     *Fluorescence intensity ratio ($I_1/I_3$) of pyrene in presence of 30 mg HA/g Al$_2$O$_3$ complex at different pH and ionic strength values.*

# 6    Summary

The aim of the present study was to investigate the effects of the interactions between two important soil components, mineral oxides and humic substances, on the sorption of the hydrophobic organic compounds (HOCs) under laboratory conditions selected to model the soil systems. The model system used in this study consisted of aluminum oxide and an  extracted  soil humic   acid (HA). 2,4-dichlorophenol (2,4-DCP) was taken as a HOC contaminant model.

Due to the extreme complexity of HA, it is difficult to elucidate the sorption mechanisms of HOCs to HA based on its currently measured structural characteristics. An alternative technique to decrease the chemical heterogeneity prior to sorption investigations is the fractionation of the HA. The HA was fractionated by using the ultrafiltration technique into eight different molecular size fractions. HA and its fractions were characterized using potentiometric acid-base titration, elemental analysis and different spectroscopic methods (NMR, UV-VIS and FT-IR spectroscopy) to obtain more information on the chemical structures and the functional groups of these macromolecules. The results presented in this work revealed that the elemental composition, the degree of aromaticity, and the amounts of major functional groups changed with the apparent molecular weight of the fractions. The general progression of changes in the chemical character of the fractionated HA with decreasing molecular size is a decrease in aliphatic carbon and an increase in chargeable groups. Moreover, the smaller humic acid fractions have larger content of aromatic carbon.

The differences in the structural characteristics, chemical environments and functional group contents of the HA fractions affect the adsorption of HOCs. Solid-state $^{19}$F-NMR was used to study the sorptive uptake of Hexafluorobenzene (HFB) by the humic acid and its fractions. It was found that HA molecules have different chemical environments into which HOCs such as HFB can sorb. Small HA molecules have at least three sorption sites

("rigid", "soft" and other new domains) that are more clearly defined and homogeneous than the sorption domains found in larger HA molecules. The larger molecular weight fractions are dominated by a rigid sorption domain. It is proposed that this sorption domain may result from regions composed of aliphatic moieties. The presence of these different sorption domains gives evidence that the interactions of HA and HOC cannot be strictly viewed as a simple partitioning process.

The adsorption of soil extracted HA on colloidal-sized aluminium oxide particles was investigated to elucidate how solution chemistry affects the formation and nature of organic surface coatings. A systematic study of the effects of pH and ionic strength on HA adsorption was performed. To better understand the binding mechanisms these results were compared to those of polyacrylic acid (PAA). The amount of HA and PAA adsorbed onto aluminium oxide particles decreased with increasing pH values for all solutions of constant ionic strength. In $KNO_3$ solutions at fixed pH values, the adsorption of HA and PAA generally increased with increasing ionic strength. This suggests that the conformation of the HA or PAA in solution significantly determines their structures on the mineral surface. At high pH and low salt concentration the HA or PAA molecules are adsorbed in a relatively stretched form on the surface and the adsorption was low, whilst, at low pH and high salt concentration a substantial fraction of the adsorbed HA or PAA is collapsed on the surface, which results in a relatively high adsorbed amount. In general, the surface complexation ligand exchange is the most important adsorption mechanism of HA and PAA onto the alumina particles regardless of solution chemistry.

By comparing the adsorption isotherms of HA and PAA on alumina, it was found that the PAA as a model for the HA adsorption on the mineral surfaces could not be applied in the plateau region because the PAA adsorption isotherms on alumina is of H-type while the HA adsorption isotherms follow the Langmuir-type (L) curve. The HA isotherms showed high affinity sorption at low surface coverage exactly as in the case of PAA adsorption but in the plateau region the HA adsorbed amount increases gradually

presumably due to hydrophobic humic-humic interactions resulting in multiple layering of humic acids on alumina.

By comparing the adsorption of the HA fractions on alumina surfaces, it was found that the adsorbed amount increases with increasing HA molecular size. The adsorption isotherms are of the L-type curves. Furthermore, an increase in the rise of the adsorption isotherm in the plateau regions by increasing the HA fraction size was also observed which indicates a higher contribution of the hydrophobic interactions (hydrophobic humic-humic interactions) due to the increase in the aliphatic carbon and the decrease in the chargeable groups.

The colloidal stability of the alumina dispersions containing increasing amounts of added HA and PAA was monitored using the dynamic light scattering technique. The maximum aggregate size was observed around the zero electrophoretic mobility indicating the importance of the charge neutralization mechanism, whilst the bridging mechanism does not seem to play a significant role in the studied system.

The sorption results of 2,4-dichlorophenol (2,4-DCP) on the immobilized humic acid at different pH and salt concentrations revealed that the value of the sorption coefficient decreases as the ionic strength decreases or the pH value increases which gives direct evidence for the importance of the conformation of the immobilized HA. These sorption isotherms can be described as a linear isotherm, which indicates that the sorption of 2,4-DCP is predominantly a partitioning process between the aqueous phase and the immobilized humic acid.

# 7.  References

(1)     W. Stumm and J.J. Morgan, Aquatic Chemistry, $2^{nd}$ ed., Wiley-Interscience, New York, (1981).

(2)     T.C. Voice and W.J. Weber, Water Res., 17, 1433, (1983).

(3)     W. Stumm, R. Schwarzenbach and L. Sigg, Angew. Chem., 22, 380, (1993).

(4)     F.J. Stevenson, Humus Chemistry, Genesis, Composition, Reactions, Wiley, New York, (1994).

(5)     C.T. Chiou, Partition Coefficient and Water Solubility in Environmental Chemistry. In: *Hazard Assessment of Chemicals: Current Developments.* J. Saxena and F. Fisher (Eds.). New York, Academic Press. 1: pp. 117-153, (1981).

(6)     J.J. Pignatello, Competitive Effects in the Sorption of nonpolar Organic Compounds by Soils. In: *Organic Substances and Sediments in Water.* M.I. Chelsea (Eds). Lewis Publishers. 1: pp. 291-309, (1989).

(7)     B. Xing, Nonlinearity and Competitive Sorption of Hydrophobic Organic Compounds in Humic Substances. In: *Humic Substances: Structures, Properties and Uses.* G. Davis, E.A. Gabbour and K.A. Khairy (Eds.). Cambrige, UK, The Royal Society of Chemistry, pp. 173-183, (1998).

(8)     A.E. Boekhold, S.E.A.T.M. Van der Zee and F.A.M. De Haan, Water, Air, Soil Pollut. 57/58, 479, (1991).

(9)     E.M. Murphy, J.M. Zachara, S.C. Smith, J.L. Philips and T.W. Wietsma, Environ. Sci. Technol., 28, 1291, (1994).

(10)    J.L. Zhou, S.J. Rowland, J. Braven, R.F.C. Mantoura and B.J. Harland, Int. J. Env. Anal. Chem. 58, 275, (1995).

(11)    G.A. Keoleian, R.L. Curl, Effects of Humic Acid on the Adsorption of Tetrachlorobiphenyl by Kaolinite, In: *Aquatic Humic Substances: Influence on Fate and Treatment of Pollutants*, I.H. Suffet and P. MacCarthy (Eds.), Acs Symp. Ser. 219, pp. 231-250, (1989).

(12)    G.R. Aiken, D.M. McKnight, R.L. Wershaw and MacCarthy, In: *Humic Substances in Soil, Sediment and Water*, G.R. Aiken, P. MacCarthy, R.L. Malcolm and R.S. Swift (Eds.), Wiley, New York, (1985).

(13)    M.H.B. Hayes, P. MacCarthy, R.C. Malcolm, and R.S. Swift (Eds.). Structures of Humic Substances: The Emergence of 'Forms'. In: *Humic*

*Substances II: In Search of Structure*, Part II, Wiley, Chichester, pp. 689-733, (1989).

(14)   M. Schnitzer, S.U. Khan, Humic Substances in the environment, Marcel Decker Inc. New York, (1972).

(15)   J. Buffle, Natural Organic Matter and Metal-organic Interactions in Aquatic Systems, In: *Metal Ions in Biological Systems*; H. Sigel (Ed.); Marcel Dekker: New York, pp. 165-221, (1984).

(16)   J. Buffle, Complexation Reactions in Aquatic Systems: An Analytical Approach; Ellis Horwood Limited: Chichester, (1988).

(17)   M.H.B. Hayes and R.S. Swift, In: *The Chemistry of Soil Constituents*, D.J. Greenland and M.H.B. Hayes (Eds.). Wiley, Chichester, pp. 179-320, (1978).

(18)   N.C. Brady, The Soil Around Us. In: *The Nature and Properties of soils*. New York, Macmillan Publishing Company: pp. 1-21, (1990).

(19)   R.S. Swift, Advances in Soil Organic Matter Research: The Impact on Agriculture and The Environment, W.S. Wilson (Ed.), The Royal Society of Chemistry, Cambridge, UK, 153, (1991).

(20)   W. Flaig, In: *Humic Substances, Peats and Sludges: Health and Environmental Aspects*, M.H.B. Hayes and W.S. Wilson (Eds.), The Royal Society of Chemistry, Cambridge, UK, 346, (1997).

(21)   B.E. Watt, R.L. Malcolm, M.H.B. Hayes, N.W.E. Clark and J.K. Chipman, Water Res., 6, 1502, (1996).

(22)   D.L. MacDonald and J.K. Chipman, In: *Humic Substances, Peats and Sludges: Health and Environmental Aspects*, M.H.B. Hayes and W.S. Wilson (Eds.), The Royal Society of Chemistry, Cambridge, UK, 337, (1997).

(23)   M.H.B. Hayes and R.S. Swift, In: *Soil Colloids and Their Associations in Aggregates*, M.F. DeBoodt, M.H.B. Hayes and A. Herbillon (Eds.), Plenum, New York, 245, (1990).

(24)   P. MacCarthy, C.E. Clapp, R.L. Malcolm and P.R. Bloom, An Introduction to Soil Humic Substances. In: *Humic Substances in Soil and Crop Sciences: Selected Readings*, American Society of Agronomy, Inc., Soil Science Society of America, Inc., pp. 1-12, (1990).

(25)   F. Scheffer and P. Schachtschabel, Lehrbuch der Bodenkunde, Ferdinand Enke Verlag, Stuttgart, 14. Aufl., (1988).

(26)    M. Schnitzer, S.U. Khan, Characterization of Humic Substances by Physical Methods. In: Humic Substances in the environment, Marcel Decker Inc. New York, pp. 55-133, (1972).

(27)    J.A. Rice and P. MacCarthy, Characterization of Stream Sediment Humin. In: *Aquatic Humic Substances: Influence on Fate and Treatment of Pollutants*. I.H. Suffet and P. MacCarthy (Eds.), American Chemical Society, pp. 41-54, (1989).

(28)    J.A. Rice and P. MacCarthy, A Model of Humin. Environ. Sci. Technol., 24, 1875, (1990).

(29)    J.A. Rice, Studies on Humus: 1. Statistical Studies on the Elemental Composition of Humus 2. The Humin Fraction of Humus. Dissertation Colorado School of Mines, Golden, CO, (1986).

(30)    K. Malekani, Organic Architecture of Humin, Dissertation South Dakota State University, SD, (1997).

(31)    F.J. Stevenson, In: *Cycles of Soil*, John Wiley & Sons, Inc., 346, (1986).

(32)    W. Flaig, In Report of FAO/IAEA Technical Meeting, Pergamon. Elmsford, NY, 103, (1966).

(33)    M.M. Kononova, Soil Organic Matter, Pergamon. Elmsford, NY, (1966).

(34)    C.E. Clapp, M.H.B. Hayes, N. Senesi, S.M. Griffith (Eds.), Humic Substances and Organic Matter in Soil and Water Environments: Characterization, Transformations and Interactions. St. Paul, MN: IHSS; (1996).

(35)    M. Schnitzer, H.R. Schulten, Adv. Agron., 55, 167, (1995).

(36)    H.R. Schulten, M. Schnitzer, Naturwissenschaften, 80, 29, (1993).

(37)    K. Ghosh and M. Schnitzer, Soil Sci. 129(5), 266, (1980).

(38)    R.S. Cameron, B.K. Thornton, R.S. Swift, and A.M. Posner, J. Soil Sci. 23(4), 394, (1972).

(39)    H.R. Schulten, Fresenius Anal. Chem., 351, 62, (1995).

(40)    Y. Chen and M. Schnitzer, Soil Sci. Soc. Am. J. 40, 866, (1976).

(41)    P.K. Cornel, R.S. Summers, and P.V. Roberts, J. Colloid Interface Sci., 110(1), 149 (1986).

(42)   R.S. Summers and P.V. Roberts, J. Colloid Interface Sci., 122(2), 367 (1988).

(43)   R.S. Swift, Fractionation of Soil Humic Substances, In: *Humic Substances in Soil, Sediment and Water*. G.R. Aiken, D.M. McKnight, R.L. Wershaw, P. McCarthy, (Eds.), Wiley. New York; pp. 387-408. (1985).

(44)   P. Burba, B. Aster, T. Nifant'eva, V. Shkinev and B.Ya. Spivakov, Talanta, 45, 977, (1998).

(45)   T.I. Nifant'eva, V.M. Shkinev, B.Y. Spivakov and P. Burba, Talanta, 48, 257, (1999).

(46)   E. Tombácz, Soil Science, 164, 814, (1999).

(47)   S. Silva, B. Zanetti, E. Burzoni, G. Dell'Agnola and S. Nardi, Agrochimica, 25, 131, (1981).

(48)   R.S. Summers, P.K. Cornel and P.V. Roberts, Science of the Total Environment, 62, 27, (1987).

(49)   R.S. Swift, R.L. Leonard, R.H. Newman, and B.K.G. Theng, Science of the Total Environment , 117/118, 53, (1992).

(50)   S. Lakhman, R. Mills and H. Patterson, Analytica Chimica Acta, 282, 101, (1993).

(51)   J.C. Lobartini, G. A. Orioli and K.H. Tan, Comminucations in Soil Science Plant Analysis, 28, 787, (1997).

(52)   I. Cristl, H. Knicker, I. Kogel-Knabner and R. Kretzschmar, European Journal of Soil Science, 51, 617, (2000).

(53)   J.A. Davis and R. Gloor, Environ. Sci. Technol., 15(10), 1223, (1981).

(54)   J. John, B. Salbu, E. Gjessing and H. Bjoerrstad, Water Res., 22, 1381, (1988).

(55)   T. Tanaka and M. Senoo, Mater. Res. Soc. Symp. Proc., 353 1013, (1995).

(56)   J. Buffle, D. Perret and M. Newman, In: *Environmental Particles*, vol. 1 J. Buffle, H.P. van Leeuwen (Eds.), Lewis, Boca Raton, FL, pp. 171–220, (1992).

(57)   J. Buffle, Complexation Reactions in Aquatic Systems—An Analytical Approach, E. Horwood, Chichester, pp. 570–591, (1988).

(58)  C.H. Giles, D. Smith and A. Huitson, J. Colloid Interface Sci. 47, 755, (1974).

(59)  C.H. Giles, A.P.D'Silva and I.A. Easton, J. Colloid Interface Sci., 47, 766 (1974).

(60)  M.A. Cohen Stuart, G.J. Fleer and B.H. Bijsterbosch, J. Colloid Interface Sci. 90(2), 310, (1982).

(61)  L.K. Koopal, J. Colloid Interface Sci., 83(1), 116, (1981).

(62)  M.A. Cohen Stuart, J.M.H.M. Scheutjens and G.J. Fleer, J. Polm. Sci. Polym. Phys. Ed., 18, 559, (1980).

(63)  V. Hlady, J. Lyklema and G.J. Fleer, J. Colloid Interface Sci., 87(2), 395, (1982).

(64)  E. Jenkel and B. Rumbach, Z. Elektrochem., 55, 612, (1951).

(65)  G.J. Fleer, M.A. Cohen Stuart, J.M.H.M. Scheutjens, T. Cosgrove and B. Vincent (Eds.), In: *Polymers at Interfaces*, Chapman and Hall, New York, (1993).

(66)  M.A. Cohen Stuart, G.J. Fleer, J. Lyklema, W. Norde, and J.M.H.M. Scheutjens, Adv. Colloid Interface Sci., 34, 477, (1991).

(67)  J.L. Zhou, S.J. Rowland, R. Fauzi, R.F.C. Mantoura and J. Braven, Water Res., 28(3), 571, (1994).

(68)  M.T. Wais Mossa and M. Mazet, Env. Technol. 12, 725, (1991).

(69)  D.M. McKnight, R.L. Wershaw, K.E. Bencala, G.W. Zellweger and G.L. Feder, Sci. Total Environ., 117/118, 485, (1992).

(70)  B. Gu, J. Schmitt, Z. Chen, L. Liang and J.F. McCarthy, Environ. Sci. Technol., 28(1), 38, (1994).

(71)  G. McD. Day, B.T. Hart, I.D. McKelvie and R. Beckett, Colloids Surfaces, 89, 1, (1994).

(72)  E. Tipping, Geochim. Cosmochim. Acta, 45, 191, (1981).

(73)  T.D. Waite, I.C. Wrigley and R. Szymczak, Environ. Sci. Technol. 22(7), 778 (1988).

(74)  E. Tombácz, M. Gilde, I. Ábrahám and F. Szántó, Applied Clay Sci., 5, 101, (1990).

(75)  E. Tombácz, M. Gilde, I. Ábrahám and F. Szántó, Applied Clay Sci., 3, 31, (1988).

(76)   K. Makoto, Soil Sci. Plant Nutr. (Tokyo), 41(2), 215 (1995).

(77)   A. Amirbahmanand and T.M. Olson, Colloids Surfaces, 95, 249, (1995).

(78)   G. Sposito, The Surface Chemistry of Soils. Oxford University Press, New York. (1984).

(79)   M.A. Schlautman and J.J. Morgan, Geochim. Cosmochim. Acta, 58(20), 4293, (1994).

(80)   J.A. Davis, Geochim. Cosmochim. Acta, 46, 2381, (1982).

(81)   G. Sposito, The Chemistry of Soils. Oxford University Press, New York. (1989).

(82)   E.M. Murphy, J.M. Zachara and S.C. Smith, Environ. Sci. Technol., 24, 1507, (1990).

(83)   R.R. Engebertson, R.V. Wandruszka, Environ. Sci. Technol. 28(11), 1934 (1994).

(84)   R. Amal, J.A. Raper and T.D. Waite, J. Colloid Interface Sci., 151(1), 244, (1992).

(85)   A. Calderbank, Reviews of Environmental Contamination and Toxicology, 108, 71, (1989).

(86)   R.P. Schwarzenbach, P. M. Gschwend, and D.M. Imboden, Environmental Organic Chemistry; John Wiley: New York, pp 255-284, (1993).

(87)   C.T. Chiou, Theoretical considerations of the partition uptake of nonionic organic compounds by soil organic matter. In: *Reactions and Movement of Organic Chemicals in Soils*. B.L. Sawhney, K. Brown (Eds.). Madison, WI: Soil Science Society of America, American Society of Agronomy, 1, (1989).

(88)   J.J. Pignatello, In: *Organic Substances and Sediments in Water*, Lewis Publishers. Chelsea, MI, p. 291, (1991).

(89)   P.M. McGinley, L.E. Katz, W.J.Jr. Weber, Environ. Sci. Technol., 27, 1524, (1993).

(90)   S.W. Karickhoff, D.S. Brown and T.A. Scott, Water Res., 13, 241, (1979).

(91)   D.H. Freeman and L.S. Cheung, Science, 214, 790, (1981).

(92)   S.W. Karickhoff, J. Hydraul. Eng., 110, 707, (1984).

(93)   P.J. Flory, J. Chemical Physics, 19, 51, (1942).

(94)   M.A. Schlautman and J.J. Morgan, Environ. Sci. Technol., 27, 961, (1993).

(95)   B. Xing, J.J. Pignatello and B. Gigliotti, Environ. Sci. Technol., 30, 2432, (1996).

(96)   D.W. Rutherford, C.T. Chiou and D.E. Kile, Environ. Sci. Technol., 26, 336, (1992).

(97)   C.T. Chiou, L.J. Peters and V.H. Freed, Science, 206, 831, (1979).

(98)   B. Xing and J.J. Pignatello, Environ. Toxicol. Chem., 15, 1282, (1996).

(99)   B. Xing and J.J, Pignatello, Environ. Sci. Technol., 31, 792, (1997).

(100)  S.D. Kohl and J.A. Rice, Organic Geochemistry, 30, 929, (1999).

(101)  T.M. Young and W.J. Weber, Environ. Sci. Technol., 29, 92, (1995).

(102)  E.J. Leboeuf and W.J. Weber, Environ. Sci. Technol., 31, 1697 (1997).

(103)  W.Huang, T.M. Young, M.A. Schlautman, H. Yu and W.J. Weber, Environ. Sci. Technol., 31, 1703, (1997).

(104)  C.T. Chiou, and D.E. Kile, Environ. Sci. Technol., 32, 338 (1998).

(105)  A.T. Kan and G. Fu and M.B. Tomson, Environ. Sci. Technol., 28, 859, (1994).

(106)  Y.O. Aochi and W.J. Farmer, Environ. Sci. Technol., 31, 2520, (1997).

(107)  G. Cornelissen, P.C.M. Van Noort and H.A.J. Govers, Environ. Sci. Technol., 32, 3124, (1998).

(108)  W. Huang, H. Yu and W. J. Weber, J. Contam. Hydrol., 31, 129, (1998).

(109)  W.J. Weber, W. Huang and H. Yu, J. Contam. Hydrol., 31, 149, (1998).

(110)  M.L.Brusseau, P. Rao and C. Suresh, Environ. Sci. Technol., 25, 134, (1991).

(111)  W. Huang, M.A. Schlautman and W.J. Weber, Environ. Sci. Technol., 30, 2993, (1996).

(112)  J.J. Pignatello and B. Xing, Environ. Sci., Technol., 30, 1, (1996).

(113)  W.J. Weber, P.M. McGinley and L.E. Katz, Environ. Sci. Technol., 26, 1955, (1992).

(114)  W.J. Weber and W. Huang, Environ. Sci. Technol., 30, 881, (1996).

(115)  J.J. Pignatello, In: *Reactions and Movements of Organic Chemicals in Soils*. B.L. Sawhney, K. Brown (Eds.), Soil Science Society of America. Madison, WI; Chapter 3. (1989).

(116)  P.J. Toscano, J. Waechter, E.J. Schermerhorn, P. Zhou and H.L. Frisch, Journal of Polymer Science: Part A: Polymer, 31, 859, (1993).

(117)  A. Bandis, B.J. Cauley, C.E. Inglefield, W.-Y. Wen, P.T. Ingelfield and A. A. Jones, J. Polym. Sci. Part B, 31, 447, (1993).

(118)  J. Clauss, K. Schmidt-Rohr, A. Adam, C. Beoffel and H.W. Spiess, Macromolecules, 25, 5208, (1992).

(119)  E.H. Immergut and H.F. Mark, In Plasticization and Plasticizer Processes. R.F. Gould (ed.), Washington, D. C.; p. 1, (1964).

(120)  J.R. Darby and J.K. Sears, In: *Encyclopedia of Polymer Science and Technology*. H.F. Mark, N.G. Gaylord and N.M. Bikales (Eds.), Interscience. New York; p. 228, (1969).

(121)  R.O.J. Hill, In Encyclopedia of Polymer Science and Technology. J.F. Mark, N.G. Gaylord and N.M. Bikales (Eds.), Interscience. New York; p. 354, (1965).

(122)  E.R. Graber and M.D. Borisover, Environ. Sci. Technol., 32, 3286, (1998).

(123)  R.G. Luthy, G.R. Aiken, M.L. Brusseau, S.D. Cunningham, P. M. Gschwend and J.J. Pignatello, Environ. Sci. Technol., 31, 3341, (1997).

(124)  S.D. Kohl, P.J. Toscano, W. Hou and J. Rice, Environ. Sci. Technol., 34, 204, (2000).

(125)  W. Mittelstaedt and F. Führ, Field Lysimeter Studies with $^{14}$C Pyridate, Report IRA 11/91 E, Study-Nr. Al 2/89, Research Centre Jülich (1991).

(126)  R.S. Swift, In: *Methods of Soil Analysis: Part 3, Chemical Methods*. D.L. Sparks, J.M. Bartels, J.M. Bigham (Eds.), Soil Science Society of America. Madison, WI; p. 1018, (1996).

(127)  I. Droppo, B.G. Krishnappan, S.S. Rao and E.D. Ongley, Environ. Sci. Technol., 29, 546, (1995).

(128) H.-S. Shin, J.M. Monsallier and G.R. Choppin, Talanta, 50, 641, (1999).

(129) S.W. Karickhoff, Sorption Kinetics of Hydrophobic Pollutants in Natural Sediments, In: *Contaminants and Sediments*, Vol. 2, R.A. Baker (Ed.), Ann Arbor Science Publishers, Inc., Ann Arbor, MI, pp. 193-205, (1980).

(130) P.H. Howard and W.M. Meylan (Eds.), In: *Handbook of Physical Properties of Organic Chemicals*. Lewis Publishers. New York; p. 322, (1997).

(131) M.A.M. Lawrence, P.A. Davies, M.G. Edwards, and K. Kimkiss, Chemosphere, 41, 1091, (2000).

(132) M. Ettlinger, Aluminiumoxid C, Titandioxid P 25 – zwei hochdisperse Metalloxide nach dem AEROSIL$^{®}$-Verfahren, in: Schriftreihe Pigmente, Firmenschrift der Degussa AG, Frankfurt/Main, Nr. 56, 3. Aufl., (1981).

(133) K.-H. Wassmer, U. Schroeder und D. Horn, Makromol. Chem. 192, 553 (1991).

(134) D.H. Everett, Pure Appl. Chem. 58, 967, (1986).

(135) M. Schnitzer, Organic Matter Characterization. In: *Methods of Soil Analysis*, Part 2, A.L. Page, R.H. Miller and D.R. Keeney (Eds.), American Society of Agronomy and Soil Science Society of America, Madison, pp. 581-594 (1986).

(136) O.B. Peersen, X. Wu, I. Kustanovich and S.O. Smith, Journal of Magnetic Resonance, 104, (1993).

(137) R. Fründ,, H.-D. Lüdemann, F.J. González-Vila, G. Almendros, J.C. del Río, and F. Martín, Sci. Tot. Environ., 81/82, 187, (1989).

(138) J.W. Emsley and L. Phillips, Progress in Nuclear Magnetic Resonance Spectroscopy, 7, 1, (1971).

(139) W. Brown (Ed.), Dynamic Light Scattering, Oxford University Press, New York, (1993).

(140) E.C. Bowles, R.C. Antweiler and P. MacCarthy, Acid-base Titration and Hydrolysis of Fulvic Acid from the Suwannee River. US Geological Survey, Open File Report 87-57, Denver, Colo., USA, pp. 209-227, (1989).

(141) A.L. Herbelin and J.C. Westall, FITEQL, version 3.2. Oregon State University, Corvallis, Ore., USA. (1996).

(142) S.A. Visser, Water Res., 17, 1393, (1983).

(143) G. Newcombe, M. Drikas, S. Assemi and R. Beckett, Water Research, 31, 965, (1997).

(144) E. Tombácz, É. Mádi, M. Szekeres and J. Rice, Electrolyte Induced Spontaneous Fractionation of Polydisperse Humate Solutions. Understanding and managing organic matter in soils, sediments, and waters, In: *Understanding and managing organic matter in soils*, sediments and waters, R.S. Swift and K.M. Spark, (Eds.), IHSS, St. Paul, pp. 53-60, (2001).

(145) L. Rao and G.R. Choppin, Radiochimica Acta, 69, 87, (1995).

(146) M. Kawahigashi, N. Fujitake, and T. Takahashi, Soil Science and Plant Nutrition, 42, 355, (1996).

(147) L. Campanella, B.M. Petronio, C. Baraguglia, R. Cini and D.N. Innocenti, Int. J. Environ. Anal. Chem., 60, 49, (1994).

(148) Y-P. Chin, G. Aiken and E. O'Loughlin, Environ. Sci. Technol., 28, 1853, (1994).

(149) M. Fukushima, S. Tanaka, H. Nakamura, S. Ito, Talanta, 43, 383, (1996).

(150) M.A. Wilson, P.F. Barron and A.H. Gillan, Geochem. Cosmochimm Acta, 45, 1743, (1981).

(151) K.A. Throne, Humic Substances in the Sueuanne River, Georgia; In: *Interactions, Properties, and Proposed Structures*, R.G. Avertt, J.A. Leenheer, D.M. McKnight, K.A. Throne (Eds.), US Geological Survey Open-File Report 87-557, Colorado, p. 251, (1989).

(152) P.J. Toscano, H.L. Frisch, J. Polymer Science, 29, 1219, (1991).

(153) W. Huang, and W.J.J. Weber, Environ. Sci. Technol., 32, 3549, (1998).

(154) J.J. Pignatello, Advances in Colloid and Interface Science, 76/77, 445, (1998).

(155) B. Xing, and J.J. Pignatello, Environ. Sci. Technol., 32, 614, (1998).

(156) F.J., Stevenson and G.F. Vance, In: The Chemistry of Aluminum. Sposito G. (Ed.), CRC, Boca Raton, pp. 117-145, (1989).

(157) J. Buffle, Complexation Reactions in Aquatic Systems: An Analytical Approach, Wiley, New York, pp. 195-383, (1988).

(158) J.E. Gebhardt and D.W. Furstenau, Colloids Surf., 7, 221, (1983).

(159) J-M, Séquaris, Interactions of Polycarboxylates with Major Inorganic Soil Components, In: *Detergents in the Environment*, M.J. Schwuger (Ed.), Marcel Dekker, New York, pp. 225-245, (1997).

(160) J. T. Kunjappu, P. Somasundaran and K Sivadasan, Colloids Surfaces, 97, 101, (1995).

(161) K. Ishiduki and K. Esumi, Langmuir, 13, 1587, (1997).

(162) N. L. Filippova, Langmuir, 14, 1162, (1998).

(163) A.W.P. Vermeer, W.H. van Riemsdijk and L.K. Koopal, Langmuir, 14, 2810, (1998).

(164) J.L. Zhou, and S.J. Rowland, Wat. Res., 31, 1708, (1997).

(165) E. Tipping and D. Cooke, Geochim. Cosmochim. Acta, 46, 75, (1982).

(166) F.M. Dunnivant, P.M. Jardine D.L. Taylor and J.F. McCarthy, Soil. Sci. Soc. Amer. J., 56, 437, (1992).

(167) J. Buffle and G.G. Leppard, Environ. Sci. Technol., 29, 2169, (1995).

(168) J. F. McCarthy and J.M. Zachara, Environ. Sci. Technol., 23, 496, (1989).

(169) J.M. Martin, J.M. Mouchel and P. Nirel, Water Sci., Technol. 18, 83, (1986).

(170) H.-R. Schulten, Int. J. Environ. Anal. Chem., 94, 147, (1996).

(171) L.T.C. Bonten, T.C. Grotenhuis and W.H. Rulkens, Chemosphere, 38, 3627, (1999).

(172) W.-Y. Shiu, K.-C. Ma, D. Varhaníčková and D. Machay, Chemosphere, 29, 1155, (1994).

(173) A. Sabljić, H. Güsten, H. Verhaar, J. Hermens, Chemosphere, 31, 4489, (1995).

(174) H.M. Seip, J. Alstad, G.E. Carlberg, K. Martinsen and R. Skanne, Sci. Total Environ., 50, 87, (1986).

(175) K. Fytianos, E. Voudrias, E. Kokkalis, Chemosphere, 40, 3, (2000).

(176) K. Schellenberg, C. Leuenberger and R.P. Schwarzenbach, Environ. Sci. Technol., 18, 652, (1984).

(177) J. Peuravuori, N. Paaso and K. Pihlaja, Talanta, 56, 523, (2002).

(178) D.G. Crosby, K.I. Beynon, P.A. Greve, F. Korte, G.G. Stil and J.W. Vonk, Pure Appl. Chem., 53, 1051, (1981).

(179) L.S. Lee, P.S.C. Rao, P. Nkedi-Kizza and J.J. Delfino, Environ. Sci. Technol., 24, 654, (1990).

(180) P. Lampi, K. Tolonen, T. Vartiainen and J. Tuomisto, Chemosphere 24, 1805, (1992).

(181) F. De Paolis and J. Kukkonen, Chemosphere, 34, 1693, (1997).

(182) J. Saarikoski, R. Lindström, M. Tyynelä, Ecotoxicol. Environ. Saf., 11 158, (1986).

(183) G. Ohlenbusch, M.U. Kumke, F.H. Frimmel, Sci. Total Environ. 253, 63, (2000).

(184) Y.–H. Yang and L.K. Koopal, Colloids Surfaces, 151, 201-212, (1999).

# 8.   List of figures

## Chapter 5

# 9.    List of tables

## Chapter 4

## Chapter 5

# CURRICULUM VITAE

| | |
|---|---|
| **Name:** | Moustafa M. R. Khalaf |
| **Date of birth:** | 20. June 1967 |
| **Place of birth:** | Al-Minia, Egypt |
| **Nationality:** | Egyptian |
| **Marital status:** | Married with one child |

**School education:**

| | |
|---|---|
| 1972-1978 | Primary School (Al-Minia, Egypt) |
| 1978-1981 | Preparatory School (Al-Minia, Egypt) |
| 1981-1984 | General Secondary School (Al-Minia, Egypt) |
| 1984 | General Secondary Education Examination |

**High education:**

**Under-graduate study**

| | |
|---|---|
| 1984-1988 | B.Sc. in Chemistry, *May 1988*, Chemistry Department, Faculty of Science, Minia University, Egypt. |

**Post-graduate study**

| | |
|---|---|
| 1988-1989 | Post-graduate courses, Chemistry Department, Faculty of Science, Minia University, Egypt. |
| 1989-1993 | M.Sc. in Physical Chemistry, *May 1993*, Chemistry Department, Faculty of Science, Minia University, Egypt. |
| 1993-2003 | Assistant Lecturer at the Department of Chemistry, Faculty of Science, Minia University, Egypt. |
| May 1997-March 2003 | Study of Ph.D. at the Institute of Applied Physical Chemistry, Research Center Jülich, Germany. |
| 24. March 2003 | Ph.D. oral exam. |